The role of Fyn kinase in CRH regulation of energy homeostasis

Styliani Ourailidou

Thesis

Submitted to the University of Warwick

for the degree of

Doctor of Philosophy

Warwick Medical School

January 2017

THE UNIVERSITY OF WARWICK

Contents

List of Figures

List of Tables

Acknowledgements

First and foremost, I would like to thank my supervisors Pr. Dimitris Grammatopoulos and Dr. Claire Bastie for their supervision of my work and guidance throughout my PhD years. I am grateful for all the opportunities they gave me to expand my knowledge.

Special thanks goes to my mentor Dr Katia Karalis at the Biomedical Research Foundation of the Academy of Athens for her support and encouragement since my MSc. *Crh* KO mice were a gift from Dr Karalis for my PhD project.

I am grateful to all the members of the Developmental Biology laboratory, BRFAA, for helping me, listening to me and creating a pleasant environment in the lab. To Yassemi Koutmani, Theodora Tzanavari, Panagiotis Giannogonas, Nasia Apostolou, Maria Moisidou, Giannis Gabierakis, Kostantia Kodela, Antonia Katsouda and Babis Sigalas, I am very thankful.

I would like to thank, last but not least, from the Dev Bio lab my PostDoc, Dr Sevasti Karaliota. I heartily thank her for trusting, assisting and believing in me. Her advice and guidance were helpful in pleasant and difficult times. Being taught from her made me a better scientist.

I would also like to thank Fragiskos Sergiou for preparing Figures 1.2 and 3.15 of this manuscript.

Many thanks to all the people at Warwick Medical School and University Hospital Coventry Warwickshire who helped me throughout my time in England.

My gratitude goes to Warwick University for the financial support (Chancellor's 3-yearScholarship).

Lastly, a special thanks goes to my parents and sister, Akis, Zetta and Marilena, and Kostas for all their support, encouragement and love that motivated me the past years.

Declarations

I hereby certify that this thesis (including data generated and data analysis) is my own work. All sources of information and contributions by others have been clearly disclosed and acknowledged. This thesis has not been submitted for a degree at another University.

Abstract

Corticotropin-releasing hormone (CRH) is the master regulator of stress responses mediated by the hypothalamic-pituitary-adrenal (HPA) axis in mammals. CRH and CRH-related ligands, termed urocortins (UCNs), along with their receptors, CRHR1 and CRHR2, are expressed both centrally and peripherally. Evidence has implicated the CRH family of peptides in mechanisms regulating energy balance in the animal. Interestingly, Fyn kinase, a member of the Src kinase family, is also involved in homeostasis regulation. Fyn knockout animals display reduced adiposity partly due to increased energy expenditure and lipid utilization in white adipose tissues. Fyn kinase expression is down-regulated by glucocorticoids, suggesting that HPA axis might regulate Fyn, thereby implying a possible interaction with CRH.

I sought to determine a possible crosstalk between CRH and Fyn kinase. Using a mouse model with total *Crh* deficiency (*Crh* KO mouse) and applying various metabolic challenges, such as cold exposure and induction of lipolysis processes, Fyn kinase expression was studied in tissues harvested from age-matched WT and *Crh* KO mice. I uncovered a novel positive correlation between CRH and Fyn kinase that was unmasked upon normalization of the *Crh* KO blood glucocorticoid. Activation of lipolysis pathways did not affect Fyn kinase expression, but unraveled differences between the two genotypes, both *in vivo* and *in vitro*.

CRH plays an important role in activating thermogenesis of brown adipose tissue and therefore I sought to determine whether Fyn kinase had similar actions. A novel role for Fyn kinase activity in controlling brown adipogenesis was reported with the use of the brown preadipocyte line, T37i. Additionally, treatment of brown adipocytes with the Fyn kinase activity inhibitor, SU6656, provided evidence of an interaction between Fyn and Akt, whereas ERK1/2 remained unaffected.

Abbreviations

ABHD5	α/β hydrolase domain-containing protein-5
AC	adenylyl cyclase
ACC	acetyl-CoA carboxylase
ACO	acyl-CoA oxidase
ACTH	adrenocorticotropin hormone
Akt	protein kinase B
AMPK	AMP-activated protein kinase
ANOVA	Analysis of variance
aP2	adipocyte protein 2
ATGL	adipose triglyceride lipase
ATP	adenosine triphosphate
BAT	brown adipose tissue
BMP7	bone morphogenic protein 7
bp	base pairs
BRFAA	Biomedical Research Foundation of the Academy of Athens
BSA	bovine serum albumin
C/EBP-β	CCAAT/enhancer-binding protein β
CaCl2	calcium chloride
cAMP	cyclic adenosine monophosphate
cDNA	complementary DNA
CGI-58	comparative gene identification-58
CIDEA	cell death activator-A
CNS	central nervous system
CO_2	carbon dioxide
CoA	coenzyme A
CPT1	carnitine palmitoyltransferase 1
CPT2	carnitine palmitoyltransferase 2
CREB	cAMP response element-binding protein
CRH	corticotropin-releasing hormone
CRH-BP	corticotropin-releasing hormone-binding protein
CRHR	corticotropin-releasing hormone receptor
CSK	C-terminal Src Kinase
Ct	threshold cycle
DEPC	diethylpyrocarbonate
DG	diglycerol
DGAT2	diglyceride acyltransferase 2
dH_2O	distilled water
DMEM	Dulbecco's Modifed Eagle Medium
DMSO	dimethyl sulfoxide
DNA	deoxyribonucleic acid
dNTP	deoxynucleoside triphosphate

DTT	dithiothreitol
Ebf2	early B cell factor-2
ECL	enhanced chemiluminescence
EDTA	ethylenediamine tetraacetic acid
ELISA	enzyme-linked immunosorbent assay
En1	engrailed-1
epiAT	epididymal adipose tissue
ERK1/2	extracellular signal-regulated kinases 1/2
F	forward
FADH	reduced flavin adenine dinucleotide
FAS	fatty acid synthase
FBS	fetal bovine serum
FFA	free fatty acid
g	gram
GAPDH	glyceraldehyde 3-phosphate dehydrogenase
GC	guanylyl cyclase
GDP	guanosine diphosphate
GLUT4	glucose transporter type 4
GPCR	G protein-coupled receptor
GR	glucocorticoid replacement
GTP	guanosine triphosphate
GTT	glucose tolerance test
Hadha	Hydroxyacyl-CoA dehydrogenase/3-ketoacyl-CoA thiolase/enoyl-CoA hydratase
HEPES	1-(3-dimethylaminopropul)-3-2-ethanesulphonic acid
HFD	high-fat diet
HPA	hypothalamus-pituitary-adrenal
HRP	horse-radish peroxidase
HSL	hormone-sensitive lipase
Hsp90	heat shock protein 90
IBMX	3-isobutyl-1-methylxanthine
IgG	immunoglobulin G
IP3	inositol 1, 4, 5-triphosphate
IRS1	insulin receptor substrate 1
ITT	insulin tolerance test
Kb	kilo base pairs
KCl	potassium chloride
KD	knockdown
kDa	kilodalton
kg	kilogram
KO	knockout
l	litre
LKB1	liver kinase B1
LPL	lipoprotein lipase
LPS	lipololysaccharide
M	molar
mA	milliampere

MAPK	mitogen-activated protein kinase
MG	monoglycerol
mg	milligram
MgCl2	magnesium chloride
MGL	monoglycerol lipase
min	minutes
ml	millilitre
mM	millimolar
MMLV	Moloney murine leukemia virus
mRNA	messenger ribonucleic acid
Myf-5	myogenin factor-5
NaCl	sodium chloride
NADH	reduced nicotinamide adenine dinucleotide
NE	norepinephrine
NEFA	non-esterified fatty acid
NF-κB	Nuclear factor kappa-light-chain-enhancer of activated B cells
ng	nanogram
NK	natural killer cell
nM	nanomolar
NOS	nitric oxide synthase
ns	not significant
O_2	oxygen
^{o}C	degree Celsius
OE	overexpressed
ORO	Oil Red O
P	phosphoryl group
p38	protein 38
Pax7	paired box protein 7
PBS	phosphate-buffered saline
PCR	polymerase chain reaction
PET-CT	positron emission tomography-computed tomography
PI3K	phosphoinositide 3-kinase
PKA	protein kinase A
PKB	protein kinase B
PKC	protein kinase C
PLC	phospholipase C
POMC	pro-opiomelanocortin
PPARα	peroxisome proliferator-activated receptor α
PPARγ	peroxisome proliferator-activated receptor γ
PRDM16	PRD1-BF-1-RIZ1 homologous domain-containing protein 16
PTP	protein tyrosine phosphatase
PVN	paraventricular nucleus
qRT-PCR	quantitative real-time PCR
R	reverse
RGS	regulators of G protein signalling
rpm	rounds per minute

RT	room temperature
SDS	sodium dodecyl sulfate
SEM	standard error of mean
Ser	serine
SH	Src homology
siRNA	small interfering RNA
SNS	sympathetic nervous system
subAT	subcutaneous adipose tissue
SVF	stromal vascular fraction
T3	triiodothyronine
TAE	Tris-acetate-EDTA
TBS	tris-buffered saline
TBS-T	tris-buffered saline-tween 20
TCR	T-cell receptor
TEMED	N, N, N1, N1-tetramethylethylenediamine
TG	triglycerol
TLE3	transducin-like enhancer protein 3
TNF-α	tumor necrosis factor-α
Tris	Tris (hydroxymethyl) aminomethane
Tris-HCl	Tris hydrochloric acid
Tyr	tyrosine
U	unit
UCN	urocortin
UCP1	uncoupling protein 1
UV	ultraviolet
V	volt
v/v	volume per volume ratio
VMN	ventromedial nucleus
w/v	weight per volume ratio
WAT	white adipose tissue
WT	wild-type
ZFP516	zing finger protein 516
β-AR	β-adrenergic receptor
µg	microgram
µl	microlitre
µm	micrometer
µM	micromolar

Chapter 1

Introduction

1.1 Adipose tissue

Adipose tissue evolved primarily to store energy in times of plenty and to provide fuel when sources become insufficient. Nowadays, it is acknowledged as the body's largest endocrine organ and it secretes hormones (adipokines), lipids, cytokines and other factors (Gesta et al., 2007; Nawrocki and Scherer, 2004; Spiegelman and Flier, 2001). This dynamic tissue is able to respond to homeostatic and external cues and play central role in controlling appetite, glucose homeostasis, insulin sensitivity, aging, fertility, fecundity and body temperature (Berry et al., 2013).

Adipose tissue is composed of adipose stem cells, adipocytes, mural, endothelial and neuronal cells (Riordan et al., 2009; Schipper et al., 2012). Various discrete depots have been described: inguinal, interscapular, perigonadal, retroperitoneal and mesenteric depots (Berry et al., 2013). In mammals, two main classes of adipose tissue exist, namely the white adipose tissue (WAT) and the brown adipose tissue (BAT), which are histologically and molecularly distinct and functionally distinguishable.

Developmentally, white and brown fat cells derive from a common multipotent precursor in the somites, which also gives rise to skeletal myocytes, dorsal dermis (Kajimura et al., 2015). Before the adipogenic commitment of this precursor, cells positive in *Pax7* (paired box protein 7), *En1* (engrailed-1), *Myf-5* (myogenin factor-5) and *Ebf2* (early B cell factor-2) give rise to brown adipocytes (Wang et al., 2014). *Ebf2* and *Bmp7* (bone morphogenic protein 7) control brown adipocyte differentiation by regulating the expression of *Prdm16* (PRD1-BF-1-RIZ1 homologous domain-containing protein 16), *C/EBP-β* (CCAAT/enhancer-binding protein β), *ZFP516* (zing finger protein 516), *PPARγ* (peroxisome proliferator-activated receptor γ) and *PPARα*

(peroxisome proliferator-activated receptor α) (Kajimura et al., 2015). White preadipocytes originate from *Pax7*-negative and *Myf-5*-negative precursors (Wu et al., 2013) and *PPARγ* and *TLE3* (transducin-like enhancer protein 3) are essential for their differentiation (Kajimura et al., 2015).

1.1.1 White adipose tissues (WAT)

WAT is designed for energy storage and is classically divided into subcutaneous and visceral depots. Histologically, subcutaneous fat is heterogeneous and contains mature unilocular adipocytes intercalated with small multilocular adipocytes, whereas visceral fat is more uniform and appears to consist primarily of large unilocular adipocytes (Tchernof et al., 2006; Tchkonia et al., 2007). These differences are physiologically significant as the expansion of subcutaneous fat may protect against from the deleterious effects of type 2 diabetes and glucose intolerance (Snijder et al., 2003a; Snijder et al., 2003b), whereas, visceral depots expansion can associate with metabolic complications and increases the risk of diabetes, hyperinsulinemia and cardiovascular diseases (Grauer et al., 1984). This discrimination between the "good fat" and "bad fat" has its roots to the distinct histology of the two depots. More specifically, the large numbers of small multilocular adipocytes that reside in the subcutaneous fat have been shown to be protective against metabolic dysfunctions (Salans et al., 1973; Weyer et al., 2000). The increased interstitial tissue found in the subcutaneous depots as well as the increased rates of adipose turnover (Bjorntorp et al., 1971; Salans et al., 1973), which constantly provides a pool of new and younger adipocytes, further enhance the "good profile" of the subcutaneous fat. Further, the anatomical localization of the fat pads is considered to be key aspect in the protection against hyperinsulinemia and glucose tolerance. In particular, the visceral fat is drained by the portal vein, which in case of nutritional imbalance, such as diet-induced obesity, provide additional fatty acids to the liver and this can cause hepatic insulin resistance (Bjorntorp, 1991; Despres et al., 1995; Randle, 1998); whereas the close proximity of subcutaneous fat with the insulin-

sensitive muscle mass at the gluteal region, promotes the beneficial effects of this adipose depot (Snijder et al., 2003a; Virtue and Vidal-Puig, 2008).

Dietary non-esterified fatty acids (NEFAs) are esterified to the chemically inert triacylglycerol (TG) and finally stored in cytosolic lipid droplets (Lass et al., 2011). The increased energy demand, for example after fasting or exercise, mobilizes the energy reserves of WAT. This hydrolysis of TG is termed lipolysis and results in production of free fatty acids (FFAs) and glycerol. FFAs enter the circulation to be further catabolized by non-adipose tissues, such as skeletal muscles, via the β-oxidation pathway. Glycerol is taken up by the liver to provide substrates either for the glycolysis or the gluconeogenesis pathways.

Lipolysis is driven mainly by three enzymes: adipose triglyceride lipase (ATGL), hormone-sensitive lipase (HSL) and monoglyceride lipase (MGL) (Lass et al., 2011). ATGL resides on lipid droplets and gains full hydrolytic activity upon binding with its co-activator, comparative gene identification-58 (CGI-58) (Lass et al., 2006). CGI-58, also termed α/β hydrolase domain-containing protein-5 (ABHD5), strongly interacts with perilipin (see below), thus reducing interaction with ATGL (Granneman et al., 2007). ATGL hydrolyzes triglycerides to diglycerides and free fatty acids (FFAs) (Zimmermann et al., 2004). The hydrolysis of diglycerides to monoglycerides and FFAs is catalyzed by HSL (Haemmerle et al., 2002; Osuga et al., 2000), and the final step of lipolysis is catalyzed by MGL, which releases glycerol and FFAs (Karlsson et al., 1997). The phosphorylated forms of HSL and MGL translocate to lipid droplets to coordinately hydrolyze stored lipids.

One of the most important activators of lipolysis are catecholamines, which bind to β-adrenergic receptors (β-AR) on plasma membranes of adipocytes (Cannon and Nedergaard, 2004). Coupling of the receptor to G_s proteins activates adenylyl cyclase and the intracellular signal is transmitted via cyclic AMP (cAMP) (Connolly et al., 1986;

Scarpace and Matheny, 1996). Subsequent activation of protein kinase A (PKA) leads to a series of phosphorylation events, which include activation of lipases and deactivation of perilipin (Figure 1.1). Perilipin is the protein that normally localizes around the triglyceride droplets within the cell (Blanchette-Mackie et al., 1995), thus protecting them against ATGL and HSL activity (Martinez-Botas et al., 2000). Modification of ATGL is not PKA-dependent (Schweiger et al., 2006; Zechner et al., 2012; Zimmermann et al., 2004). Activated PKA phosphorylates perilipin (Chaudhry and Granneman, 1999), which changes conformation and binds to phosphorylated HSL (Miyoshi et al., 2007; Shen et al., 2009; Wang et al., 2009). Lastly, HSL translocates to these sites of action (Egan et al., 1992; Londos et al., 1995).

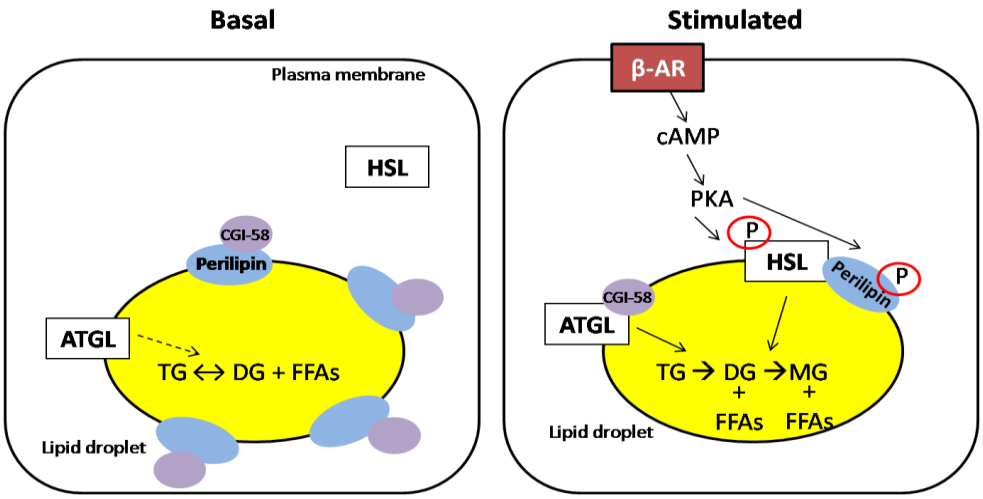

Figure 1.1: The lipolysis process. Under basal conditions, the lipid droplet is surrounded by perilipin molecules, which prevent lipolysis from both ATGL, because it strongly binds the ATGL co-activator, CGI-58, and HSL, because it has no access to lipid droplets. ATGL, which normally resides on lipid droplet surface, catalyzes (low activity denoted by the doted arrow) the first step of lipolysis: TG to DG and FFAs. Under stimulated conditions, catecholamines bind to β-AR and cAMP and PKA are activated. PKA, in turn, phosphorylates and deactivates perilipin, which changes conformation and binds to phosphorylated HSL, thus allowing HSL to translocate to the lipid droplets, where it gains full hydrolytic capacity and hydrolyzes DG to MG and FFAs. Upon perilipin phosphorylation, CGI-58 binds to ATGL, which has full hydrolyzing activity and catalyzes the first step of lipolysis (arrow). HSL = hormone-sensitive lipase, ATGL = adipose triglyceride lipase, TG = triglyceride, DG = diglyceride, FFAs = free fatty acids, MG = monoglyceride, CGI-58 = comparative gene identification-58, β-AR = β-adrenergic receptor, cAMP = cyclic AMP, PKA = protein kinase A, P = phosphoryl group.

The product of lipolysis, FFA, are activated to acyl-CoA (Coenzyme A) by acyl-CoA synthase, turned into acylcarnitine by carnitine acyltransferase I (CPT1) on the outer mitochondrial membrane, shuttled inside the mitochondria by carnitine-acylcarnitine translocase and converted to acyl-CoA by carnitine acyltransferase II (CPT2) on the inner mitochondrial membrane. The ensuing β-oxidation of FFA (acyl-CoA) produces acetyl-CoA, which enters the citric acid (or Krebs) cycle, leading to the formation of the reduced electron carriers, FADH and NADH, which are then oxidized by the electron transport chain (respiratory chain), ultimately through oxygen consumption. This results in a pumping out of protons from the mitochondrial matrix and the formation of a proton-motive force that drives the protons back into the matrix and produces energy in the form of ATP (Lowell and Flier, 1997).

1.1.2 Brown adipose tissue (BAT)

Morphologically, BAT differs from WAT because of its rich vasculature and numerous un-myelinated nerves, which provide sympathetic stimulation to the adipocytes (Nnodim and Lever, 1988). Opposite to the single large lipid droplet found in white adipocytes, brown cells contain smaller lipid droplets and a large number of mitochondria (Weber, 2004), giving the characteristic colour of this tissue. The primary role of BAT is to convert nutrients into chemical energy in the form of heat (Cannon and Nedergaard, 2004). This role has given mammals an evolutionary advantage, which is to survive and to be active during periods of nocturnal or hibernal cold, to survive the cold stress of birth and probably to survive on diets low in essential macronutrients, such as protein (Cannon and Nedergaard, 2004). BAT was thought to be present only in neonatal life, in the interscapular region (Gregoire et al., 1998; MacDougald and Mandrup, 2002; Spiegelman and Flier, 2001). However, more recent studies provide evidence that brown cells exist in adult humans and in several discrete areas and these depots are metabolically functional (Nedergaard et al., 2007). Positron emission tomography-computed tomography (PET-CT) identified the supraclavicular region as the main BAT

depot in adult humans, although it is heterogeneous tissue and as it contains cells expressing the classical markers for BAT but also cells that do not express these typical markers (Cypess et al., 2009; Cypess et al., 2013; Virtanen et al., 2009). Other BAT containing regions are the cervical and perirenal areas, which comprise cells expressing the classical brown marker genes (Cypess et al., 2013; Nagano et al., 2015; Xue et al., 2015). Importantly, PET imaging detects higher amounts of BAT in young and lean subjects, suggesting that BAT activity is necessary for the natural regulation of body weight (Kajimura et al., 2015). As WAT, BAT can also be regulated by environmental signals, particularly low temperatures. Interestingly, the original BAT cells, which appear in neonatal life, are distinct from the ones that are present or can be induced in adults (Wu et al., 2012).

The heat generated from BAT cells is a product of a complex system consisting of mitochondrial biogenesis, energy uncoupling and energy dissipation (Kajimura et al., 2010). Uncoupling protein 1 (UCP1), a mitochondrial protein, is responsible for this unique function of BAT. UCP1 gives the mitochondria an ability to uncouple oxidative phosphorylation and utilizes substrates to generate heat rather than ATP.

1.1.2.1 The thermogenic machinery

Signals such as “a meal was just consumed”, “too much energy has been stored” or “body temperature is lowering” activate a signalling cascade that initiates from the ventromedial hypothalamic nucleus (VMN) of the brain (Cannon and Nedergaard, 2004). Norepinephrine (NE) is released, binds to the β3-adrenergic receptor on the plasma membrane of brown adipocytes (Cannon and Nedergaard, 2004) and activates a signalling cascade described in Figure 1.1. Phosphorylation of the transcription factor cAMP response element-binding protein (CREB) (Thonberg et al., 2002) results in expression of genes like UCP1 (Figure 3.15), and activation of MAP kinases, like ERK1/2 (Lindquist and Rehnmark, 1998; Shimizu et al., 1997), which inhibits

apoptosis, and p38 (Cao et al., 2001), which further stimulates the adrenergic-activated UCP1 expression.

Lipolysis processes and β-oxidation occur in BAT. However, when protons are driven back into the mitochondrial matrix through UCP1, the proton gradient is dissipated, thereby uncoupling fuel oxidation from ATP synthesis and generating heat (Cannon and Nedergaard, 2004).

1.1.2.2 Physiological roles of BAT in energy metabolism and browning of white adipose tissues

Apart from its thermoregulatory role, BAT plays an important role in regulating total body fat. The anti-obesity role became evident when caloric excess could stimulate BAT expansion and thermogenesis, known as diet-induced thermogenesis (Rothwell and Stock, 1997). Transgenic mice with decreased BAT have glucose intolerance and insulin resistance as well as enhanced susceptibility to diet-induced obesity and diabetes (Hamann et al., 1993; Hamann et al., 1995; Lowell et al., 1993). Experiments under ambient temperatures further supported the above role of BAT as the UCP1 KO mice display increased metabolic efficiency (Enerback et al., 1997) and gain more weight than WT controls only when housed under thermoneutral conditions (=temperature at which the lowest metabolic rate is observed, 29-31^{o} C for mice) (Feldmann et al., 2009).

Adult humans when exposed to cold, accumulate more BAT in the supraclavicular region (Kajimura and Saito, 2014). Despite their multilocular appearance and UCP1-positive staining, these areas contain cells that express both brown- and white-specific genes (Sharp et al., 2012; Wu et al., 2012). This expansion of BAT further resulted in improvement of postprandial insulin sensitivity (Chondronikola et al., 2014; Lee et al., 2014) and induced energy expenditure (van der Lans et al., 2013; Yoneshiro et al., 2013). However, the anti-obesity role of BAT has been disputed as studies have shown that upon cold exposure, increased glucose uptake was only reported

for BAT and not in other tissues, thus not influencing whole-body insulin sensitivity (Orava et al., 2011; Orava et al., 2013; Ouellet et al., 2012). To support this argument, studies have shown that the primary substrate for BAT was oxidation of intracellular free fatty acids and to a lesser extent plasma substrates (Ouellet et al., 2012), thus strengthening the notion of intra-tissue benefits. These contradictory effects resulted from differences in the duration of cold exposure and therefore, for future studies, this should be considered in order to elucidate the role of BAT in whole-body energy homeostasis.

Newborns have relatively large deposits of BAT. It is believed that with age, but probably more with body size, our relative functionality of BAT decreases and disappears (Kajimura and Saito, 2014). However, in addition to the supraclavicular and perirenal regions of BAT found in humans, islets of BAT are also found in WAT depots (Kajimura et al., 2015). These brown-like or beige cells express UCP1 and in rodents, they take on a multilocular appearance upon prolonged cold stimulation or elevation of intracellular cAMP (Cousin et al., 1992; Young et al., 1984). Although classical brown adipocytes derive from a *myf-5* positive lineage, similar to skeletal muscle cells (Seale et al., 2008), the beige cells do not (Ishibashi and Seale, 2010; Petrovic et al., 2010; Seale et al., 2008).

The beige adipocyte homeostasis may be maintained through two mechanisms. First, they can be generated *de novo* from a population of beige preadipocytes (Wang et al., 2013; Wu et al., 2012), which express the early B cell factor-2 (*Ebf2*), a brown preadipocyte marker (Wang et al., 2014). Second, they can be bi-directionally converted from and to white adipocytes under the control of environmental temperature or sympathetic nerve innervation (Cao et al., 2011; Rosenwald et al., 2013; Ye et al., 2013). Although these two theories may seem contradictory, both are still examined to elucidate the precise mechanisms that underlie the browning effect of white adipose tissues. The appearance of beige cells is “location dependent” (site dependent), as subcutaneous

rather than epididymal fat undergoes browning (Ohno et al., 2012; Vitali et al., 2012). This is due to increased expression of the BAT-specific marker, PRDM16, in the subcutaneous adipose tissue, which has higher density of sympathetic nerves compared to epididymal fat (Seale et al., 2011). Further, great variability is reported for the browning responses among inbred strains of mice, where C57BL/6J mice have less beige in their white fat depots compared to the A/J mice (Collins et al., 1997).

Environmental cues that control the appearance of beige cells have largely been studied and consist of the well-known stimulus cold exposure and subsequent β-adrenergic activation, exercise, bariatric surgery, cancer and others, which are reviewed in Kajimura et al., 2015. Notably, the presence of beige adipocytes in humans is inversely correlated with obesity and type 2 diabetes (Kajimura et al., 2015), indicating their important role in regulating metabolism. However, the exact mechanisms of glucose clearance are not completely understood as beige cells can potentially secrete hormones. The latter was proven from the beneficial effects of transplanted subcutaneous fat from exercised mice on glucose homeostasis compared to transplantations of subcutaneous fat from sedentary mice (Stanford et al., 2015). Further evidence on the beneficial effects of beige cells on energy expenditure and propensity for weight gain comes from rodent studies. Particularly, mouse strains with high propensity for browning of WAT (mice overexpressing *Prdm16* and mice with genetic ablation of *myf-5* resulting in loss of brown adipocytes) are more resistant to diet-induced obesity (Kajimura and Saito, 2014).

Overall, BAT and beige cells should be considered more than a heat-generating organ/cells. Therefore, their implication in whole-body metabolism could have a therapeutic effect in humans with small or actively absent BAT, like obese humans or elderly people. While PET-CT detects only the metabolically active BAT and not the BAT mass *per se*, it was shown that young and lean subjects have increased BAT activity compared to obese (Lee et al., 2010; Yoneshiro et al., 2011) and elderly

(Yoneshiro et al., 2011). Hence, although the precise mechanisms are still unknown, it is implied that BAT has a protective role against body fat accumulation and its activity decreases with age.

Stressful stimuli can disturb the energy balance, either by mobilizing the energy reserves or by increasing the energy pools. The most important mediator in stress responses is Corticotropin-Releasing Hormone (CRH) and its implication in regulation of whole-body homeostasis will be reviewed in the next section.

1.2 Stress response: CRH and implications in energy homeostasis

Stress involves external and/or internal challenges that threaten survival (e.g. depletion of ATP, increased utilization of substrates, etc). Thus, maintenance of homeostasis must be tightly controlled to face these challenges. The integrated stress responses are regulated by the Hypothalamo-Pituitary-Adrenal (HPA) axis and its main mediator Corticotropin-Releasing Hormone or Factor (CRH or CRF) (Chrousos and Gold, 1992). In response to stressful stimuli, CRH initiates and coordinates a series of adaptation mechanisms involving the autonomic, endocrine, immune, cardiovascular, and reproductive systems. Dysregulation of the stress response can have severe physiological and psychological consequences, such as anxiety, anorexia nervosa and depression (Sarnyai et al., 2001; Sasaki et al., 1988; Arborelius et al., 1999; Bale, 2005; Chrousos and Gold, 1992; de Kloet et al., 2005; Heinrichs and Koob, 2004; Holmes et al., 2003; Holsboer, 1999; McEwen, 2004; Zorrilla and Koob, 2004).

1.2.1 Corticotropin-Releasing Hormone (CRH)

CRH is a 41 amino acid peptide (Vale et al., 1981), released from the hypothalamus and regulates adrenocorticotropin (ACTH) secretion from the anterior pituitary. This, in turn, triggers glucocorticoid release from the adrenal gland (Bale and Vale, 2004), which suppresses CRH secretion via a negative-feedback loop. The physiological role of CRH is much wider than the central nervous system (CNS) alone as CRH is also produced and secreted in the periphery by a plethora of tissues (Table 1.1). Therefore, CRH exerts a wide spectrum of actions that emphasize its critical role in integrating the activity of diverse physiological mechanisms. One such example is the effects of CRH on the immune system. Although CRH exerts anti-inflammatory effects through glucocorticoids, its production in sites of inflammation suggests a pro-inflammatory role (Baigent, 2001). In this context CRH appears to be an important regulator of inflammatory responses in both autocrine and paracrine ways (Karalis et al., 1991).

Table 1.1: Examples of tissues and cells shown to express CRH mRNA and/or protein. Taken from Grammatopoulos and Ourailidou, review accepted for publication in Current Molecular Pharmacology.

Tissues/Cells	References
Placenta	(Sasaki et al., 1988)
Endometrium	(Makrigiannakis et al., 1997; Makrigiannakis et al., 1995)
Adrenal	(Bruhn et al., 1987)
Ovary	(Mastorakos et al., 1993)
Testis	(Fabbri et al., 1990; Thompson et al., 1987)
Gut	(Suda et al., 1984)
Anterior pituitary	(Suda et al., 1984)
Lung	(Suda et al., 1984)
Liver	(Suda et al., 1984)
Heart	(Muglia et al., 1994)
Lymphatic organs	(Aird et al., 1993)
Murine splenic T lymphocytes	(Muglia et al., 1994)
Immune cells	(Baigent, 2001)
Skin	(Slominski et al., 2001)
Joints	(Crofford et al., 1992)
Synovium	(McEvoy et al., 2001)

1.2.2 The CRH family of peptides

The first mammalian CRH peptide was isolated from ovine hypothalamic extracts in 1981 (Vale et al., 1981). Urotensin I in fish (*Catostomus commersoni*) (Lederis et al., 1982) and sauvagine in frogs (*Phyllomedusa sauvagei*) (Montecucchi et al., 1980) consist the ancient paralogs of CRH (Lovejoy et al., 2014). Following CRH isolation, a novel family of mammalian CRH-related ligands was discovered. The family consists of three members: urocortin 1 (UCN1) (Vaughan et al., 1995), urocortin 2 (UCN2 or stresscopin-related peptide) (Reyes et al., 2001), and urocortin 3 (UCN3 or stresscopin) (Lewis et al., 2001). UCNs are expressed in distinct areas of the brain and the periphery (Hillhouse and Grammatopoulos, 2006; Suda et al., 2004), including the immune (Kageyama et al., 1999), digestive (Harada et al., 1999), cardiovascular systems (Hsu and Hsueh, 2001; Takahashi et al., 2004), and reproductive organs (Yamauchi et al., 2005). Although UCNs display only 45% sequence homology with CRH, they exert complementary and/or distinct actions (Suda et al., 2004). The interplay between CRH and UCNs in physiology and underlying integrated responses are poorly understood. Studies employing knockout (KO) animal models revealed that *Crh*-deficient mice have normal behaviour (similar to control animals) under basal conditions, normal increase in anxiety-like behaviours after restraint stress or CRH administration into the brain (Weninger et al., 1999b) and almost normal feeding and energy homeostasis in basal and under restraint stress conditions (Weninger et al., 1999b), suggesting potential compensatory roles of UCNs. Despite these normal behavioural characteristics of *Crh* KO mice, the endocrine response, comprised from the release of glucocorticoids, is significantly blunted in these mice both under basal and stressful conditions (Bale and Vale, 2004). The compensatory roles of UCNs are summarized by the fact that all three UCNs have been linked to metabolism regulation (Chen et al., 2006; Kotz et al., 2002; Kuperman and Chen, 2008; Li et al., 2007; Zalutskaya et al., 2007), a finding that supports the hypothesis of overlapping and possibly synergistic roles. Additionally, in

the immune or cardiovascular systems, UCNs have been reported to either mimic CRH actions or exert more potent effects (Suda et al., 2004). In contrast, in physiological processes controlling the level of anxiety, UCN2 and UCN3 exhibit distinct actions and stress-coping characteristics compared to CRH (Suda et al., 2004). Other examples of contrasting roles between UCNs and CRH include effects on colonic motility and gastric emptying (Suda et al., 2004), where UCNs inhibit and CRH stimulates this process.

The bioactivity of CRH and related peptides is regulated by a circulating binding protein, called CRH-binding protein (CRH-BP). It is produced by the liver and the placenta and it can either enhance or inhibit the effects of CRH (Linton et al., 1988; Potter et al., 1991; Seasholtz et al., 2002; Sehringer et al., 2004). CRH-BP exhibits differential selectivity towards CRH and UCNs and also plays additional roles to regulate ligand – CRH receptor interaction by increasing the half-life of CRH or UCNs and protecting them from degradation and delivering the ligand to the receptors in target tissues (Seasholtz et al., 2002). Moreover some reports raise the possibility that CRH-BP might possess intrinsic bioactivity on its own (Seasholtz et al., 2002).

1.2.3 CRH Receptor subfamilies

Signals from CRH and UCNs are transduced across the cell membrane through activation of two types of receptors, termed CRH receptor 1 (CRHR1) and CRH receptor 2 (CRHR2), which are encoded by different genes (Hillhouse et al., 2002). Both belong to the family of seven transmembrane domain (7TMD) G protein-coupled receptors (GPCRs, family B) (Chang et al., 1993). The ligands for B1 subfamily receptors (receptors for “brain-gut” neuropeptides) are polypeptide hormones that act in a paracrine and/or autocrine manner, including secretin, glucagon, vasoactive intestinal peptide, CRH and parathyroid hormone. The homology between CRHR1 and CRHR2 is 71% on the amino acid level (Lovenberg et al., 1995). All members of the B1 family of GPCRs have multiple coding exons, possibly due to gene duplication during evolution

(Lovejoy et al., 2014). Subsequent alternative splicing produces several receptor subtypes for both CRHRs, which are expressed in various tissues: CRHR1α (main functional receptor), CRHR1β, CRHR1c-h and CRHR2α, CRHR2β and CRHR2γ (Chen et al., 1993; Grammatopoulos et al., 1999; Kostich et al., 1998; Liaw et al., 1996; Pisarchik and Slominski, 2001; Ross et al., 1994; Valdenaire et al., 1997).

Despite the great homology between CRHRs, considerable divergence is exhibited at their N-termini (only 40% sequence similarity), consistent with their pharmacological characteristics (Grammatopoulos and Chrousos, 2002). CRHR1 binds CRH as well as UCN1, with equivalent high affinity, but not UCN2 and UCN3 (Figure 1.2). In contrast, all UCNs are the natural ligands for CRHR2, which binds them with significantly higher affinity compared to CRH (Chen et al., 1993; Hsu and Hsueh, 2001; Lewis et al., 2001; Lovenberg et al., 1995; Reyes et al., 2001; Vaughan et al., 1995).

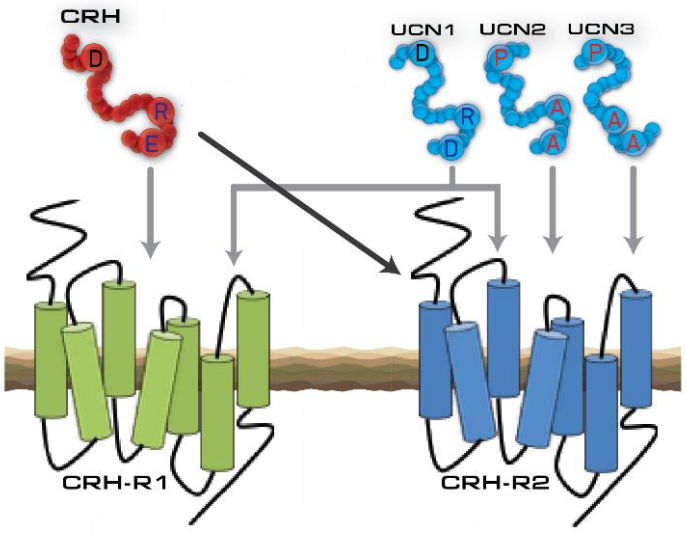

Figure 1.2: CRHRs' pharmacological characteristics. CRHR1 recognizes and binds CRH and UCN1 with equivalent high affinity (grey arrows), but not UCN2 and UCN3, and CRHR2 binds all thee UCNs with significantly higher affinity (grey arrows) than CRH (black arrow). Specific amino acid signatures determine ligand binding affinity: proline (P) and alanine (A) residues (coloured red) are found only in CRHR2 selective ligands, UCN2 and UCN3, while the CRHR non-selective peptides contain an invariant arginine (R) and an acidic (E or D) amino acid (coloured blue). Taken from Grammatopoulos and Ourailidou, review accepted for publication in Current Molecular Pharmacology.

Both CRHRs are widely distributed in the central nervous system (CNS) and the periphery. CRHR1 is expressed in the pituitary corticotrophs, where its CRH-dependent activation induces pro-opiomelanocortin (POMC) gene transcription and subsequent ACTH secretion (Chen et al., 1993; Hsu and Hsueh, 2001; Lewis et al., 2001; Lovenberg et al., 1995; Reyes et al., 2001; Vaughan et al., 1995). Levels of CRHR1 are also detected in other brain areas (Van Pett et al., 2000) and the periphery (Hillhouse and Grammatopoulos, 2006). The expression pattern of CRHR2 differs from that of CRHR1. Although, it is detected in the CNS (Kostich et al., 1998; Van Pett et al., 2000), it does not co-localize with CRHR1, therefore suggesting that these receptors exert distinct roles. In the periphery, CRHR2 has been detected in skeletal, smooth and cardiac muscle (Hillhouse and Grammatopoulos, 2006). The diverse and distinct physiological functions of CRHR1 and CRHR2 were confirmed by the *Crhr1* and *Crhr2* KO mouse models, which showed different and sometimes opposite phenotypes. Whilst *Crhr1* KO mice display decreased anxiety-like behaviour and impaired stress response (Smith et al., 1998; Timpl et al., 1998), *Crhr2* deficient mice show increased anxiety-like behaviour, accelerated HPA axis response to stress, and impaired cardiovascular function (Bale et al., 2000; Coste et al., 2000; Kishimoto et al., 2000).

CRHRs exert their actions upon ligand binding, which allosterically changes the receptor and initiates G protein coupling (Grammatopoulos, 2012). The CRHRs preferentially couple to the G_s-adenylyl cyclase signalling pathway, but also exhibit alternative coupling to and activation of other G proteins such as G_i, G_o, G_q and G_z (Figure 1.3) (Chen et al., 1986; Grammatopoulos et al., 2001). Interestingly, not only the CRHRs have the ability to bind to different G proteins, but also the pattern of G protein activation is unique for each tissue and controlled by tissue-specific mechanisms (Grammatopoulos and Ourailidou, review accepted for publication in Current Molecular Pharmacology). Further downstream signalling molecules include the protein kinases A (PKA), PKC, MAP kinases p38 and ERK1/2 and also signalling molecules such as Ca^{2+}

and nitric oxide synthase (NOS) (Brar et al., 2004a; Cantarella et al., 2001; Kiang, 1997; Ulisse et al., 1990).

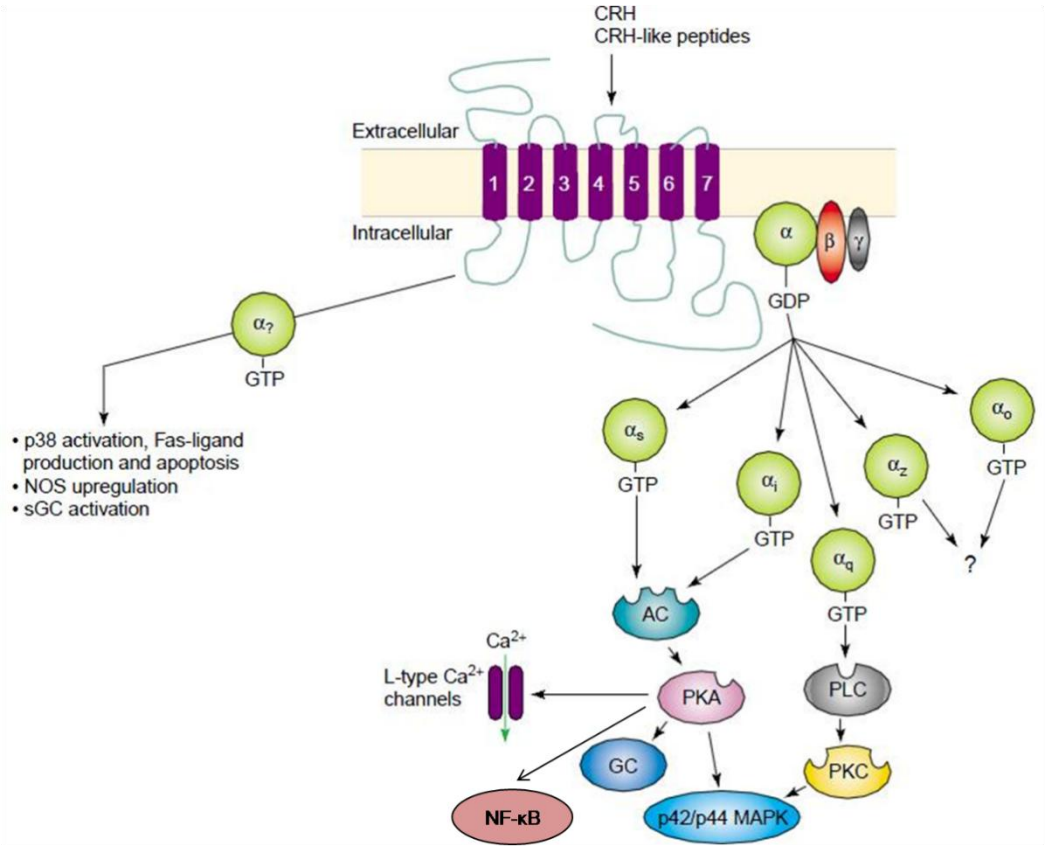

Figure 1.3: CRHR signalling. Upon CRH or CRH-like peptides binding to CRHRs, a plethora of downstream signalling cascades is activated in a tissue-specific manner. AC = adenylyl cyclase, GC = guanylyl cyclase, GDP = guanosine diphosphate, GTP = guanosine triphosphate, MAPK = MAP kinase, NOS = nitric oxide synthase, PKA = protein kinase A, PKC = protein kinase C, PLC = phospholipase C, sGC = soluble GC, NF-κB = nuclear factor kappa-light-chain-enhancer of activated B cells. Modified from (Grammatopoulos and Chrousos, 2002).

1.2.4 Metabolic roles of CRH

The CRH family of neuropeptides also plays an important role in the regulation of food intake (Bradbury et al., 2000; Contarino et al., 2000; Cullen et al., 2001; Spina et al., 1996), anxiety (Britton et al., 1986; Stenzel-Poore et al., 1994), and stress (Vaughan et al., 1995), as well as stimulation of sympathetic outflow (Brown et al., 1982;

Udelsman et al., 1986), therefore suggesting their involvement in energy balance. The first indirect indications of CRH metabolic actions arose in 1990 (Rothwell, 1990) and included experiments with adrenalectomized genetically obese rodents, which displayed reduced food intake, body weight gain and increased metabolic rates evident from the increased thermogenesis. However, this role of CRH in metabolism was almost invalidated when Muglia et al. (Muglia et al., 1995) generated the *Crh* KO mouse. These mice display normal body weight gain and food intake relative to their control (wild-type, WT) littermates, when allowed *ad libitum* access to food. Similarly, the observation that *Crh* KO and WT mice exhibit indistinguishable anorectic responses to restraint stress (Swiergiel and Dunn, 1999) could emphasize the importance of other modulators, such as urocortins, in the control of food intake.

Further, eating disorders, such as anorexia nervosa, can arise from dysregulation of the HPA axis (Rothwell, 1990). Stress-induced anorexia begins when CRH is released after a stressful stimulus (Kuperman and Chen, 2008). Acute central administration of CRH causes hyperglycemia (Rothwell, 1990) (Table 1.2), while chronic infusions alter the energy balance markedly in male rats, whereas no effects are seen in females (Rivest et al., 1989). Other differences are observed between obese and lean animals, with the obese being more responsive to CRH-induced suppression of food intake and activation of brown fat thermogenesis than their leaner controls (Rothwell, 1990). Finally, a functional link between CRH and leptin has been described, as leptin administration increases hypothalamic CRH expression (Schwartz et al., 1996; Huang et al., 2006) and release (Costa et al., 1997). However, since corticosterone levels were unaffected after leptin injections, it is suggested that leptin actions are independent of the HPA axis (Harris, 2010). Simultaneous injections of leptin and CRH receptor antagonist (alpha-helical CRH 9-41) prevented leptin-induced hypophagia (Uehara et al., 1998; Gardner et al., 1998). The elevated CRHR2 expression after leptin administration (Figure 1.4) indicated that this receptor may mediate the effects of leptin (Huang et al., 2006;

Nishiyama et al., 1999; Masaki et al., 2003). However, studies using the *Crhr2* KO mouse showed that CRHR2 is not essential for the anorectic effects of leptin (Harris, 2010). Due to compensatory mechanisms that might have developed in mice with global *Crhr2* deficiency (Harris, 2010), further studies are needed in order to elucidate the role of CRHRs in regulation of leptin effects.

Considerable evidence supports the effects of CRH on both energy intake and energy utilization. Chronic central CRH infusions attenuate weight gain by reducing food intake (Table 1.2). Furthermore, CRH induces energy utilization by activating the sympathetic nervous system (SNS) (Cullen et al., 2001): it stimulates thermogenesis in brown adipose tissue (BAT), increases uncoupling protein (UCP) 1 in BAT, elevates norepinephrine released in CNS as well as increases plasma norepinephrine, increases heart rate and stimulates glucocorticoid release. This increases substrates' availability in liver and muscle and enhances catecholamine-induced lipolysis in adipose tissue. These findings suggest that chronic CRH infusions negatively affect the energy balance, partially by reducing food intake and partially by activating SNS.

Table 1.2: Effects of centrally or intraperitoneally (ip) administered CRH and UCNs on feeding behaviour of mice.

CRH infusions	UCNs infusions
Eating disorders Stress-induced anorexia Hyperglycemia ↓ Food intake ↓ Weight gain ↑ SNS activity	↓Food intake

The anorectic effects of CRH, as discussed above, also occur after central or intraperitoneal (ip) administration of UCNs (Table 1.2), but without increasing the SNS outflow and therefore resulting in a less dramatic state of negative energy balance (Cullen et al., 2001; Seres et al., 2004). The metabolic phenotype of *Ucn1* KO mice has

not been described yet, but it is reported that they have a normal body size and exhibit impaired stress response to restraint and cold (Zalutskaya et al., 2007). *Ucn2* KO mice are characterized by increased tissue-specific insulin sensitivity (Figure 1.4) and increased glucose utilization (Chen et al., 2006; Kuperman and Chen, 2008), suggesting a role for UCN2 as a modulator of these functions. Furthermore, both *Ucn2* (Chen et al., 2006) and *Ucn3* (Li et al., 2007) KO mice are protected against high-fat diet (HFD)-induced insulin resistance (Table 1.3). Remarkably, *Ucn3* KO mice secrete less insulin than their control littermates under high glucose-stimulating concentrations and UCN3 signals through islet CRHR2 to promote insulin secretion (Li et al., 2007), supporting a role for UCN3 as an important regulator of β cell insulin release (Figure 1.4). Finally, transgenic $UCN3^{+}$ (overexpressing, OE) mice show a lean phenotype complemented with increased carbohydrate metabolism, without modulation of the insulin transduction signal and up-regulated catabolic processes (Jamieson et al., 2011) (Table 1.3).

Table 1.3: Metabolic phenotypes and other parameters from mice deficient (indicated by KO) in CRH family of peptides and transgenic (indicated by OE) mice compared to control mice

	UCN2 KO	UCN3 KO	UCN3 OE	CRHR1 KO	CRHR2 KO
Phenotype	Feeding: N Weight gain: N	Feeding: N Weight gain: N	Feeding: ↑ Weight: heavier ↑ Lean mass ↑ Carb utilization	Feeding: N Weight: N	Feeding: N Weight gain: N
Glucose utilization	↑	ND	↑ Skeletal muscle	N	N
Insulin sensitivity	↑ Skeletal muscle	↓ Secretion from β cells	N	↑	N
Stress	ND	ND	ND	Do not lose weight & low anxiety (*)	↓ Food intake, ↑ heat production & ↓ fat stores
HFD challenge	Insulin sensitive	Insulin sensitive	Protected from obesity & hyperglycemia	↓ Weight gain, ↑ lipid oxidation & insulin sensitive	Insulin sensitive, no weight gain & ↑ SNS activity

(*): (Chotiwat et al., 2010)
(N): Normal
(ND): Not Determined

Studies with CRHR KO mice show that CRHR2 normally inhibits or dampens the stimulatory actions of CRHR1 (Bale et al., 2003). More specifically, *Crhr2* KO mice exhibit normal basal feeding behaviour and weight gain. However, following a challenge, like high-fat diet (HFD) or cold, food intake is reduced, heat production is enhanced and fat stores are depleted in the *Crhr2* KO mice (Table 1.3). Under HFD, *Crhr2* KO mice are protected against insulin resistance and the SNS outflow is increased (Bale et al., 2003; Kuperman and Chen, 2008). Body mass and food intake are normal in the *Crhr1* KO mice (Bradbury et al., 2000; Muller et al., 2000), but there is a significant disruption of the circadian pattern of food intake. In particular, mice lacking *Crhr1* gene consume more food during the resting period (light period) (Muller et al., 2000). This effect is rescued with glucocorticoid replacement in the drinking water of the mice. Further evidence suggests that *Crhr1* KO mice have reduced adiposity that could not be attributed to differences in food intake and locomotor activity, rather it could result partially from increased lipid oxidation in the liver (Sakamoto et al., 2013). *Crhr1* KO mice have increased insulin sensitivity and when fed HFD, they have reduced weight gain and increased energy expenditure (Lu et al., 2015; Sakamoto et al., 2013).

Recent evidence from *in vitro* and *in vivo* experiments (*Crhr1* KO mice) suggests that CRHR2, and subsequently its ligand UCN2, play a significant role in adipose depots development, especially the white adipose tissue (WAT). More specifically, they stimulate the differentiation of white adipocytes to brown-like cells, whereas CRHR1 and its ligand CRH prevent that, allowing the expression of a white phenotype (Lu et al., 2015). These favorable actions of UCN2/CRHR2 are abolished by corticosterone replacement in *Crhr1* KO mice, thus showing that the brown characteristics in the WAT are secondary to the low levels of circulating corticosterone (Lu et al., 2015).

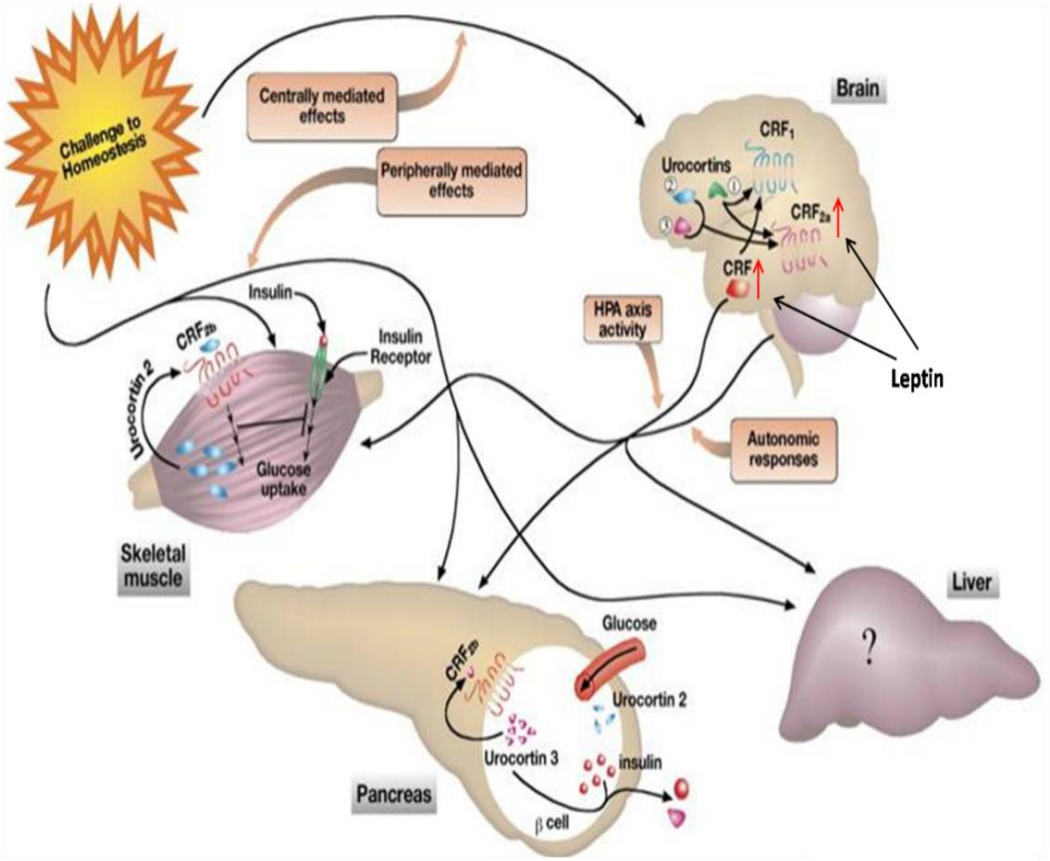

Figure 1.4: Schematic representation of the proposed roles of central and peripheral CRH, UCNs and CRHRs in modulating glucose homeostasis. After a stressful stimulus, hypothalamic CRH stimulates glucocorticoid release, which in parallel to changes in autonomic activity will modulate skeletal muscle, pancreatic and hepatic function. Brain: CRH and UCNs, functioning through CRHR1 and CRHR2, will modulate food intake and glucose homeostasis. Leptin increases CRH and CRHR2 expression levels. Skeletal muscle: UCN2 produced and acting locally on CRHR2 will regulate glucose uptake by inhibiting insulin signaling. Pancreas: UCN3, produced by β cells, regulates high glucose-induced insulin secretion. Although, both *Ucn2* and *Ucn3* deficient mice demonstrate alterations in metabolic liver functions, studies have failed to demonstrate hepatic expression of CRH-related peptides or receptors (denoted by '?' in the liver). Therefore, these observed effects in the mutant mice would seem likely to be secondary to their altered energy homeostasis resulting from the direct effects on muscle or pancreatic physiology. Modified from (Kuperman and Chen, 2008).

1.2.5 CRH in spleen

There is considerable amount of evidence for interactions between the immune and the central nervous systems (Jessop et al., 1997). CRH, through activation of the HPA axis and subsequent glucocorticoid production, exerts its anti-inflammatory role;

whereas peripherally expressed CRH acts as a pro-inflammatory mediator (Karalis et al., 1991). CRH has been detected in human lymphocytes (Ekman et al., 1993; Stephanou et al., 1990), rat thymocytes and splenocytes (Aird et al., 1993; Redei, 1992) and mouse spleen (Muglia et al., 1994). Inflammatory diseases, such as arthritis, enhance the expression of CRH (Crofford et al., 1992; Jessop et al., 1995; Karalis et al., 1991). CRH influences the inflammatory response in various ways: it enhances natural killer (NK) cell activity (Carr et al., 1990), it induces rat splenocyte proliferation (McGillis et al., 1989) and exerts pro-inflammatory effects in inflamed tissues measured by exudate volume after carageenin injection (Webster et al., 1996), monocyte infiltration in arthritic joints of rats (Crofford et al., 1992) and skin mast cell degranulation and release of histamine (Singh et al., 1999; Theoharides et al., 1998).

Exogenous administration of CRH in rats reduces spleen weight by 43% compared to control animals (Labeur et al., 1995). Splenocyte proliferation is attenuated after lipopolysaccharide (LPS) stimulation in CRH-infused animals (Labeur et al., 1995). Further, using an antisense oligonucleotide complementary to CRH, which blocked CRH expression, showed an impaired splenocyte activation upon concanavalin A, indicating that endogenous splenic CRH plays a functional role in mediating immune cell activation, thus enhancing the pro-inflammatory role of CRH (Jessop et al., 1997).

Transgenic mice overexpressing CRH have reduced cellularity in lymphoid organs, which reaches 90% in the spleen (Boehme et al., 1997). This resulted from impaired development of T and B lymphocytes in primary lymphoid tissues (thymus and bone marrow, respectively). On the other hand, mice deficient in *Crh* exhibit diminished inflammatory response to two models of inflammation (carageenin-induced local inflammation and turpentine-induced abscess), confirming the pro-inflammatory role of peripheral CRH (Karalis et al., 1999; Venihaki and Majzoub, 2002). Upon LPS administration in *Crh* KO mice, a compromised splenic cytokine response was reported as measured from tumor necrosis factor α (TNF-α) and interleukin 1β (IL-1β) (Venihaki

et al., 2003). Cultured WT and *Crh* KO splenocytes have differential responses to proliferation, as, although *Crh* KO basal proliferation was higher compared to WT, *Crh* KO proliferation rates decreased the following days in culture and WT rates remained stable (Venihaki et al., 2003). This highlighted the role of endogenous CRH in normal proliferation of splenocytes. The absolute numbers of total splenocytes are increased in naive *Crh* KO mice compared to WT (Benou et al., 2005); whereas, similar distributions of the major splenic T and B lymphocyte populations are reported between the two genotypes (Benou et al., 2005).

Other members of the CRH family of peptides, such as UCNs and CRHRs, are also expressed in splenic cell populations and their overall contribution to the inflammatory stimulation consists mainly in generating a rapid response; whereas the released cytokines and other immune mediators activate the HPA axis, which results in production of glucocorticoids and a delayed and generalized down-regulation of the inflammation (Baigent, 2001).

Overall, CRH initiates the HPA axis in response to stressful stimuli and thus coordinates a series of homeostatic mechanisms. In addition, HPA axis and its mediators, such as glucocorticoids, have also been shown to regulate, either directly or indirectly, another molecule, Fyn kinase.

1.3 Fyn kinase and the Src kinase family

Fyn kinase is a member of the large Src family of non-receptor tyrosine kinases, which catalyzes phosphorylation of tyrosine residues in proteins (Kefalas et al., 1995). Most of them are cytoplasmic enzymes but others, like Fyn, are also localized in the membrane and in the nucleus. The Src kinase family consists of nine members: Src, Fyn,

Yes, Fgr, Lck, Hck, Blk, Yrk and Lyn kinases (Brickell, 1992; Sudol et al., 1993). Interestingly, all members share a common structure (Kefalas et al., 1995) that contains four Src homology (SH) domains (Figure 1.5). The SH1 domain contains the enzymatic activity and the SH2 and SH3 domains allow them to bind to phosphorylated tyrosine residues on their substrates (Boggon and Eck, 2004). The SH4 domain is more variable between the members of the family and its post-translational modifications, such as myristoylation or palmitoylation, likely participate to their cellular localization (Resh, 1999).

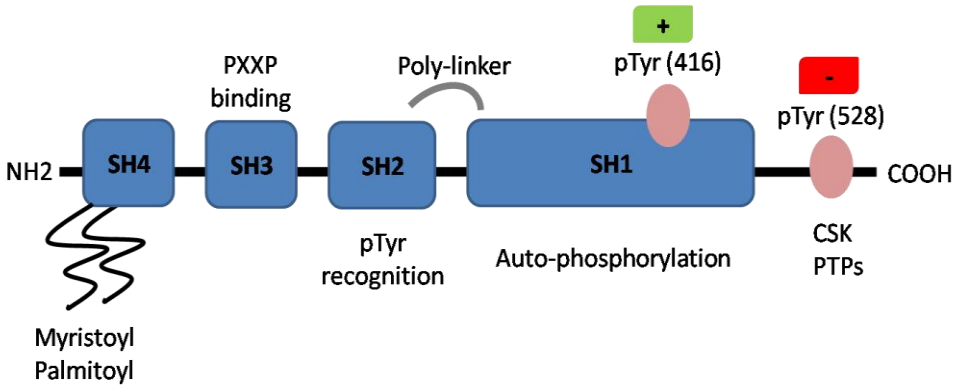

Figure 1.5: Fyn kinase structure and regulation. SH1 domain contains the catalytic activity (denoted by the green "+" symbol). SH2 binds the phosphorylated Tyr(528) at the C-terminus, stabilizing the structure in an inactive conformation (denoted by the red "-" symbol). Kinases, such as CSK, can phosphorylate Tyr(528), whereas phosphatases can dephosphorylate this residue. SH3 domain further represses Fyn activity by binding to a polyproline helix between SH2 and SH1. SH4 domain's post-translational modifications (myristoylation and/or palmitoylation) enable cellular localization and trafficking. CSK = C-terminal Src Kinase, PTPs = Protein Tyrosine Phosphatases. Modified from (Vatish et al., 2009).

Fyn, in humans, has 3 transcript isoforms. Isoform 1 encodes the FynB protein, while isoform 2 encodes the FynT (Saito et al., 2010). The third isoform, FynΔ7, has been reported (Goldsmith et al., 2002) but no translated protein has been documented. However, in mice, only two isoforms exist, FynT and FynB (Cooke and Perlmutter, 1989). Both isoforms, as a mixture, are expressed in most tissues (Yamada et al., 2012). For example, FynT is more expressed in muscle, white adipose tissue, spleen, heart and T cells and FynB is highly expressed in the brain and in the liver.

1.3.1 Biological roles of Fyn kinase and its signalling pathways

Extracellular signals that activate Fyn originate from integrins, G protein-coupled receptors, specifically Angiotensin II type 1 receptor (Yin et al., 2003), antigen and Fc receptors, and cytokine receptors (Sun et al., 2005). The signalling output of this activation has several effects on growth and motility pathways. Fyn has been extensively studied in its relation to the immune system, especially in T and B cells. Of note is Fyn's important role during the initial T cell receptor (TCR) activation upon antigen recognition (Palacios and Weiss, 2004). Other biological actions include (Saito et al., 2010; Thomas and Brugge, 1997): proliferation, survival, fertilization, growth factor and cytokine receptor signalling, integrin-mediated signalling, cell-cell adhesion, ion channel function, platelet activation, axon guidance, entry into mitosis and differentiation of NK-T cells, oligodendrocytes (Sperber and McMorris, 2001) and keratinocytes. Fyn has also been implicated in thymic involution (Nishio et al., 2005).

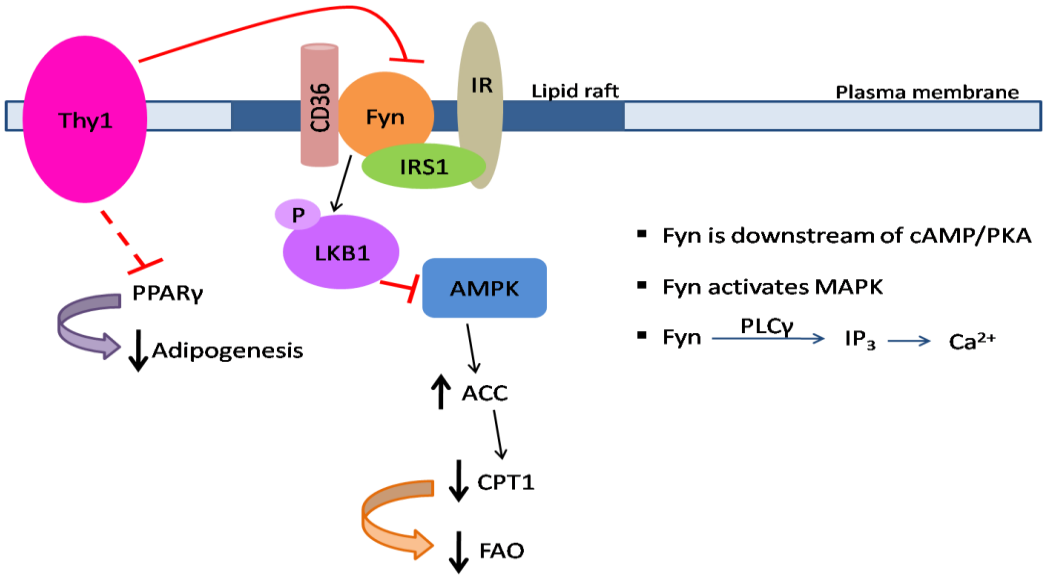

Figure 1.6: Schematic representation of Fyn signalling pathways. Fyn is localized on lipid rafts of the plasma membrane, where it is implicated in the regulation of insulin-activated pathways (IR and IRS1). Fyn interacts with CD36 and in states of low fatty acid availability (Samovski et al., 2015), Fyn phosphorylates LKB1 thus inhibiting AMPK. Consequently, ACC is increased and CPT1 is decreased, resulting in a reduced state of fatty acid oxidation. Adipogenesis is also down-regulated (left panel) since Thy1 inhibits Fyn and PPARγ (dotted line = Thy1 indirectly inhibits PPARγ via Fyn). Additional cascades where Fyn is implicated are shown in bullets (right panel).

Emphasis has been given on the role of Fyn in insulin-stimulated adipogenesis. Studies have shown that Fyn is implicated in the regulation of insulin-activated pathways (Liu et al., 2005; Saltiel and Pessin, 2003) (Figure 1.6). Firstly, Fyn was discovered to be directly associated with insulin-stimulated tyrosine phosphorylated insulin receptor substrate 1 (IRS1) and the adaptor protein c-Cbl (Myers et al., 1996; Ribon et al., 1998; Sun et al., 1996). Secondly, Fyn participates in the tyrosine phosphorylation of caveolin upon insulin stimulation in 3T3L1 cells (Mastick and Saltiel, 1997). Caveolin is highly expressed in adipocytes, its expression increases during differentiation and it is phosphorylated in result to insulin (Mastick et al., 1995). Thirdly, Fyn is located in lipid-raft microdomains, where it co-localized with insulin receptor (Dykstra et al., 2003; Liang et al., 2001; van't Hof and Resh, 1997, 1999). Furthermore, Fyn associates with flotillin, which is highly expressed in lipid rafts during differentiation of 3T3L1 adipocytes. Lastly, Fyn binds to CD36, a fatty acid transporter (Bull et al., 1994; Huang et al., 1991; Liu et al., 2005; Samovski et al., 2015). Importantly, either pharmacological inhibition of Fyn kinase activity or genetic deletion or overexpression of Fyn in 3T3L1 cells highlighted the role of Fyn in modulating the differentiation of white preadipocyte cells (Sun et al., 2005; Tse et al., 2013). *In vivo* studies using *Fyn* KO mice describe a lean phenotype characterized by increased fatty acid oxidation and energy expenditure (Bastie et al., 2007), thus strengthening the notion of Fyn participating in the regulation of whole-body metabolism.

Studies reported previously helped elucidate, partly, the molecular pathways of Fyn (Figure 1.6). It is known that Fyn negatively regulates AMPK through phosphorylation of its upstream kinase, liver kinase B1 (LKB1) (Yamada et al., 2010). Inhibition of AMPK, in turn, increases acetyl-CoA carboxylase (ACC) activation and subsequently decreases carnitine palmitoyl-transferase (CPT1) levels, affecting the fatty acid oxidation pathway (Bastie et al., 2007). Thy1 (or CD90), a cell surface glucophosphatidylinositol-anchored glucoprotein, is an upstream inhibitor of Fyn and

PPARγ, thus negatively regulating adipogenesis (Woeller et al., 2015). Other Fyn signalling pathways that have been identified are the following (Figure 1.6): Fyn is localized downstream of cAMP/PKA (Klinger et al., 2002; Yang et al., 2011) and plays a role in activating MAPK (Klinger et al., 2002), Fyn regulates calcium release by catalyzing the activation of phospholipase (PL) Cγ to generate pools of inositol 1,4,5 triphosphate (IP_3) (Harr et al., 2010).

The effects of HPA axis on regulation of Fyn kinase are evident from *in vivo* and *in vitro* studies. Firstly, behavioural studies have shown that *Fyn* KO mice display increased anxiety (Belzung and Griebel, 2001). Secondly, *in vitro* studies with T lymphocytes concluded that administration of glucocorticoids reduces the expression of Fyn kinase (Harr et al., 2010; Lowenberg et al., 2005; Lowenberg et al., 2006).

1.4 Thesis aims

My research project investigated the potential association between CRH and Fyn kinase. I based my working hypothesis on data accumulated from *in vivo* settings with *Crh* and *Fyn* knockout mice and *in vitro* experiments. In particular, Fyn was shown to regulate β-oxidation (Bastie et al., 2007) and *Crh* KO mice have increased β-oxidation in their white adipose tissues (Karaliota et al., unpublished data; Dr Karalis lab; a project in which I was also involved). Secondly, differential behavioural responses, such as increased anxiety, where exhibited by mice deficient in peptides of the CRH family and *Fyn* KO mice, indicating that Fyn might be regulated by the HPA axis. Finally, an indirect association between CRH and Fyn was postulated by the glucocorticoid insufficiency of *Crh* KO mice (Muglia et al., 1995) and the down-regulation of *Fyn* by glucocorticoids (Harr et al., 2010). The latter places Fyn downstream of the HPA axis. I used suitable models, such as the *Crh* KO mouse (gift from Dr Katia Karalis, Biomedical Research Foundation of the Academy of Athens, Greece), complemented with *in vitro* studies to achieve my aims, as listed below:

1. Determination of Fyn expression in *Crh* KO mice.

2. Investigation of alterations in Fyn expression under metabolically challenging conditions, such as cold exposure or induced lipolysis, and whether this expression was tissue-specific and/or cell-autonomous.

3. Elucidation of the role of Fyn in brown adipogenesis and its implication in CRHR signalling pathways.

Chapter 2

Material and Methods

2.1 Animals

2.1.1 Housing, breeding and experimental protocol

Wild-type (WT) mice (genetic background C57/Bl6) were provided by the animal facility, Clinical, Experimental Surgery and Translational Research Center, Biomedical Research Foundation of the Academy of Athens (BRFAA). Corticotropin-Releasing Hormone knockout (*Crh* KO) mice (genetic background C57/Bl6) were a gift from Dr Katia Karalis, Clinical, Experimental Surgery and Translational Research Center, BRFAA.

All studies were approved and performed in compliance with the prefectural Veterinary Service of Athens, Greece. Experimentation was performed in the Laboratory Animal Facilities of the Biomedical Research Foundation of the Academy of Athens (BRFAA), which are approved by the competent authority as breeding (EL25BIO001) and experimental (EL25BIO003) facilities.

Mice were housed and maintained in accordance with the European legal framework for the protection of animals used for experimental and other scientific purposes (European Directive 86/609/EEC and European Convention 123/ETS). Husbandry conditions were in accordance with the current guidelines of international organizations, such as the Association for the Assessment and Accreditation of Laboratory Animal Care International (AAALAC Int) and the Federation of European Laboratory Animal Science Associations (FELASA).

Mice were housed in ventilated cages (Techniplast, Varese, Italy) (up to 8 mice per cage) under specific pathogen-free (SPF) conditions and constant environmental conditions (12:12 hour light: dark cycle (0700-1900), temperature 22±2^{0}C, and relative humidity 45±10%). The mice were fed irradiated pellets (2918 Teklad Global 18% Protein Rodent Diet, Harlan Laboratories, Indianapolis, USA; 18% protein, 6% fat and 3.1 kcal/g) and had access to filter-sterile tap water *ad libitum*. The cage bedding comprised corncob granules (REHOFIX®, J. Rettenmaier & Söhne Co., Rosenberg, Germany). Cages and bedding were changed once a week. All mice were routinely screened (twice a year) under a health-monitoring program, in accordance to the Federation of European Laboratory Animal Science Associations' recommendations, and were classified as free of pathogens.

All researchers were required to follow mandatory training prior to starting animal studies. This training included seminars on animal handling, animal anesthesia and analgesia and animal necropsy and histopathology. These seminars discuss warnings and safety regulations, safety rules within the facility and procedures to follow in case of injury.

2.1.2 Genotyping

Despite the glucocorticoid insufficiency (Muglia et al., 1995), *Crh* KO mice are viable and fertile without glucocorticoid replacement. However, litters from homozygous mating die within the first 12 hours of life due to lung dysplasia. This phenotype can be rescued with glucocorticoid replacement (corticosterone final concentration 20 μg/ml; Sigma-Aldrich, USA) in the drinking water of the breeding pairs, from day 12 of gestation until weaning day.

In the case of mating a *Crh* heterozygous mother with a homozygous father or two heterozygous parents will also give rise to *Crh* KO pups and corticosterone replacement is not required because one maternal physiological *Crh* allele is sufficient to

produce the corticosterone needed for survival of litters (Muglia et al., 1995). However, identification of the *Crh* KO pups in this setting requires genotyping due to the mixed genotype of the litters and the lack of obvious phenotypes to isolate the *Crh* KO from the *Crh* heterozygous and the WT littermates.

2.1.2.1 Tagging, tail clipping and DNA isolation

Tagging the animals (ear marking, performed under anesthesia) was required to identify each individual. DNA was obtained from a small piece of tail (cut under anesthesia). Tails were incubated in 200 μl of tail buffer (100 mM Tris-HCl pH 8.5, 200 mM NaCl, 5 mM EDTA, 0.2% SDS) and Proteinase K 0.1 mg/ml (Sigma-Aldrich, USA) overnight at 55^{o}C. Proteinase K was deactivated at 95^{o}C for 5 minutes. DNA isolation continued as follows: 200 μl of Phenol-Chloroform-Isoamyl Alcohol (Sigma-Aldrich, USA) were added and samples were vortexed, centrifuged at 13,000 rpm for 5 minutes at room temperature, the upper aqueous phase was collected in 600 μl of ethanol (VWR Chemicals, USA), centrifuged at 13,000 rpm for 5 minutes at room temperature, the DNA pellet was washed with 500 μl of 70% ethanol in distilled dH_2O, centrifuged at 13,000 rpm for 5 minutes at room temperature, the pellet was air dried and re-suspended into 200 μl of dH_2O.

2.1.2.2 Polymerase chain reaction (PCR)

PCR multiplied the sequence of interest in 25 μl total volume (Table 2.1).

Table 2.1: PCR for genotyping. Volume of reagents for the PCR.

Reagent	Volume in µl
10x Buffer (Invitrogen)	2.5
$MgCl_2$ 50 mM (Invitrogen)	1
dNTPs 5 mM (Invitrogen)	1
LM6 primer (10 pmol/µl)	0.5
LM3 primer (10 pmol/µl)	0.25
MS1 primer (10 pmol/µl)	0.25
dH_2O	17.3
Taq Polymerase 5 U/µl (Invitrogen)	0.2
DNA	2

Table 2.2: PCR for genotyping. Denaturation, annealing, elongation temperatures, and incubation times.

95°C 3 min	
55°C 1 min	34 cycles
72°C 4 min	
95°C 1 min	
55°C 1 min	
72°C 10 min	
4°C 10 min	

Table 2.3: Primers' sequence for genotyping.

Primer	Sequence 5' - 3'
mLM6	GAG CTT ACA CAT TTC GTC C
mLM3	ATC GCC TTC TTG ACG AGT TC
mMS1	GCT CAG CAA GCT CAC AGC AA

The *Crh* KO mouse was generated by targeted disruption in embryonic stem cells (Muglia et al., 1994). Homologous recombination resulted in replacement of the entire pre-proCRH coding region with the neomycin resistance gene. Primers mLM6 and mMS1 were designed to bind to the WT allele, outside the coding region, whereas the mLM3 primer binds to the neomycin cassette, thus recognizing the *Crh* KO allele

(https://www.jax.org/strain/002783). Under these conditions, a DNA fragment with 400 bp size characterized the WT, a DNA fragment with 600 bp size characterized the *Crh* KO, since the neomycin cassette is larger in size (bp) compared to the pre-proCRH coding region, and two DNA fragments with 400 and 600 bp sizes characterized the *Crh* heterozygotes.

2.1.2.3 Agarose (1%) gel electrophoresis

Gel preparation: 1 g of agarose (Sigma-Aldrich, USA) was added in 100 ml of TAE 1x (50x TAE: 2 M Tris acetate, 0.05 M EDTA, 1 M Glacial Acetic Acid pH 8.2-8.4). The mixture was melted and cooled down under tap water until it reached approximately 40^{o}C. 7 μl of ethidium bromide (Sigma-Aldrich, USA) to visualize the DNA were then added. Biorad trays and combs for the gel were used.

Sample preparation: DNA loading dye 6x (ThermoFischer Scientific, USA) was added in 25 μl of PCR product before loading the gel. 1 Kb Plus DNA ladder (ThermoFisher Scientific, USA) was used as marker.

Electrophoresis was performed with the following settings: 120 V for 30 minutes in TAE 1x.

Products were visualized under UV light and a picture of the gel was taken (Figure 2.1).

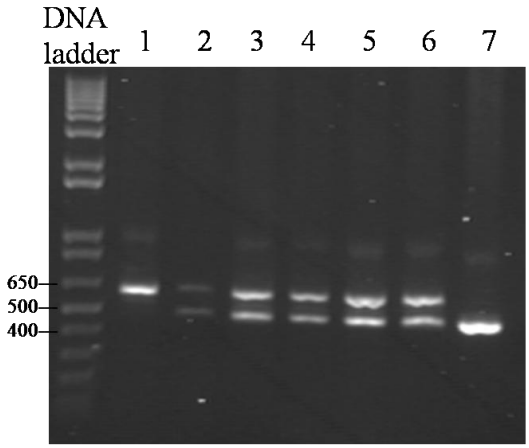

Figure 2.1: Genotyping results. 1 Kb Plus DNA ladder was loaded on the first lane. The samples follow: lane 1-*Crh* KO mouse at 600 bp, lanes 2 to 6-*Crh* heterozygous mice at 400 and 600 bp and lane 7-WT mouse at 400 bp.

2.1.3 Intraperitoneal injection

On the day of the experiment, mice were fasted for 3 hours to achieve a baseline. This was to avoid potential experimental variations due to random and uncontrolled food intake. PBS (Gibco, USA) was injected to the control groups and isoproterenol 10 mg/kg in PBS, was injected to the treated groups in a maximum volume of 100 µl. Animals were sacrificed 10 minutes later.

2.1.4 Glucocorticoid replacement

Corticosterone supplementation (20 µg/ml) in the drinking water of *Crh* KO parents restored blood levels of corticosterone and secured survival of litters (section 2.1.2). A similar method was used to restore blood corticosterone in 3 months old male *Crh* KO mice for 11 days.

2.1.5 Cold exposure

In order to metabolically stimulate (=fatty acid break down and brown adipose tissue thermogenesis) the mice, animals were acclimatized at 16^{o}C for 24 hours (Lim et

al., 2012) before being maintained at 4°C for another 24 hours. Mice were then sacrificed.

2.1.6 Sacrifice, blood collection and dissection

3-hour fasted male mice (3 months old) were anesthetized with sevoflurane (Abbvie) and sacrificed by cervical dislocation. Blood (100 µl) was collected retro-orbitally under anesthesia, prior to sacrifice and samples were kept on ice, before being centrifuged at 8,000 rpm for 8 minutes at 4°C to collect serum. Dissections included the collection of subcutaneous adipose tissue (subAT), epididymal adipose tissue (epiAT), brown adipose tissue (BAT), spleen and liver. All samples collected were stored at -80°C until further analysis.

2.2 Cell culture – T37i cell line

T37i cell line derived from a hibernoma (malignant brown adipose tissue tumour) of the transgenic mouse founder 37 carrying a hybrid gene composed of the human mineralocorticoid receptor proximal promoter fused to the SV40 large T antigen (Zennaro et al., 1998). These cells are capable of differentiating into mature brown adipocytes after exposure to insulin and triiodothyronine (T3). Their characteristics resembled the ones of mature brown adipocytes: multilocular intracytoplasmic lipid droplets and specific adipogenic gene activation (Penfornis et al., 2000), which includes uncoupling protein 1 (*Ucp1)*, peroxisome proliferator-activated receptor γ *(PPARγ)*, lipoprotein lipase *(LPL)*, adipocyte-specific fatty acid binding protein 2 *(aP2)* (Buyse et al., 2001; Penfornis et al., 2000; Viengchareun et al., 2002; Zennaro et al., 1998).

2.2.1 T37i culture

T37i cells were a gift from Dr Marc Lombès, Institut National de la Santé et de la Recherche Médicale, Unité 693, Le Kremlin-Bicêtre, France.

T37i cells were removed from liquid nitrogen, warmed in a water bath for 2-3 minutes until thawed, diluted in DMEM/F12 (Gibco, USA) media supplemented with 10% fetal bovine serum (FBS; Gibco, USA), 1% Penicillin/Streptomycin (5,000 U/ml Penicillin and 5,000 μg/ml Streptomycin; Gibco, USA) and 20 mM HEPES (Gibco, USA) (=complete DMEM/F12), transferred in a cell culture flask and incubated under 37^{o}C, 5% CO_2, 20% O_2 for 24 hours. Fresh media was added, unless confluence was more than 70% of the flask surface when cells were then split.

To split T37i cells, media were aspirated and cells were washed with PBS (Gibco, USA). 1 ml of 0.25% Trypsin-EDTA (Gibco, USA) was added in a 75 cm^2 flask for 3-4 minutes at 37^{o}C. To collect cells and deactivate the trypsin, complete DMEM/F12 was added in five volumes of trypsin. Cells were collected in a falcon tube, centrifuged at 1,000 rpm for 4 minutes at room temperature and they were re-suspended in complete DMEM/F12 and plated in new 75 cm^2 flasks.

For cell freezing, cells were centrifuged after trypsinization at 1,000 rpm for 4 minutes at room temperature. Medium was aspirated and cells were diluted in 45% complete DMEM/F12, 45% FBS and 10% dimethyl sulfoxide (DMSO; Sigma-Aldrich, USA) and placed in a cryo-freezing container at -80^{o}C for 24 hours before being stored in liquid nitrogen.

2.2.2 T37i differentiation

10^5 T37i cells per well were plated in 6-well plates. Two days after reaching 100% confluence, differentiation was initiated. The differentiation medium contained complete DMEM/F12, 2 nM T3 (Sigma-Aldrich, USA) and 20 nM insulin (Sigma-Aldrich, USA) (Penfornis et al., 2000). Fresh differentiation media was added every two days until day 11 or 12.

2.2.3 SU6656 treatment

SU6656 is a selective Src kinase family inhibitor, which acts by competing with ATP, therefore inhibiting the enzymatic activity of Fyn (Blake et al., 2000). During the whole differentiation process, SU6656 10 μM (Cayman Chemical, USA) was added in the differentiation media (Bastie et al., 2007).

2.2.4 *Fyn* knockdown in T37i cells

Fyn was silenced using siRNA technology. Control and *Fyn* knockdown (KD) T37i cells were a gift from Dr Elena Tarabra, Albert Einstein, New York, USA.

2.3 Cell culture – Isolation and culture of primary preadipocytes

Stromal vascular fraction (SVF) was isolated from 3 months old male WT and *Crh* KO mice. The SVF of adipose tissue contains preadipocytes, mesenchymal stem cells, endothelial cells, immune cells and blood cells (Riordan et al., 2009; Schipper et al., 2012). After 16 hours in culture, media were changed in order to remove all cells that were not preadipocytes (Aune et al., 2013).

2.3.1 Isolation of stromal vascular fraction (SVF) from subcutaneous, epididymal and brown adipose tissues

Subcutaneous, epididymal and brown adipose tissues were dissected from mice under sterilized conditions. Briefly, scissors and tweezers were sterilized before the experiment and a different pair of scissors and tweezers was used to cut the mouse skin and to dissect tissues. Working area and all other instruments (e.g. beakers) were cleaned with 70% ethanol. The dissected tissues were placed in PBS (Gibco, USA) at 37^{o}C until further processing. Fat pads were transferred in beakers without PBS. Tissues

were finely minced and pieces were transferred in 50 ml falcon tubes, which contained the digestion buffer. 10 ml of digestion buffer were used for 12 fat pads (from 6 mice).

The composition of the digestion buffer for subcutaneous and epididymal adipose tissues was as follows: in 10 ml PBS (Gibco, USA) collagenase D (Roche, USA) 10 mg/ml was added along with 20 μl of dispase II and 4 μl of $CaCl_2$ 2.5 M. The solution was filtered with a 0.2 μm filter and warmed at 37^{o}C.

The digestion buffer for brown adipose tissue contained: 125 mM NaCl, 5 mM KCl, 1.3 mM $CaCl_2$, 5 mM glucose and 100 mM HEPES (Gibco, USA) were added in PBS (Gibco, USA) to a volume up to 100 ml. Aliquots of the digestion buffer were stored at -20^{o}C. On the day of the experiment 4% bovine serum albumin (BSA; Sigma-Aldrich, USA) and collagenase B 1.5 mg/ml (Roche, USA) were added to the buffer. The solution was filtered with a 0.2 μm filter and warmed at 37^{o}C.

Homogenized fat pads were incubated in digestion buffer with collagenase at 37^{o}C for 60 to 75 minutes depending on the size of the pieces, with gentle shake every 10 minutes. When all tissue was digested, it was filtered through a 100 μm mesh to discard adipocytes and undigested pieces of tissue. Collagenase was inactivated with three volumes (v/v) DMEM high glucose (4.5 g/l) (Gibco, USA) supplemented with 10% FBS (Gibco, USA) and 1% Pen/Strep (Gibco, USA) (=complete DMEM). Samples were centrifuged at 500 xg for 5 minutes at room temperature. Supernatant was discarded and pellet was washed with 20 ml complete DMEM. Samples were centrifuged at 500 xg for 5 minutes at room temperature. Supernatant was discarded and the pellet (=SVF) was re-suspended in 20 ml complete DMEM and filtered through a 40 μm mesh to discard any adipocytes that might have pelleted within the SVF. Samples were centrifuged at 500 xg for 5 minutes at room temperature. Supernatant was discarded and cells were re-suspended in 5 ml of complete DMEM by vigorously

pipetting and then plated in 25 cm^2 flask. Cells were placed in an incubator (37^oC, 5% CO_2, 20% O_2).

2.3.2 Preadipocyte culture and splitting

16-24 hours after the plating of freshly isolated SVF, preadipocytes attached and looked like fibroblasts. Since epithelial cells can also attach, they were removed (along with other immune and blood cells floating in the media). For this, media was aspirated and cells were washed twice with PBS supplemented with 1% Pen/Strep. During each wash the flask was shaken vigorously to achieve detachment of the epithelial cells. If the confluence of preadipocytes was more than 70% of the flask surface, then cells were split.

To split the preadipocytes, trypsinization was performed as described in section 2.2.1. Cells were plated in a 75 cm^2 flask. For the second split, cells were plated in three 75 cm^2 flasks and for the final split, cells were cultured in nine 75 cm^2 flasks. No more than three passages were performed to avoid loss of cellular proliferation potency and other characteristics, such as inability to differentiate into mature adipocytes.

2.3.3 Preadipocyte differentiation

5 x 10^4 to 10^5 white and brown preadipocytes were plated per well of 6-well plates. Two days after reaching 100% confluence, differentiation was initiated. The differentiation medium contained complete DMEM, insulin 5 μg/ml (Sigma-Aldrich, USA), dexamethasone 2 μg/ml (Sigma-Aldrich, USA), 0.5 mM 3-isobutyl-10methylxanthine (IBMX; Sigma-Aldrich, USA), 125 μM indomethacine (Sigma-Aldrich, USA) and 1 nM T3 (Sigma-Aldrich, USA). Fresh differentiation media was added every two days. On the 4th day, differentiation media contained complete DMEM, insulin 5 μg/ml and 1 nM T3 (Aune et al., 2013), which was changed every two days until day 8 or 10, depending on the maturation status of the adipocytes (numbers of lipid droplets accumulated).

2.3.4 CRH, UCN2, SU6656 and isoproterenol treatments

CRH (Bachem, USA) and UCN2 (Bachem, USA) 100 nM (Markovic et al., 2011; Punn et al., 2006) were added for 5 and 15 minutes in primary brown adipocyte cultures at the end of the differentiation process (day 8).

SU6656 5 μM (Cayman Chemical, USA) was added for 2 hours (Bastie et al., 2007) in primary brown adipocyte cultures at the end of the differentiation process (day 8).

Isoproterenol 0.1 μM (Sigma-Aldrich, USA) (Richelsen and Pedersen, 1987; Zhang et al., 2009) and SU6656 5 μM (Cayman Chemical, USA) were added in primary subcutaneous, epididymal and brown adipocytes at the end of the differentiation process (day 10) for 15 and 120 minutes, respectively.

2.4 mRNA quantification

2.4.1 mRNA isolation

Total RNA was isolated using Tri Reagent (Sigma-Aldrich, USA). 500 μl of reagent were used in a well of a 6-well plate and 1 ml was used for tissues (all volumes used below are applicable to 1 ml of Tri Reagent). Cells were homogenized using a 23G syringe and tissues were homogenized with the Tissue Master 125 homogenizer (OMNI International, USA). The homogenates were left on ice for 5 minutes before adding 200 μl of chloroform (Sigma-Aldrich, USA), followed by vortex for 15 seconds. Tubes were left on ice for 15 minutes and samples were centrifuged at 13,000 rpm for 20 minutes at 4^{o}C. To precipitate the isolated RNA, the upper aqueous phase was transferred in 500 μl of isopropanol (ApplichemGmbH, Germany) and stored at -80^{o}C for 20 minutes. Samples were then centrifuged at 13,000 rpm for 30 minutes at 4^{o}C and the pellet was washed with 500 μl of ice-cold 70% ethanol in DEPC water (Applichem GmbH,

Germany). Samples were centrifuged at 8,000 rpm for 10 minutes at 4^{o}C and two more washes followed. Pellet was left to air dry and was re-suspended in 20-100 µl of DEPC water.

2.4.1.1 Determination of mRNA amount

The isolated mRNA was quantified by measuring the absorbance at 260 nm using a Nanophotometer (Implen GmbH, Germany). The RNA quality was verified by assessing the A260/A280 ratio (with the nanophotometer), which was between 1.8 and 2.0.

2.4.2 DNase treatment of isolated mRNA

Genomic DNA was removed from the samples by using a DNaseI (RNase free) kit (Ambion, USA) according to the manufacturer's instructions. Briefly, 10x DNaseI buffer was added to 1x final concentration in the RNA sample and 1 µl of DNaseI (2 U) was used for up to 10 µg RNA. Samples were incubated at 37^{o}C for 30 minutes and DNaseI was deactivated at 75^{o}C for 10 minutes.

2.4.3 cDNA synthesis of isolated mRNA

Reverse transcription was performed using MMLV Reverse Transcriptase (Invitrogen, Carlsbad, USA). Up to 2 µg mRNA were used in the following reaction: 2 µg of mRNA in 6 µl of DEPC water were incubated with 2 µl of 0.3 µg/µl of random primers (Invitrogen, Carlsbad, USA) at 75^{o}C for 5 minutes. The mix was left to chill on ice for 5 minutes and 12 µl of mix B were added (Table 2.4). All samples were incubated at 42^{o}C for 45 minutes followed by 95^{o}C for 10 minutes and finally at 4^{o}C for 10 minutes.

Table 2.4: cDNA synthesis of mRNA using the MMLV Reverse Transcriptase. Volumes of reagents needed for cDNA synthesis.

Reagents for mix B	Volume in µl
5x First-Strand Buffer	4
dNTPs 5 mM	4
DTT 0.1 M	2
MMLV 200 U/µl	1
RNaseOUT™ Recombinant Ribonuclease Inhibitor 40 U/µl	1

2.4.4 Quantitative RT-PCR – SYBR® Green-based quantitative RT-PCR

2.4.4.1 Primer design

Primers for SYBR® Green-based quantitative RT-PCR were designed using the PrimerQuest Tool from Integrated DNA Technologies (IDT). The target sequence was obtained from PubMed nucleotide and the primer specificity was verified by making a BLAST search.

2.4.4.2 SYBR® Green-based quantitative RT-PCR (qRT-PCR) of mRNA

mRNA expression of genes shown on Table 2.5 were quantified using a SYBR Green-based quantitative RT-PCR. The *β-actin* and *cyclophilin* genes were used as housekeeping genes. *Cyclophilin* was a more suitable reference gene than *β-actin* or *GAPDH* for adipocytes undergoing differentiation (Zhang et al., 2014). *β-actin*, on the other hand, was stable in mouse tissues analyses (Lu et al., 2015). 15 µl of mastermix (Qiagen, United Kingdom) were mixed with 5 µl of cDNA diluted five times in distilled dH_2O and incubated using the following program: 50°C for 2 minutes, 95°C for 10 minutes and 40 cycles of 95°C for 15 seconds and 60°C for 60 seconds. In order to confirm a single PCR product, melting curve analysis was performed after the amplification of the PCR product.

Table 2.5: Primers for SYBR® Green qRT-PCR.

Primer	Sequence 5' - 3'	Amplicon size (bp)
Fyn	F: ACCTCCATCCCGAACTACAAC	135
	R: CGCCACAAACAGTGTCACTC	
UCP1	F: TCTTCTCAGCCGGAGTTTCAGCTT	86
	R: ACCTTGGATCTGAAGGCGGACTTT	
CIDEA	F: ATCACAACTGGCCTGGTTACG	136
	R: TACTACCCGGTGTCCATTTCT	
PRDM16	F: CAGCACGGTGAAGCCATTC	87
	R: GCGTGCATCCGCTTGTG	
ACO	F: TGCCTTTGTTGTCCCTATCCGTGA	191
	R: TTACATACGTGCCGTCAGGCTTCA	
Hadha	F: AGCAAGTGTTCAAAGGGCTGAACG	165
	R: TGTGCTTTACACCGAGGTCCTCAA	
DGAT2	F: GGCTACCTACCTCAGCTCTC	161
	R: CTGAAGCCAATGCACGTCAC	
FAS	F: CTCCGTGGACCTTATCACTA	201
	R: CTGGAGAGGTTGTAGTCAG	
PPARγ	F: CAGGCTTGCTGAACGTGAAG	117
	R: GGAGCACCTTGGCGAACA	
β-actin	F: CCCAGGCATTGCTGACAGG	141
	R: TGGAAGGTGGACAGTGAGGC	
Cyclophilin	F: CATCCTAAAGCATACAGGTCCTG	165
	R: TCCATGGCTTCCACAATGTT	

2.4.4.3 Analysis of qRT-PCR

The results were analyzed with the ΔΔCt method to calculate the fold mRNA expression compared to the basal treatment condition (Livak and Schmittgen, 2001). The following equations were used to calculate the relative quantity (RQ):

$$\Delta Ct = Ct_{(\text{gene of interest})} - Ct_{(\text{housekeeping gene})}$$

$$\Delta\Delta Ct = \Delta Ct_{(\text{sample})} - \Delta Ct_{(\text{control})}$$

$$RQ = 2^{-\Delta\Delta Ct}$$

In order to calculate the error, the following equation was used:

Positive error=$2^{-(\Delta\Delta Ct\text{-}SEM)}$-RQ

2.5 Protein quantification

2.5.1 Preparation of cellular protein lysates

Media were aspirated and cells were washed with ice-cold PBS (Gibco, USA). 100 μl of RIPA buffer (50 mM Tris-HCl pH 7.4, 1% NP-40, 0.5% Na-deoxycholate, 0.1% sodium dodecyl sulfate (SDS), 150 mM NaCl, 2 mM EDTA, dH_2O up to 500 ml) supplemented with 1% protease (Calbiochem, USA) and phosphatase inhibitor cocktail (Sigma-Aldrich, USA) were added per well (6-well plate). Cells were collected with cell scrapers and homogenization with a 23G syringe was performed. Lysates were kept on ice for 60 to 90 minutes. Samples were centrifuged at 13,000 rpm for 30 minutes at 4^{o}C. Supernatant was collected and stored at -80^{o}C.

2.5.2 Preparation of protein lysates from animal tissues

200 to 500 μl of RIPA buffer (same as above) supplemented with 1% protease (Calbiochem, USA) and phosphatase inhibitor cocktail (Sigma-Aldrich, USA) were added to the tissues. More specifically, 200 μl were used for BAT, 300 μl for subAT and epiAT and 500 μl for liver. Homogenization using the Tissue Master 125 homogenizer (OMNI International, USA) followed and lysates were kept on ice for 60 to 90 minutes. Samples were centrifuged at 13,000 rpm for 30 minutes at 4^{o}C. Supernatants were collected and stored at -80^{o}C.

2.5.3 Measurement of protein concentration

Protein concentration was determined using the Bradford assay (BIORAD, USA) according to manufacturer's instructions.

2.5.4 SDS loading buffer lysates

Protein samples were diluted in dH_2O to achieve a final concentration of 15-40 µg/µl. 5x SDS loading buffer (0.25 M Tris-HCl pH 6.8, 15% SDS, 50% glycerol, 0.01% bromophenol blue, 1:20 DTT, 10% β-mercaptoethanol) was added into the lysates. Samples were incubated at 95^{o}C in a heating block for 5 minutes.

2.5.5 Gel electrophoresis

2.5.5.1 Gel preparation

10% resolving gels (Table 2.6) and stacking gels were prepared. BIORAD instruments were used.

Table 2.6: Volumes for gel preparation.

Solution components (for 4 gels)	**Resolving gel**	**Stacking gel**
dH_2O	9.9 ml	8.9 ml
30% bis-acrylamide	8.3 ml	2.2 ml
1.5 M Tris-HCl pH 8.8	6.3 ml	-
1 M Tris-HCl pH 6.8	-	1.63 ml
10% SDS	0.25 ml	0.13 ml
10% ammonium persulfate	0.25 ml	0.13 ml
TEMED	0.01 ml	0.013 ml

2.5.5.2 Electrophoresis

Samples and markers (Pink protein ladder; Nippon Genetics Europe GmbH, Germany) were loaded onto the gel. Electrophoresis settings were as follows: 30 mA/gel for 90 to 120 minutes. The composition of the 10x running buffer was: 14.4 g Glycine, 30.2 g Tris base, dH_2O up to 1 l. 1x running buffer was supplemented with 0.1% SDS before use.

2.5.6 Immunoblotting

Proteins were transferred onto a nitrocellulose membrane (GE Healthcare Life Sciences, United Kingdom) for 75 minutes at 100 V using BIORAD instruments (wet transfer). The composition of the transfer buffer was 1x running buffer and 20% methanol.

2.5.7 Visualization of proteins – Enhanced Chemiluminescence (ECL) detection

Nitrocellulose membranes were blocked for 1 hour at room temperature with 5% milk (Regilait, France) in Tris-buffered saline (TBS 10x: 14 g Tris base, 60 g Tris-HCl, 87.5 g NaCl, dH_2O up to 1 l) containing 0.1% Tween 20 (Sigma-Aldrich, USA) (=TBS-T). Membranes were incubated with the primary antibody (Table 2.7) diluted in 5% milk in TBS-T overnight at 4^oC under continuous shaking. Membranes were washed three times with TBS-T before being incubated with the secondary antibody (horse anti-mouse IgG-HRP (Vector, USA) or goat anti-rabbit IgG-HRP (Millipore, USA)) diluted 1:5000 in 5% milk in TBS-T for 2 hours at room temperature. Membranes were visualized on film (Fuji Film, Greece) using ECL (ThermoFischer Scientific, USA). Signal intensities were quantified using an Image J software, normalized to GAPDH or β-tubulin signal intensities (Table 2.7). β-tubulin was used to normalize the results from the adipose tissues' lysates because GAPDH showed variability between groups (data not shown). β-tubulin was also used to normalize results from T37i cells, as previously published (Geerling et al., 2014). To re-probe the membranes, membranes were incubated in stripping buffer (75 ml dH_2O, 4.16 ml 1.5 M Tris-HCl pH 6.8, 20 ml 10% SDS, 700 μl β-mercaptoethanol) for 10 minutes at 58-60^oC and the blotting process was re-applied.

Table 2.7: Primary antibodies and dilutions used for immunoblotting.

Primary Antibody	Dilution
Fyn (sc-16 Santa-Cruz)	1:500
phospho-HSL (Ser 563; 4139 Cell Signaling)	1:500
UCP1 (ab10983 Abcam)	1:1000
phospho-Akt (Ser473; 9271 Cell Signaling)	1:1000
total Akt (9272 Cell Signaling)	1:1000
phospho-ERK1/2 (9106 Cell Signaling)	1:1000
total ERK1/2 (9102 Cell Signaling)	1:1000
GAPDH (AM4300 Ambion)	1:4000
β-tubulin (2146 Cell Signaling)	1:1000

*****The Fyn BD antibody produced two bands (Figure 3.1).

2.6 Oil Red O (ORO) staining

ORO stock solution: 0.5% (w/v) ORO (Sigma-Aldrich, USA) in isopropanol.

ORO working solution (freshly prepared): 60% ORO stock solution in dH_2O, filtered with Whatman filter paper (Whatman, United Kingdom).

ORO staining was used to visualize the lipid droplets accumulated in adipocytes. The protocol used was as follows: cells were fixed in 10% formalin for 15 minutes, washed three times with PBS, rinsed with 60% isopropanol to remove residual aqueous solutions, stained with freshly prepared ORO for 30 minutes, rinsed with 60% isopropanol to remove excess ORO stain and washed with PBS. The stained cells were stored with PBS at 4^o C until microscopy was performed.

2.7 Microscopy

ORO stained adipocytes were visualized with a bright-field microscope (Leica) and images were taken with the LAS imaging software. Scale bars were added with the Image J software.

Unstained adipocytes were visualized, when in culture, with a bright-field stereoscope (Leica) and images were taken with a digital camera (Nikon).

2.8 Statistical analysis

Data were analyzed and graphs were prepared using the GraphPad Prism 5 software. Experiments with the T37i cell line were repeated independently three times to allow statistical analysis. Depending on the design of the experiment, comparisons among treatment groups were made using Student's t-test (when comparing two groups), 1-way or 2-way ANOVA (when comparing more than two groups) to test for statistical significance. In case of ANOVA analysis, Bonferroni post-test analysis was applied to perform multiple comparison tests. These parametric tests were based on the assumption of normally distributed data. To fulfill this requirement, data of qRT-PCR were log-transformed prior to analysis. To perform parametric tests with small sample numbers, it is important that the measured samples are representative of the population. Small sample size is only reasonable under the assumption that the variability within the population is small.

Chapter 3

Regulation of Fyn kinase in *Crh*-deficient mice

I investigated whether the lack of *Crh*, using the *Crh* knockout (KO) mouse, affected Fyn expression/function in various tissues that are implicated in metabolic processes. *Crh* KO mice are a suitable tool in my experimental design due to impaired hypothalamo-pituitary-adrenal (HPA) axis, which affects behavioural responses to stressful stimuli (Bale and Vale, 2004) and is characterized by glucocorticoid insufficiency (Muglia et al., 1995). Further, behavioural studies using *Fyn* KO mice (Belzung and Griebel, 2001) and glucocorticoid treatment studies measuring the effects on Fyn expression (Harr et al., 2010) suggested that Fyn kinase may be regulated by the HPA axis. Therefore, I studied male wild-type (WT) and *Crh* KO mice (3 months of age). Although lack of *Crh* does not seem to affect the female to male ratio, females were excluded from this study as hormonal changes more predominant in females can affect fat accumulation, deposition and utilization, and food intake (Wade and Gray, 1979). Mice were maintained *ad libitum* (standard diet and ambient temperature are defined as normal conditions). *Crh* KO mice are glucocorticoid insufficient (Muglia et al., 1995), therefore, they were also supplemented with corticosterone in their drinking water. I also examined whether metabolic challenges, such as cold exposure, which has been shown to increase glucocorticoid production (Harper and Austad, 2000; Karp, 2012) or induced lipolysis, which mobilizes fatty acids similarly to the catabolic role of glucocorticoids, could alter Fyn expression, as Fyn is involved, at least partly, in energy homeostasis regulation (Bastie et al., 2007; Yamada et al., 2010). Therefore, I examined the effects of a cold challenge (4^{o}C) or a combination of cold exposure and glucocorticoid replacement in the *Crh* KO mice. Lastly, I investigated the effects of intraperitoneal injections of isoproterenol, a lipolytic agent, on lipolytic processes in

these mice. Subcutaneous (subAT), epididymal (epiAT) and brown (BAT) adipose tissues, spleen and liver were harvested.

3.1 Determination of Fyn expression under normal conditions

Fyn protein expression in WT and *Crh* KO white and brown adipose tissues as well as in spleen and liver is shown in Figure 3.1. Fyn was significantly reduced in the spleen, while other tissues did not show any change in Fyn protein expression. The latter did not exclude an effect from global *Crh* deficiency on Fyn kinase activity, which was not measured in this study and could differ between genotypes.

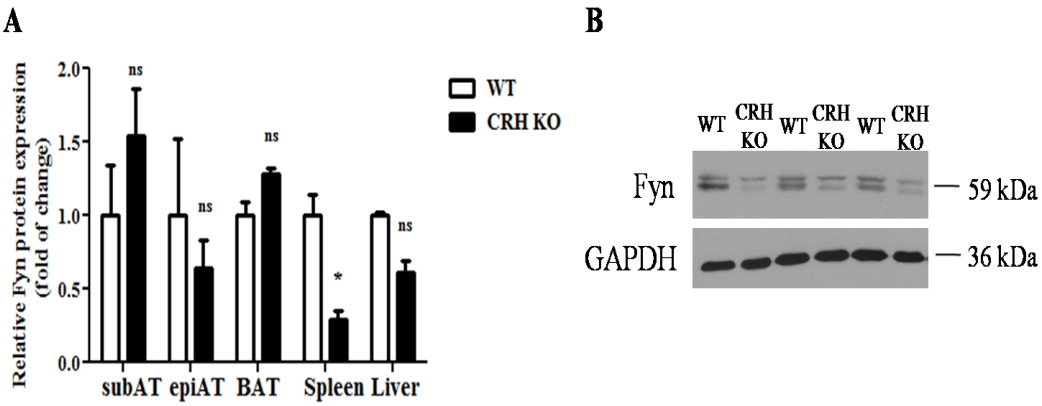

Figure 3.1: Levels of Fyn protein expression in subcutaneous, epididymal and brown adipose tissues, spleen and liver. (A) Fyn results are shown, normalized to β-tubulin, except for the spleen samples, which were normalized to GAPDH. (B) Fyn and GAPDH immunoblots for spleen. (Representative immunoblots for the other tissues are shown in Fig. 3.12). 40 µg of lysate were used for subAT, epiAT and spleen, whereas 25 µg were used for BAT and liver. Data are expressed as mean values ± SEM, n=4 for WT samples, n=3 for *Crh* KO samples, t-test: * $p<0.05$, ns=not significant.

3.2 Glucocorticoid replacement and/or cold exposure reduces *Fyn* expression

Crh KO mice are glucocorticoid insufficient (Muglia et al., 1995). Corticosterone supplementation in *Crh* KO mothers increases blood levels of corticosterone and secures the survival of the litters (Muglia et al., 1995). In models of glucocorticoid deficiency, such as the *Pomc* (pro-opiomelanocortin) knockout mice (Coll et al., 2005), glucocorticoid replacement (GR) successfully restored blood levels. Therefore, it is considered that corticosterone supplementation at a final concentration of 20 μg/ml in the drinking water of *Crh* KO mice normalized blood levels to those found in WT control animals. ELISA tests determined corticosterone levels and confirmed that although baseline (=no supplementation) *Crh* KO blood levels were significantly decreased compared to WT, after supplementation corticosterone levels were restored (Karaliota et al., unpublished data). This was evident from the first 24 hours of GR and remained stable throughout the experiment (11 days).

To measure the effects of GR on *Fyn* expression, mice were sacrificed after 11 days of GR. Just like glucocorticoids enhance thermogenesis in BAT (Soumano et al., 2000; Viengchareun et al., 2001), cold exposure has been reported to induce BAT thermogenesis (Gasparetti et al., 2003; Lim et al., 2012) and mobilize fat stores in white and brown adipose tissues. Therefore, in order to examine mice under this metabolically challenging condition, WT and *Crh* KO mice were placed at 16^{o}C for 24 hours in order to acclimatize them (Lim et al., 2012) before being placed at 4^{o}C for additional 24 hours. They were also supplemented with corticosterone or sterile tap water in order to specifically investigate the absence of *Crh*, independently of the effects due to the lack of glucocorticoids. I did not observe any differences in *Fyn* mRNA expression between WT and *Crh* KO mice under normal conditions (Figures 3.2-1A, B, C and 3.2-2E, two first columns). Consistently with protein expression (Figure 3.1), *Fyn* mRNA levels

were only significantly reduced in the spleen of *Crh* KO mice, compared to control animals (Figure 3.2-2D).

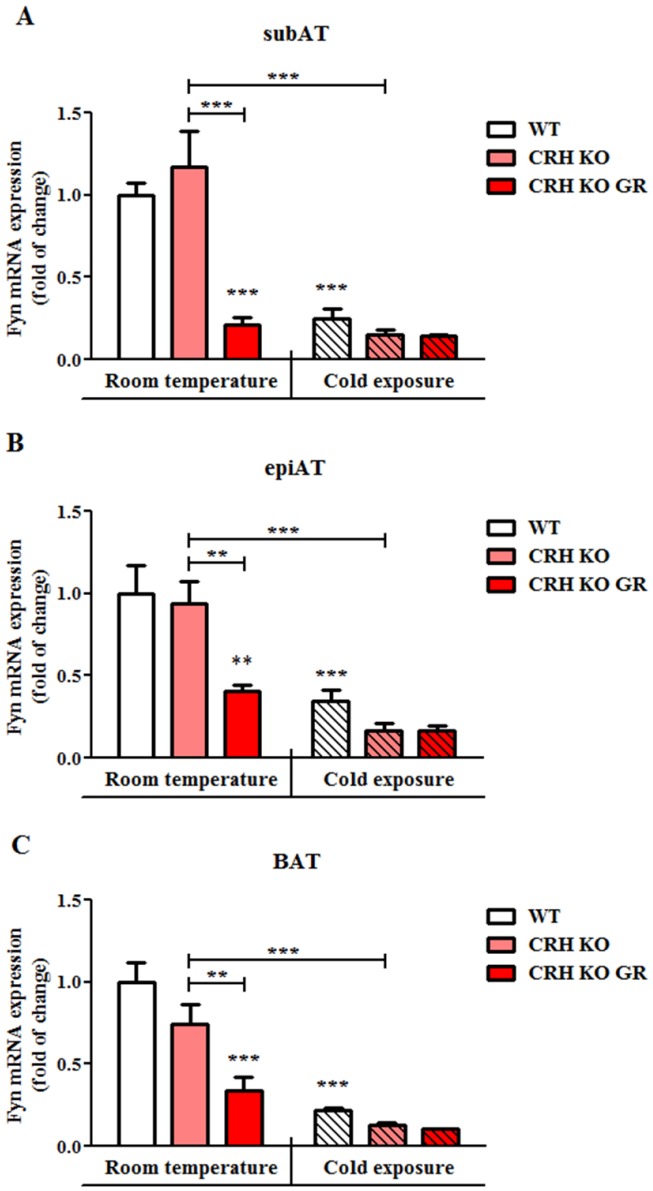

Figure 3.2-1: *Fyn* mRNA expression after glucocorticoid replacement and/or cold exposure. WT and *Crh* KO mice were either i) maintained under standard conditions (*ad libitum* access to chow diet and ambient temperatures), or ii) supplemented with corticosterone for 11 days or iii) were maintained at 4°C (cold challenge) for 24 hours with or without corticosterone. Mice were fasted for 3 hours prior to sacrifice and subAT (A), epiAT (B) and BAT (C) were dissected. Quantitative RT-PCR was performed for *Fyn* and results were normalized to *β-actin*. GR=glucocorticoid replacement. Data are expressed as mean values ± positive error, n=4 for WT room temperature (RT), *Crh* KO RT and *Crh* KO cold, n=3 for *Crh* KO GR RT, n=5 for WT cold and n=2 for *Crh* KO GR cold, 2-way ANOVA with Bonferroni post-test: * $p<0.05$, ** $p<0.01$, *** $p<0.001$. Data are normalized to WT RT and the statistical analysis has been performed to the control, WT RT, unless otherwise stated by solid lines.

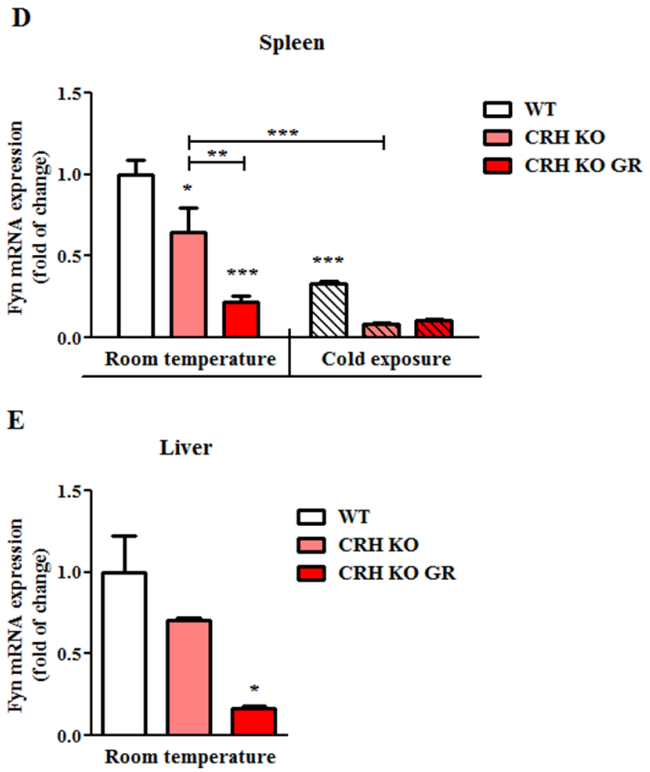

Figure 3.2-2: *Fyn* mRNA expression after glucocorticoid replacement and/or cold exposure. Similar description as in Figure 3.2-1. Spleen (D) and liver (E) were dissected.

Interestingly, across all tissues investigated, corticosterone supplementation significantly decreased *Fyn* expression levels in *Crh* KO (Figures 3.2-1 and 3.2-2), suggesting that a CRH-dependent mechanism controlled *Fyn* expression. In addition, cold exposure significantly decreased *Fyn* levels in WT and *Crh* KO mice. Reduction was also measured for the glucocorticoid replaced *Crh* KO tissues after cold exposure compared to *Crh* KO GR at room temperature and these levels were similar to *Crh* KO cold exposed mice, indicating that this effect was independent of glucocorticoid replacement.

3.3 Fyn regulates adipogenesis in the T37i brown preadipocyte cell line

Although Fyn protein levels did not appear to be affected by the lack of *Crh* in mice when animals were maintained in neutral conditions, I uncovered that conditions that typically activate thermogenesis, such as glucocorticoid treatment (Soumano et al., 2000; Viengchareun et al., 2001) or cold exposure (Gasparetti et al., 2003; Lim et al., 2012), dramatically affected *Fyn* expression in control mice and this was enhanced by the lack of *Crh*. Interestingly, I observed that *Crh* KO mice had increased browning characteristics in white adipose tissue depots, particularly in the subcutaneous depot (Figure 3.3) (Karaliota et al., unpublished data). Therefore, I investigated whether Fyn and differences of Fyn expression in BAT, the main tissue for thermogenesis, could affect BAT function.

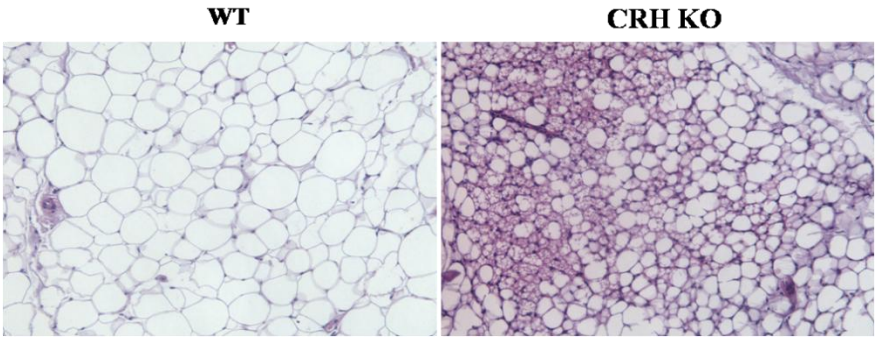

Figure 3.3: Browning of *Crh* KO subcutaneous white adipose tissue. Hematoxylin and eosin staining of WT and *Crh* KO subcutaneous fat pads. Representative images using a bright-field microscope with 10x magnification. (Taken from Karaliota et al., unpublished data)

The evolutionary advantage of the appearance of BAT in mammals has been previously discussed (chapter 1). One of the functions of this highly specified organ is to produce energy from food in the form of heat, a process known as thermogenesis. Major role in the process plays uncoupling protein 1 (UCP1), which functions as a mitochondrial proton translocator, uncoupling β-oxidative phosphorylation and ATP production, resulting in heat release. All mechanisms that induce lipolysis in brown

adipocytes also induced thermogenesis, and no thermogenesis can be evoked without simultaneously evoking lipolysis (Cannon and Nedergaard, 2004). This pathway has been discussed in the general introduction (chapter 1). The genetic switch that determines the formation and function of brown adipocytes, originating from a progenitor that expresses the myoblast marker *myf-5*, is PRD1-BF-1-RIZ1 homologous domain-containing protein 16 (*Prdm16*) (Seale et al., 2008). The presence of PRDM16 causes significant up-regulation of BAT molecular signature genes, such as *Ucp1* and cell death activator-A (*CideA*). The expression of PRDM16 in subcutaneous adipose tissue regulates a functional thermogenic program (Seale et al., 2011), thus pointing to a conserved mechanism that controls brown adipocyte development.

I first investigated how variations of Fyn expression affected the differentiation of the brown preadipocyte cell line, T37i. T37i cell line derived from a hibernoma (malignant brown adipose tissue tumour) of the transgenic mouse founder 37 carrying a hybrid gene composed of the human mineralocorticoid receptor (MR) proximal promoter fused to the SV40 large T antigen (Zennaro et al., 1998). These cells are capable of differentiating into mature brown adipocytes after exposure to insulin and triiodothyronine (T3). Normally, their characteristics resemble the ones of mature brown adipocytes: multilocular intracytoplasmic lipid droplets and specific adipogenic gene activation (Penfornis et al., 2000), which includes *Ucp1*, peroxisome proliferator-activated receptor γ *(PPARγ)*, lipoprotein lipase *(LPL)*, adipocyte-specific fatty acid binding protein 2 *(aP2)* (Buyse et al., 2001; Penfornis et al., 2000; Viengchareun et al., 2002; Zennaro et al., 1998).

To investigate the role of Fyn in these cells, Fyn was either inhibited using a pharmacological inhibitor, the SU6656 (Blake et al., 2000), or silenced using siRNA technology in these cells. Differentiation processes were assessed by quantitative RT-PCR of differentiation markers and by visualization of lipid accumulation using Oil Red O staining.

Figure 3.4 shows representative images of T37i cell differentiation. Staining of triglycerides stored in the droplets using Oil Red O, which gives a typical red color, assessed differentiation. As expected, no staining was observed in undifferentiated cells (day 0). Two days after initiation of differentiation, cells had a globular morphology but did not display lipid accumulation (not shown). At day 6 of differentiation, clusters of differentiated cells were identified. These clusters became predominant at day 8, as cells accumulated lipids. Additionally, the number of droplets per cell had increased, as visualized by the red color. More than 70% of the cells contained lipids at day 10 and they reached 80% at day 12.

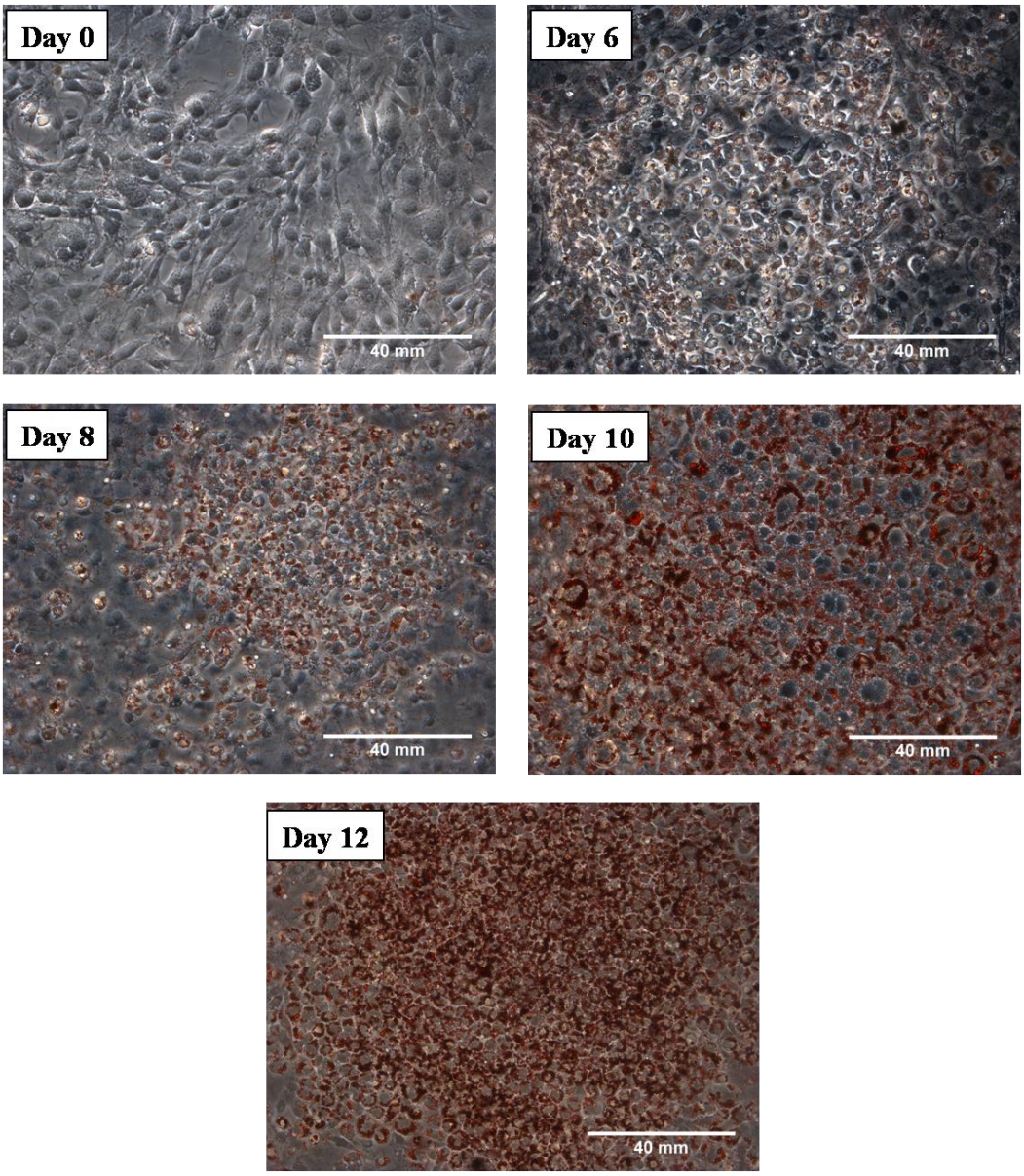

Figure 3.4: Oil Red O staining of T37i cells during differentiation. Cells were induced to differentiate to mature brown adipocytes. At days 0, 6, 8, 10 and 12, cells were washed with PBS, fixed in 10% formalin and stored at 4^{o}C with PBS until the Oil Red O staining was performed for all plates. Representative images are shown. Images were taken using a bright-field microscope (Leica) with 20x magnification. Scale bar is 40 mm.

As shown in Figure 3.5, cell differentiation was not associated with changes in Fyn protein levels. However, blocking Fyn activity using the specific Fyn inhibitor SU6656 resulted in reduced differentiation (Figures 3.6, 3.7-1, 3.7-2 and 3.7-3), therefore and although Fyn activity was not directly measured, it is likely that Fyn

activity played an important role in brown adipose tissue differentiation. As shown in Figure 3.6, DMSO had no effect on cell differentiation (as visualized by accumulation of lipid droplets); in contrast, cells treated with the Fyn inhibitor showed a reduced number of lipid-containing cells, suggesting impaired differentiation.

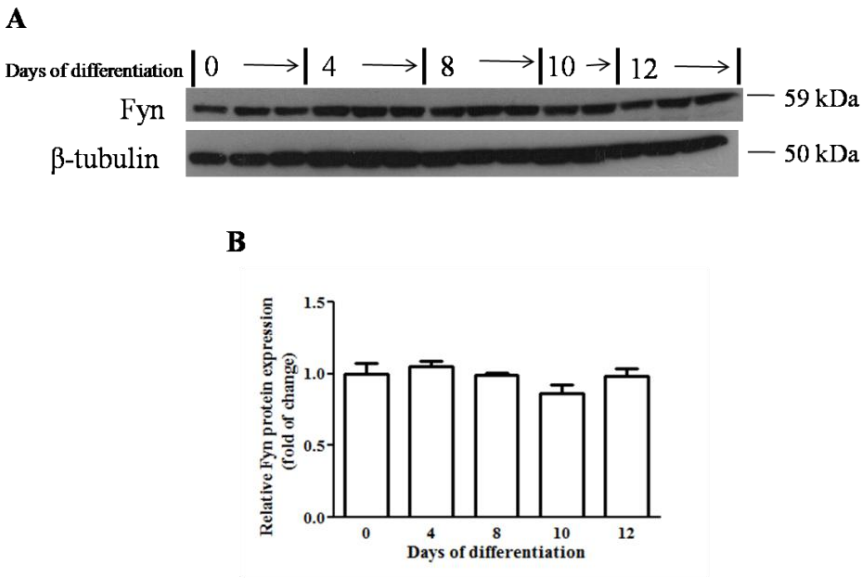

Figure 3.5: Levels of Fyn protein expression during differentiation of T37i cells. Cells were collected at days 0, 4, 8, 10 and 12, and Fyn immunoblots are shown (A). Results were normalized to β-tubulin (B). 20 μg of lysate were used. Data are expressed as mean values ± SEM, n=3 except for samples from day 10 n=2, 1-way ANOVA with Bonferroni post-test: the results are not significantly different.

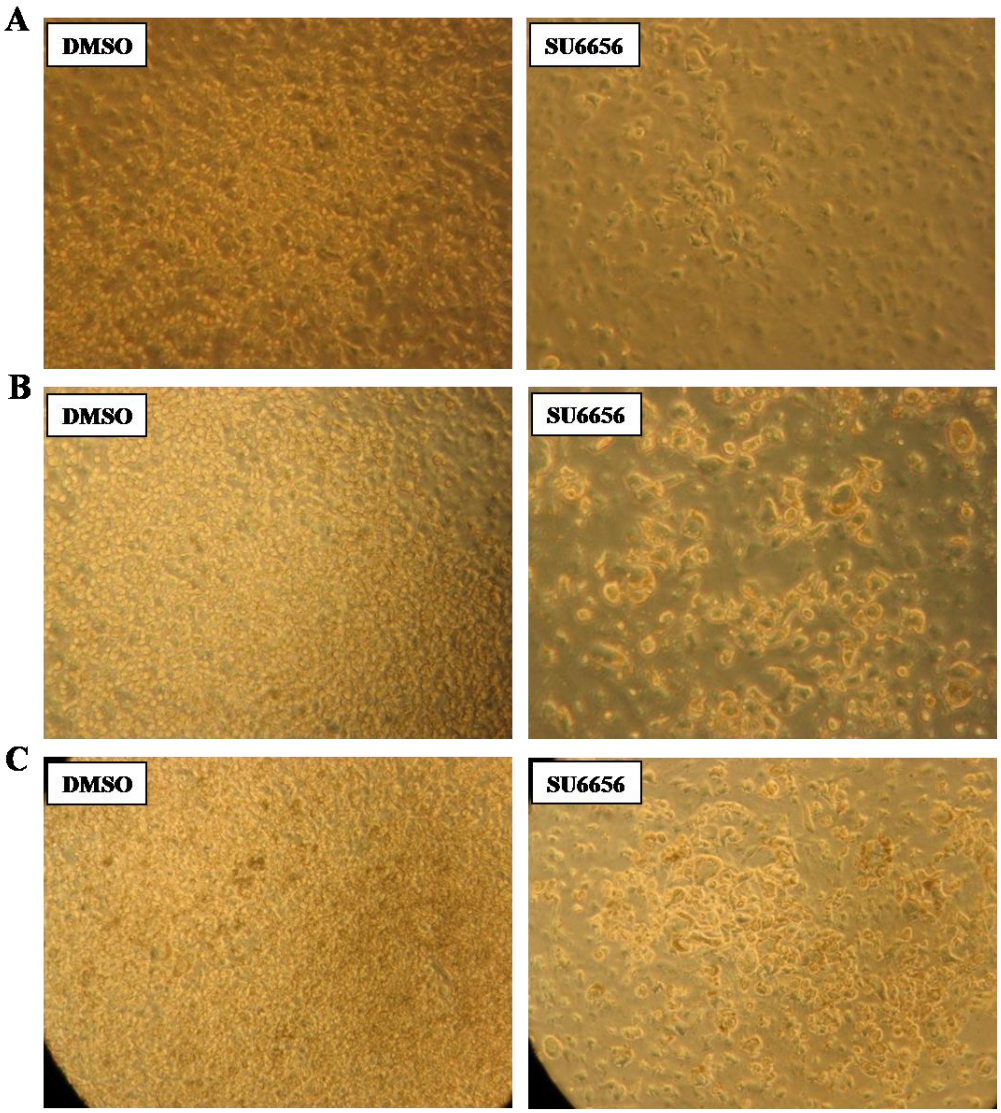

Figure 3.6: SU6656 inhibits the differentiation of T37i cells. From the beginning of differentiation, cells were treated either with DMSO (control cells) or SU6656 10 μM. Representative images are shown from cells in culture. Images were taken using a bright-field stereoscope at (A) day 5, (B) day 9 and (C) day 11 with 10x magnification.

The impaired differentiation of T37i cells treated with SU6656 was also evident in gene analysis experiments by using quantitative RT-PCR from cells collected at the undifferentiated state (day 0) and fully differentiated cells (day 11) (Figures 3.7-1, 3.7-2 and 3.7-3). Differentiation markers specific for brown adipocytes, such as *Ucp1* (Figure 3.7-1A), *CideA* (Figure 3.7-1B) and *Prdm16* (Figure 3.7-1C), were decreased (by 86%, 85%, 43%, respectively) in SU6656-treated cells compared to control cells, indicating

less thermogenic capacity of these cells. *Aco* (acyl-CoA oxidase; Figure 3.7-2D) and *Hadha* (hydroxyacyl-CoA dehydrogenase/3-ketoacyl-CoA thiolase/enoyl-CoA hydratase; Figure 3.7-2E) expressions were increased (5- and 1.5-fold, respectively), pointing to increased fatty acid oxidation. The expression of *Dgat2* (diglyceride acyltransferase 2; Figure 3.7-3F) and *Fas* (fatty acid synthase; Figure 3.7-3G) was slightly increased in SU6656-treated cells, which along with the unchanged levels of *Pparγ* (Figure 3.7-3H) suggested that although cells were not differentiating, cells were equipped to accumulate lipids. Taken together, these data point to fatty acid oxidation being predominant to lipid synthesis and storage in the SU6656-treated cells; and this could explain the lack of lipid accumulation in these cells.

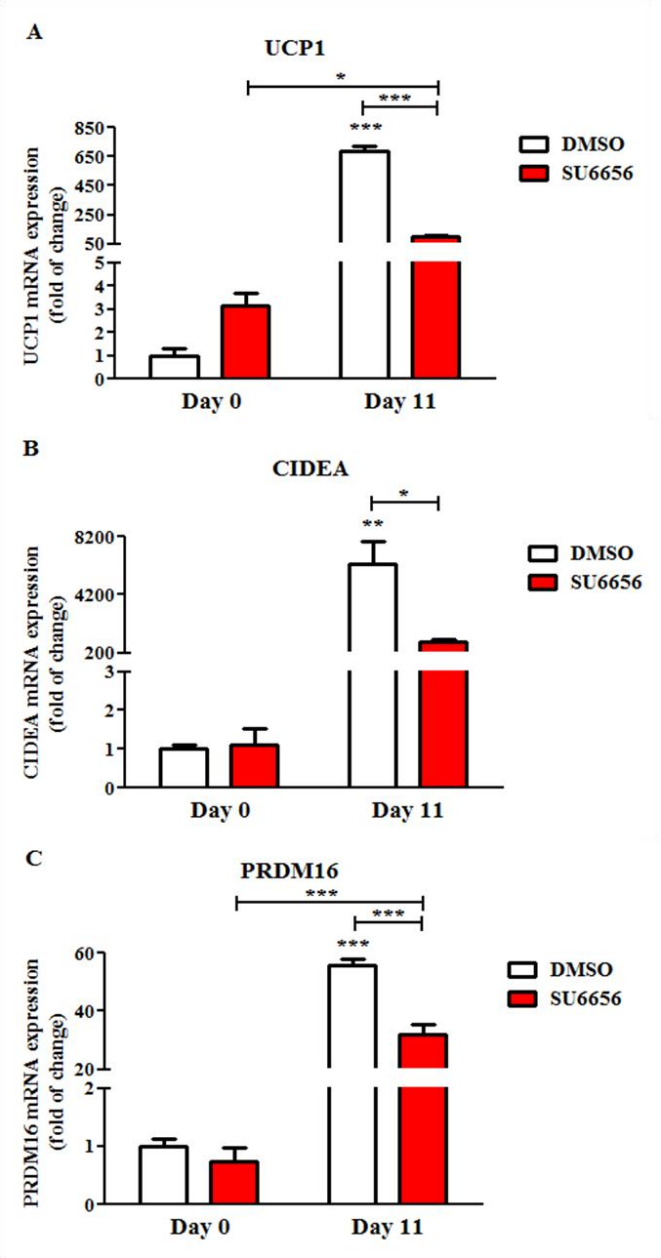

Figure 3.7-1: Effects of SU6656 on brown adipocyte markers' gene expression in T37i cells. From the beginning of differentiation, cells were treated either with DMSO (control cells) or SU6656 10 µM. Quantitative RT-PCR was performed for (A) *Ucp1*, (B) *CideA*, (C) *Prdm16* and results were normalized to *cyclophilin*. Data are expressed as mean values ± positive error, n=3, 2-way ANOVA with Bonferroni post-test: * $p<0.05$, ** $p<0.01$, *** $p<0.001$. Data are normalized to control cells at day 0 and the statistical analysis has been performed to the control cells at day 0, unless otherwise stated by solid lines.

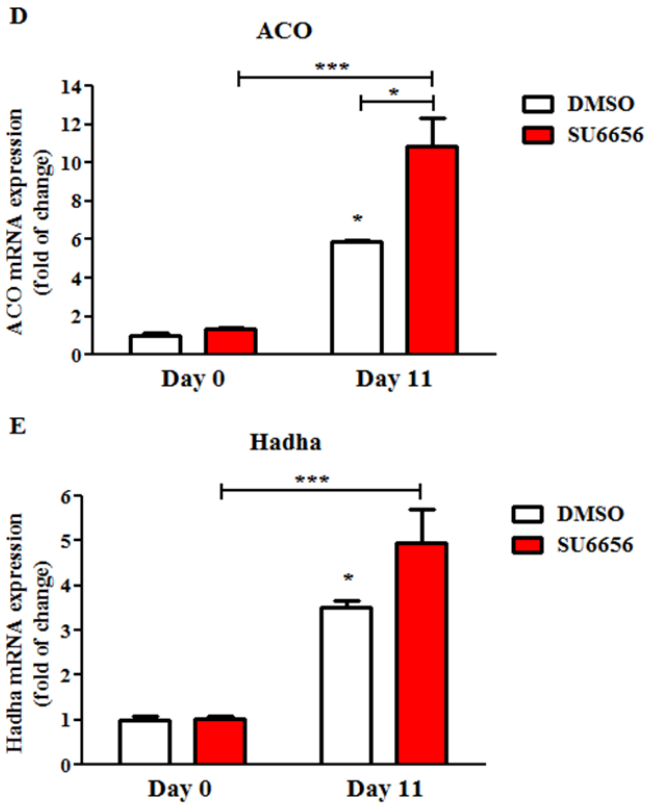

Figure 3.7-2: Effects of SU6656 on fatty acid oxidation markers' gene expression in T37i cells. Similar description as in Figure 3.7-1. Quantitative RT-PCR was performed for (D) *Aco* and (E) *Hadha*.

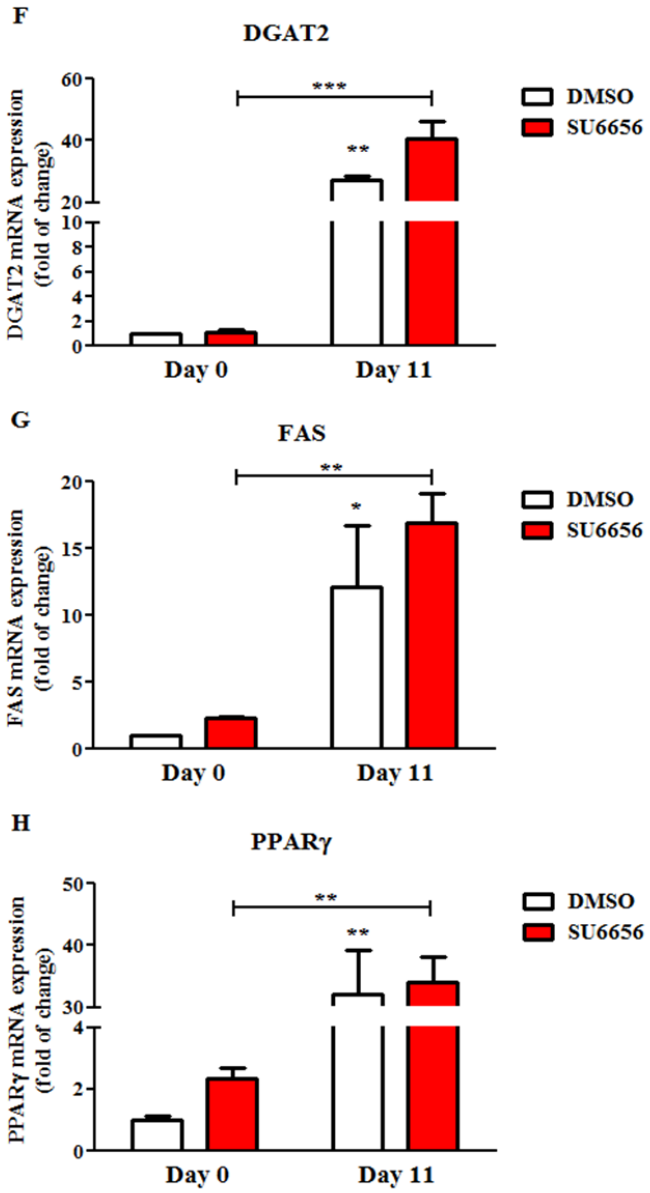

Figure 3.7-3: Effects of SU6656 on lipid storage and synthesis markers' gene expression in T37i cells. Similar description as in Figure 3.7-1. Quantitative RT-PCR was performed for (F) *Dgat2*, (G) *Fas* and (H) *Pparγ*.

Because there is always a risk of off-target effect of pharmacological inhibitor, I next investigated the effect of *Fyn* deletion in T37i cells. For this, *Fyn* was knockdown in the T37i cells using the siRNA technology (gift from Dr Elena Tarabra, Albert Einstein, NY, USA).

As evident in Figure 3.8, *Fyn* was successfully silenced in T37i cells, as *Fyn* mRNA expression was completely abolished (A) and Fyn protein expression was absent (B).

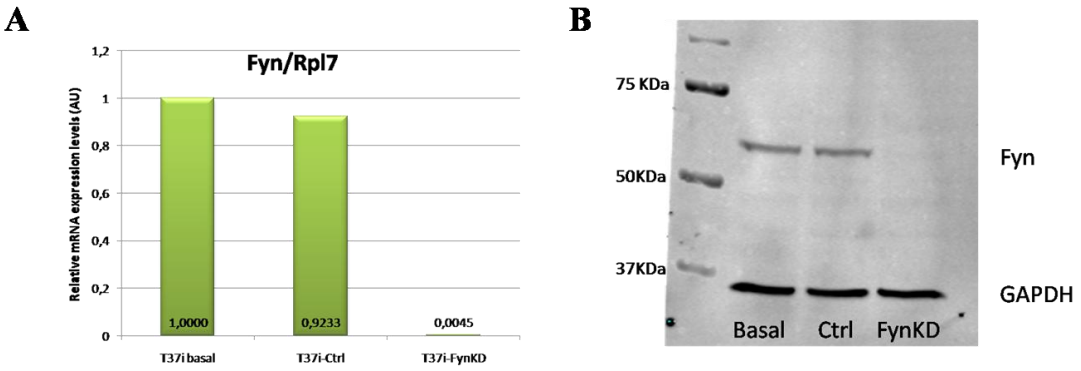

Figure 3.8: *Fyn* knockdown (KD) in T37i cells. *Fyn* was silenced with siRNA. (A) *Fyn* mRNA expression normalized to *Rpl7* using qRT-PCR in undifferentiated cells. (B) Immunoblot for Fyn normalized to GAPDH in untreated cells (=basal), in cells treated with the control siRNA (=Ctrl) and in Fyn KD cells without differentiation. (Tarabra's results)

I next investigated the differentiation processes in *Fyn* KD cells, compared to control cells. This was done by visualizing lipid droplets using Oil Red O (Figure 3.9) and by analyzing the main marker of BAT differentiation, *Ucp1* (Figure 3.10). Consistently with the data with the Fyn inhibitor, silencing *Fyn* in T37i cells resulted in blocking lipid accumulation (Figure 3.9) and a decrease in *Ucp1* expression (Figure 3.10).

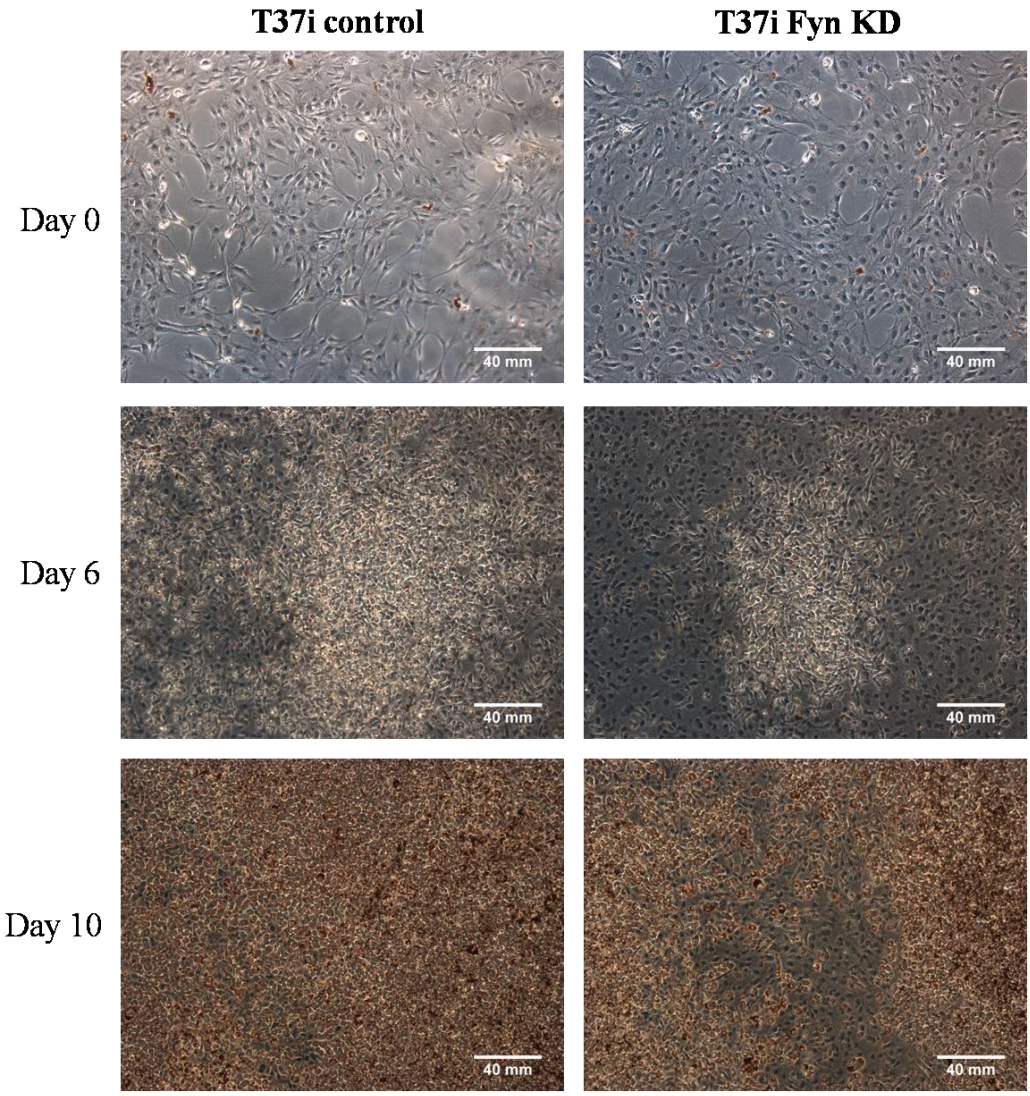

Figure 3.9: Oil Red O staining of T37i control and *Fyn* KD cells. Control and *Fyn* KD cells were induced to differentiate to mature brown adipocytes. At days 0, 6 and 8 cells were washed with PBS, fixed in 10% formalin and stored at 4^{o}C with PBS until Oil Red O was performed for all plates. Representative images are shown. Images were taken using a bright-field microscope (Leica) with 10x magnification. Scale bar is 40 mm.

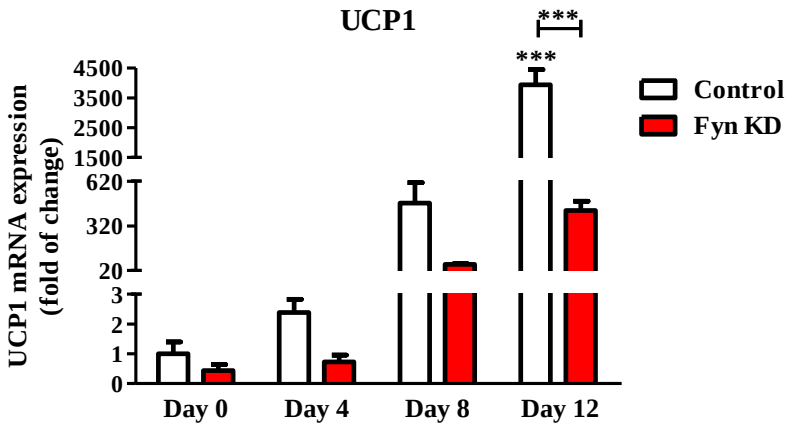

Figure 3.10: *Ucp1* mRNA expression in T37i control and *Fyn* KD cells. Cells were induced to differentiate to mature brown adipocytes and samples were collected at days 0, 4, 8 and 12. Quantitative RT-PCR was performed for *Ucp1* and results were normalized to *cyclophilin*. Data are expressed as mean values ± positive error, n=3, 2-way ANOVA with Bonferroni post-test: *** $p<0.001$. Data are normalized to control cells at day 0 and the statistical analysis has been performed to the control cells at day 0, unless otherwise stated by the solid line.

3.4 Isoproterenol increases lipolysis in the white adipose tissue of *Crh* KO mice

Lipolysis processes were investigated using intraperitoneal injection of isoproterenol, traditionally used for these purposes (Girousse et al., 2013; Lucas et al., 2003; Viswanadha and Londos, 2006). Isoproterenol was injected to mice (10 mg/kg) and phosphorylation levels of hormone-sensitive lipase (HSL), one of the major enzymes involved in lipolysis (chapter 1) were assessed in subAT, epiAT, BAT and liver after 10 minutes. HSL has five phosphorylation sites. Serine 563, serine 659 and serine 660 sites are PKA-dependent and increase the hydrolytic activity of HSL (Anthonsen et al., 1998); whereas phosphorylation of serine 565 by AMPK inhibits HSL phosphorylation at serine 563 resulting in reduced HSL activity (Anthonsen et al., 1998; Garton and Yeaman, 1990). ERK-dependent phosphorylation at serine 600 was also shown to increase phosphorylation at serine 563 (Greenberg et al., 2001), thus enhancing the hydrolytic activity and making this site important during hormonal stimulation, such as after insulin or isoproterenol administration. Levels of HSL phosphorylation at serine 563 were assessed by Western blot and results are shown in Figure 3.11.

Basal lipolysis was not significantly changed between WT and *Crh* KO tissues. Isoproterenol induced lipolysis in the subcutaneous (Figure 3.11A), epididymal (Figure 3.11B) and brown (Figure 3.11C) fat pads of WT and *Crh* KO mice. However, the response to isoproterenol in *Crh* KO was attenuated compared to WT and was abolished in BAT (Figure 3.11C). I did not observe any effects in liver (Figure 3.11D), consistently with the fact that this tissue is not a major site of lipolysis.

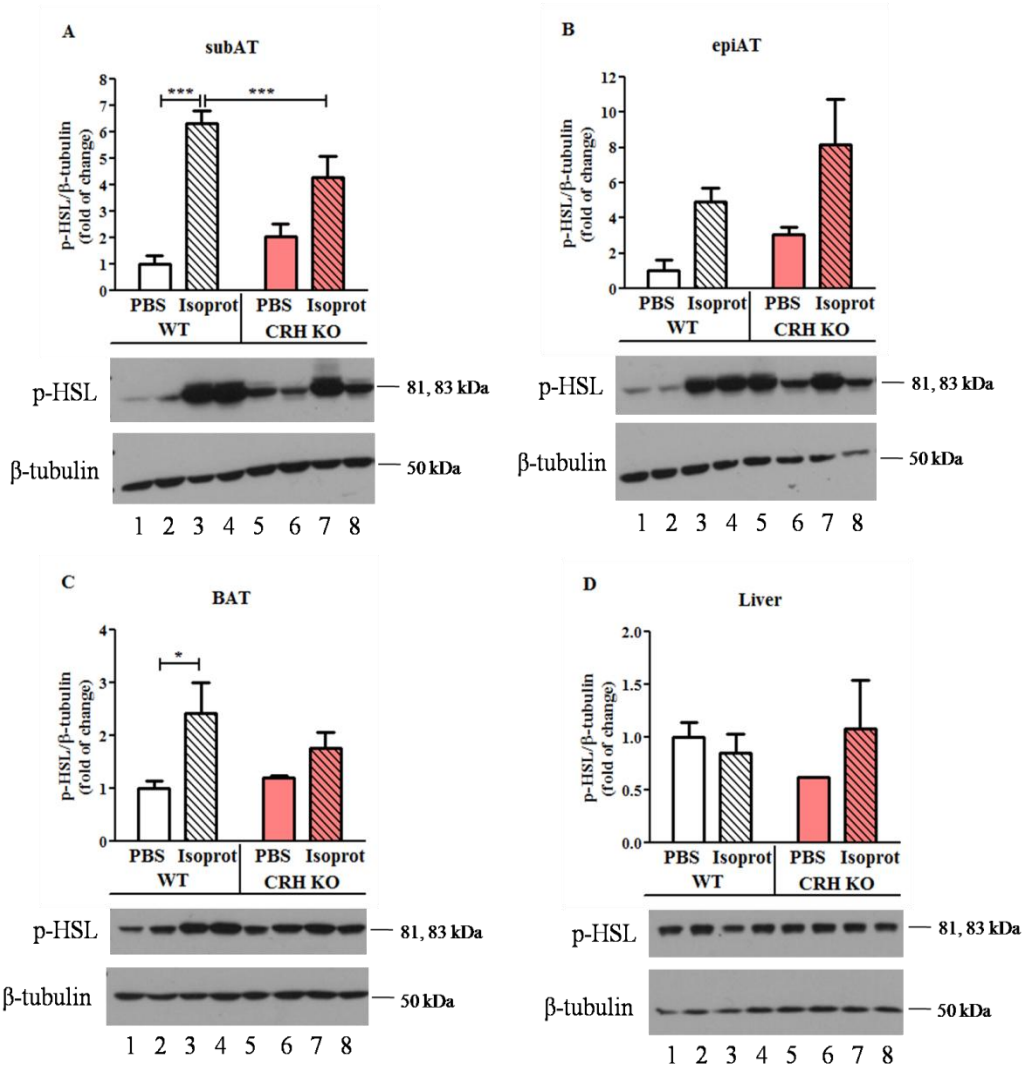

Figure 3.11: Levels of phospho-HSL expression in WT and *Crh* KO mice injected with PBS or isoproterenol 10 mg/kg. Mice were fasted for 3 hours before the injections and they were sacrificed 10 minutes after the injections. subAT (A), epiAT (B), BAT (C) and liver (D) were harvested. Immunoblots are shown for phospho-HSL and results were normalized to β-tubulin. 40 μg of lysate were used for subAT and epiAT, whereas 25 μg were used for BAT and liver. Data are expressed as mean values ± SEM, for subAT n=4 for WT PBS and WT isoprot, n=2 for *Crh* KO PBS and n=3 for *Crh* KO isoprot, for epiAT n=3 for WT PBS and *Crh* KO isoprot, n=4 for WT isoprot and n=2 for *Crh* KO PBS, for BAT n=4 for WT PBS and WT isoprot, n=2 for *Crh* KO PBS and n=3 for *Crh* KO isoprot, for liver n=4 for WT PBS, n=3 for WT isoprot and *Crh* KO isoprot and n=2 for *Crh* KO PBS, 2-way ANOVA with Bonferroni post-test: * $p<0.05$, ** $p<0.01$, *** $p<0.001$. Data are normalized to WT PBS and the statistical analysis has been performed to the control, WT PBS.

To test whether Fyn protein levels were altered or not after isoproterenol injection, immunoblots for Fyn were also performed (Figure 3.12). No differences were measured between the isoproterenol-treated and control groups and between genotypes.

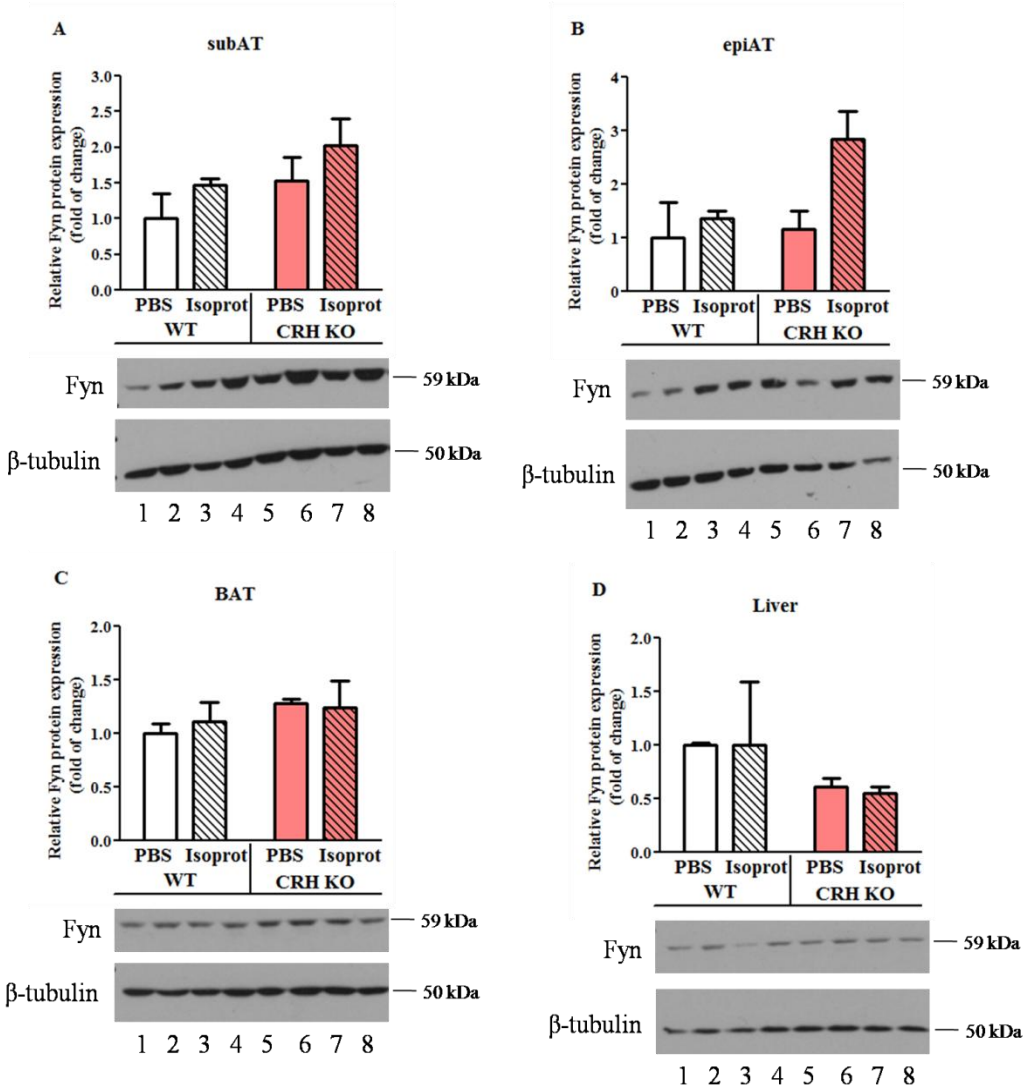

Figure 3.12: Levels of Fyn expression in WT and *Crh* KO mice injected with PBS or isoproterenol 10 mg/kg. Mice were fasted for 3 hours before the injections and they were sacrificed 10 minutes after the injections. subAT (A), epiAT (B), BAT (C) and liver (D) were harvested. Immunoblots are shown for Fyn and results were normalized to β-tubulin. 40 μg of lysate were used for subAT and epiAT, whereas 25 μg were used for BAT and liver. Data are expressed as mean values ± SEM, for subAT n=4 for WT PBS and WT isoprot, n=2 for *Crh* KO PBS and n=3 for *Crh* KO isoprot, for epiAT n=3 for WT PBS, WT isoprot and *Crh* KO isoprot and n=2 for *Crh* KO PBS, for BAT n=4 for WT PBS and WT isoprot, n=2 for *Crh* KO PBS and n=3 for *Crh* KO isoprot, for liver n=4 for WT PBS, n=3 for WT isoprot and *Crh* KO isoprot and n=2 for *Crh* KO PBS, 2-way ANOVA with Bonferroni post-test: the results are not significantly different. Data are normalized to WT PBS.

Isoproterenol increases BAT thermogenesis in rodents (Bachman et al., 2002) after binding to β-adrenergic receptors. However, in this study, as shown from UCP1 protein levels (Figure 3.13), I did not observe BAT thermogenesis activation. Possibly, the 10-minute treatment was not enough to stimulate UCP1 expression.

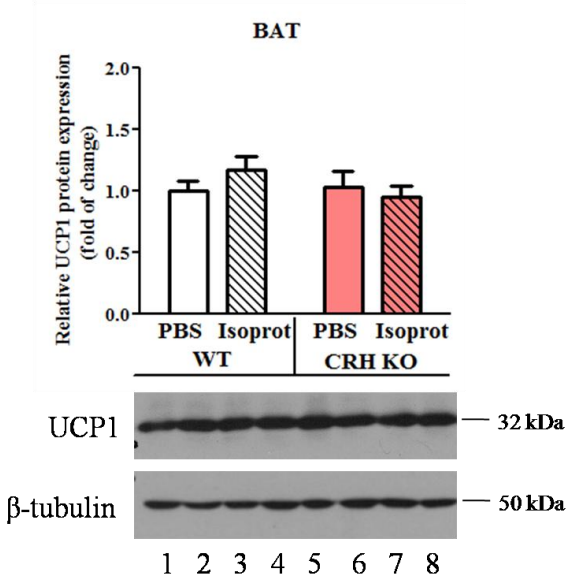

Figure 3.13: Levels of UCP1 expression in WT and *Crh* KO mice injected with PBS or isoproterenol 10 mg/kg. Mice were fasted for 3 hours before the injections and they were sacrificed 10 minutes after the injections. BAT was harvested. Immunoblots are shown for UCP1 and results were normalized to β-tubulin. 25 μg of lysate were used. Data are expressed as mean values ± SEM, n=4 for WT samples, n=2 for *Crh* KO PBS and n=3 for *Crh* KO isoprot, 2-way ANOVA with Bonferroni post-test: the results are not significantly different. Data are normalized to WT PBS.

3.5 Discussion

Extensive literature implicates the CRH family of peptides in whole-body metabolism. It is widely acknowledged that stress induces anorexia via CRH release (Kuperman and Chen, 2008). Other eating disorders, such as anorexia nervosa, can arise from HPA axis dysregulations (Rothwell, 1990). Studies that focused on injecting CRH centrally, either acutely (Rothwell, 1990) or chronically (Cullen et al., 2001; Rivest et al., 1989), unraveled the effects of CRH on both energy intake and energy utilization. Briefly, it is suggested that CRH decreases body weight gain (Bornstein et al., 1998; Brown et al., 1982; Buwalda et al., 1997; Krahn et al., 1990; Rivest et al., 1989; Rohner-Jeanrenaud et al., 1989) by reducing food intake (Arase et al., 1988; Krahn et al., 1990; Morley and Levine, 1982). On the other hand, CRH's effects on energy expenditure are mainly via activation of the sympathetic nervous system (Cullen et al., 2001). This includes stimulation of thermogenesis in BAT accompanied by increased expression of UCP1, induction of norepinephrine release and increase in heart rate and glucocorticoid release. Other reports claim that CRH does not only increase body temperature (Buwalda et al., 1997; Morimoto et al., 1993), but also transiently increases locomotor activity (Buwalda et al., 1997), explaining, at least in part, the effects of CRH on body mass. Infusions of UCNs, on the other hand, solely affect (reduce) food intake and do not increase sympathetic nervous system outflow as reported for CRH (Cullen et al., 2001; Seres et al., 2004).

Deficiency or overexpression of members of CRH family in mice presents intriguing metabolic phenotypes (discussed in chapter 1). These mice exhibit either normal weight (similar to control animals) and food intake or are leaner compared to controls. Additionally, they have distinct responses, such as different levels of insulin sensitivity, which are triggered upon metabolically challenging conditions, such as high-fat diet or stress (Table 3.1). Lastly, UCN2/CRHR2 modulate white adipose tissue development as they promote a brown-like (beige) phenotype compared to the white

characteristics driven by CRH/CRHR1 (Lu et al., 2015). The latter was also confirmed by *in vivo* studies using the *Crhr1* KO mice, which exhibit increased brown characteristics in WAT and BAT due to increased CRHR2 activity (Lu et al., 2015).

Preliminary evidence from the Karalis' lab, BRFAA, suggests that the *Crh* KO mice display a lean phenotype compared to their controls, characterized by reduced adiposity in all white (subcutaneous and epididymal) adipose pads (Karaliota et al., unpublished data). *Crh* KO mice have a higher metabolic rate (data accumulated from indirect calorimetry approach with metabolic cages), increased glucose tolerance and insulin sensitivity measured by intraperitoneal injections of glucose and insulin tolerance tests (GTT and ITT, respectively). The expanded and functional beige compartment in the subcutaneous adipose tissue (Figure 3.3), which promotes an enhanced thermogenesis due to increased *Ucp1* expression, is another characteristic of *Crh* KO mice. The aforementioned metabolic characteristics along with the lower activity, the increased energy expenditure and unchanged food intake compared to WT, make the *Crh* KO resistant to high-fat diet (HFD)-induced obesity.

Bastie et al. were the first to report the metabolic profile of the *Fyn* KO mice (Bastie et al., 2007). *Fyn* KO mice have reduced adiposity, accompanied by a reduction in adipocyte cell size. Although a recent publication (Tse et al., 2013) suggests contradictory results on the effect that causes the reduced adiposity, it is noteworthy that the first paper showed smaller adipocytes in the epididymal fat pad, whereas the second studied the subcutaneous depot and reported that the total number of adipocytes is reduced in *Fyn* KO mice compared to controls. *Fyn* KO mice also display reduced plasma and intra-tissue triglyceride and non-esterified fatty acid levels and improved glucose clearance associated with increased peripheral tissue insulin sensitivity (Bastie et al., 2007). Increased fatty acid oxidation in skeletal muscle and white adipose tissues and increased energy expenditure, resulted in a lean phenotype. Surprisingly, *Fyn* KO mice on HFD become obese but they remain glucose tolerant and insulin sensitive (Lee

et al., 2013). The latter, along with the preferential accumulation of fat within the subcutaneous rather than the visceral (epididymal) depot and the reduced inflammatory processes within the white depots protected *Fyn* KO mice from the deleterious effects of HFD. An overview of *Fyn* KO mouse's metabolic characteristics and a comparison to the metabolic phenotypes of various KO models with deficiency in genes of the CRH family of peptides is demonstrated in the table below (Table 3.1).

Table 3.1: Metabolic characteristics of *Fyn* KO and mice deficient in genes of the CRH family of peptides.

	Food intake	Weight gain	Glucose utilization	Insulin sensitivity	Energy expenditure	Lipid utilization	HFD	Stress
Fyn KO	N	↓	↑	↑	↑	↑	Insulin Sensitive	ND
UCN-I KO	ND	Normal size	ND	ND	ND	ND	ND	Impaired corticosterone response
UCN-II KO	N	N	↑	↑	ND	ND	Insulin sensitive	ND
UCN-III KO	N	N	ND	↑β cell secretion	ND	ND	Insulin sensitive	ND
CRH-R1 KO	N	Normal weight	N	↑	ND	ND	↓Weight gain, ↑lipid oxidation & insulin sensitive	Do not lose weight & low anxiety
CRH-R2 KO	N	N	N	N	ND	ND	Insulin sensitive no weight gain & ↑SNS activity	↓Food intake, ↑heat production & ↓fat stores

(N): Normal
(ND): Not determined

Strong evidence that supported the rationale to investigate Fyn function in *Crh* KO mice came from the direct regulation of β-oxidation by Fyn (Bastie et al., 2007) and the increased β-oxidation pathway in *Crh* KO mice (Karaliota et al., unpublished data). Secondly, under stressful conditions various mouse models lacking genes of the CRH family of peptides, such as *Crh receptor 1* KO, *Crh receptor 2* KO, *Crh* transgenic and

Crh binding protein KO mice (Bale and Vale, 2004), exhibit differential behavioural responses, whereas *Fyn* KO mice display increased anxiety under normal conditions (Belzung and Griebel, 2001). Lastly, an indirect association between CRH and Fyn was postulated by the glucocorticoid insufficiency of *Crh* KO mice (Muglia et al., 1995) and the direct down-regulation of *Fyn* by glucocorticoids (Harr et al., 2010), another linking point that Fyn is a target of the HPA axis.

Crh KO mice have been extensively studied for their responses under basal and stressful conditions. Although *Crh* KO mice exhibit adrenocortical atrophy (Muglia et al., 1995), they are capable of releasing small amounts of corticosterone under normal and stressful conditions, perhaps due to vasopressin which has been shown to act synergistically with CRH to augment ACTH release (Bale and Vale, 2004). However, this basal and stress-induced endocrine response is significantly blunted compared to WT mice (Bale and Vale, 2004). *Crh* KO mice exhibit normal anxiety to stressful stimuli, indicating that CRH is not required for these networks (Dunn and Swiergiel, 1999; Weninger et al., 1999a). *Fyn* KO mice, on the other hand, are characterized by anxiety and fear under normal conditions (Belzung and Griebel, 2001; Miyakawa et al., 1994).

Interestingly, glucocorticoids regulate, either directly or indirectly Fyn kinase expression at the mRNA and protein level. The direct effects have been studied in T lymphocytes where dexamethasone, a synthetic glucocorticoid, down-regulated *Fyn* expression (Harr et al., 2010). The indirect role of glucocorticoids on Fyn was studied in T cells providing evidence of the mechanism that is activated in order for glucocorticoids to exert their fast, non-genomic immunosuppressive effects on T cells. This indirect role appears when glucocorticoids break down the complex of TCR, Lck/Fyn, glucocorticoid receptor and heat-shock protein (Hsp) 90, necessary for T cell activation (Lowenberg et al., 2005; Lowenberg et al., 2006). In that way, the role of Fyn makes it a potential target for anti-inflammatory therapy as Fyn is tightly connected to

mediate TCR signalling (Palacios and Weiss, 2004). Furthermore, glucocorticoid effects on immune modulation are either complemented or antagonized by CRH. Particularly, CRH-induced activation of the HPA axis and the ensuing glucocorticoid release promote anti-inflammatory effects; whereas the peripherally expressed CRH, in various immune cells, enhance the inflammatory response (Karalis et al., 1991), thus indicating an antagonistic role of CRH to glucocorticoids.

This study aimed to investigate whether Fyn expression is under the same regulatory framework of interactions, as CRH and glucocorticoids. My research has provided evidence that Fyn may be unaffected by the global deficiency of *Crh*, associated with adrenal hypofunction and glucocorticoid deficiency, when mice were maintained at normal conditions. Both mRNA (Figures 3.2-1 and 3.2-2) and protein levels (Figure 3.1) were unchanged between WT and *Crh* KO mice in a number of metabolic tissues (white and brown adipose tissues and liver). There was one notable exception, the results from spleen, which are discussed below.

CRH has a complex role in immunity and inflammation. As discussed above, it has been shown that CRH not only attenuates inflammation through stimulation of glucocorticoid release (anti-inflammatory role), but also the peripherally expressed CRH acts as a pro-inflammatory mediator (Karalis et al., 1991). Due to *Crh* KO glucocorticoid insufficiency (Muglia et al., 1995) and the reported decrease of *Fyn* by glucocorticoids (Harr et al., 2010), I anticipated that *Fyn* expression in *Crh* KO spleens would be increased or maybe unchanged compared to WT spleens. Unexpectedly, Fyn expression was reduced in *Crh* KO spleens compared to WT (Figures 3.1 and 3.2-2D). Interestingly, this effect was greater when circulating corticosterone levels were normalized to the WT levels (Figure 3.2-2D). Published reports indicated that exogenous corticosterone administration caused reduction in splenic cell populations (Pruett et al., 2000). The latter in combination with the known down-regulation of *Fyn* expression by glucocorticoids (Harr et al., 2010), could support the greater effect of corticosterone on

Fyn expression in *Crh* KO spleens (Figure 3.2-2D). However, this does not exclude the requirement of performing experiments where the absolute numbers of splenocytes and major splenic cell populations should be counted after glucocorticoid replacement. Under normal conditions, it has been shown that naïve *Crh* KO spleens have increased cellularity compared to control spleens (Benou et al., 2005). This was also evident from my experiments, where *Crh* KO spleen weight was two times heavier compared to WT spleens (Figure 3.14A and B), even when spleen weight was normalized to body weight (Figure 3.14C; 30% increase). Further, splenic cell subpopulations (mostly T and B lymphocytes) were similarly distributed, in absolute numbers, in WT and *Crh* KO spleens (Benou et al., 2005). Overall, the reduced levels of Fyn in *Crh* KO spleens could not be a result of differences in major splenic cellular populations. Rather, it could depend on variations of other immune cells, like macrophages and dendritic cells.

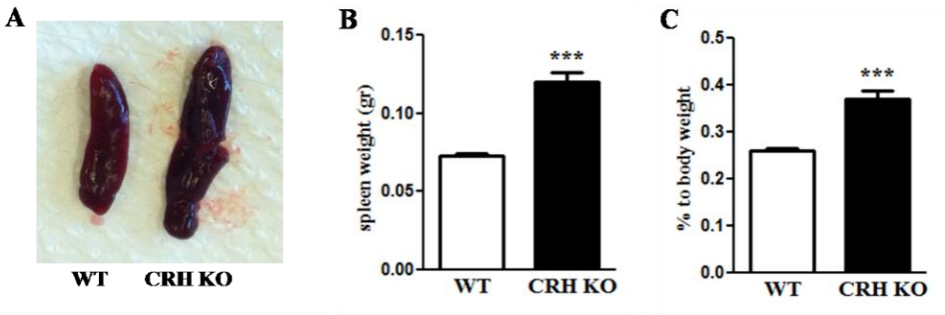

Figure 3.14: *Crh* KO spleen morphology. (A) Image of WT and *Crh* KO spleens. (B) WT and *Crh* KO spleen weights. (C) Spleen weight normalized to body weight. Data are expressed as mean value ± SEM, n=6, t-test: *** $p<0.001$.

Glucocorticoid replacement has been the preferred method to normalize blood levels in glucocorticoid deficient mice, like the *Pomc* knockout mice (Coll et al., 2005) or to restore the levels after adrenalectomy (Sterzer et al., 2004). A dose ranging from 10 to 30 μg/ml is needed for the survival of pups born from homozygous (*Crh* KO) parents (Muglia et al., 1995). The dose used in this study was 20 μg/ml and successfully replaced *Crh* KO mice (Karaliota et al., unpublished data) and secured survival of litters.

Because the effects of *Crh* deficiency on *Fyn* could be a result of the subsequent glucocorticoid insufficiency, I examined whether glucocorticoid replacement for 11 days could have altered *Fyn*. Notably, in all tissues examined, *Fyn* was decreased upon corticosterone delivery (Figures 3.2-1 and 3.2-2). This suggested that after normalization of corticosterone levels to the ones measured in WT mice, only *Crh* deficiency could have an impact on differences recorded. Therefore, this unmasked a CRH-dependent mechanism that positively regulated *Fyn*. However, it should be noted that since the levels of urocortins (UCNs) were not determined in this study, their involvement in the regulation of Fyn expression/activity cannot be excluded. It has been shown that deletion of *Crhr1* resulted in variable alterations in the expression of other peptides of the CRH family (Bale et al., 2002; Chen et al., 2004a). Additionally, a study using *Crhr1* KO mice, which are glucocorticoid insufficient (Smith et al., 1998), reported that UCN2 and CRHR2 were increased compared to WT littermates in WAT and BAT and that this effect was reversed after normalization of circulating corticosterone (Lu et al., 2015). This suggested that the UCN system could be altered due to deletion of *Crh*, as a compensatory mechanism, and that this could regulate Fyn expression. Therefore, it is essential to elucidate the expression levels of UCNs in the *Crh* KO mouse, under normal conditions and upon glucocorticoid administration, to determine whether CRH directly exerts its effects on Fyn or indirectly by inducing alterations in UCNs expression levels.

Initially thought to be present only in newborns, BAT was recently revealed in adults as well (Chatterton et al., 2002; Hany et al., 2002; Okuyama et al., 2002). It is active and responsive to cold or β-adrenergic treatment (Cypess et al., 2014; Cypess et al., 2009; Cypess et al., 2015; Nedergaard et al., 2007; Saito et al., 2009; van Marken Lichtenbelt et al., 2009; Virtanen et al., 2009). When exposed to cold, the sympathetic nervous system releases norepinephrine, which binds to β3 adrenergic receptors, activating the cAMP-PKA pathway leading to increased *Ucp1* expression in BAT and heat release (Figure 3.15). Activated PKA in turn phosphorylates lipases, such as HSL,

which translocates to lipid droplets (Figure 1.1) and begin the hydrolysis of stored lipids (lipolysis) (Zhang et al., 2016).

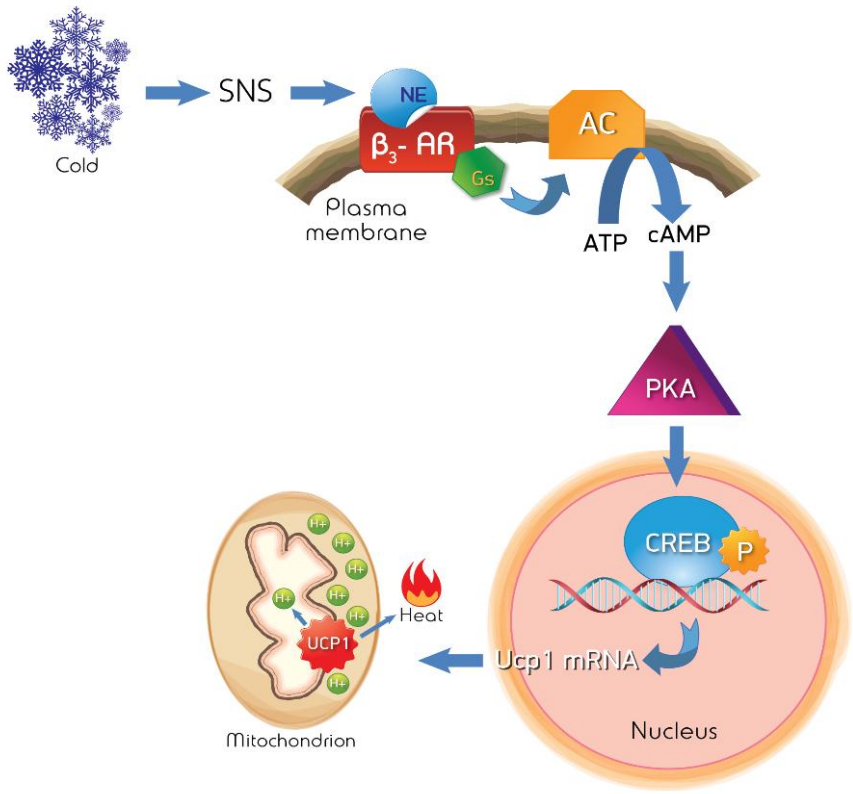

Figure 3.15: Norepinephrine stimulates heat release in brown adipocytes. A cold stimulus activates the SNS, which releases norepinephrine. Upon binding to its receptor, the β3-AR, and coupling to G_s proteins, the AC is activated and the cAMP-PKA pathway results in increased phosphorylation of CREB. Subsequent transcription of *Ucp1*, translation and translocation to the inner membrane of mitochondria, dissipates the proton gradient (H^+) and uncouples the oxidative phosphorylation from ATP synthesis and generates heat. SNS = sympathetic nervous system, NE = norepinephrine, β3-AR = β3-adrenergic receptor, AC = adenylyl cyclase, PKA = protein kinase A.

Growing evidence suggests that cold exposure *in vivo* induces browning in WAT (Loncar et al., 1988b; a; Loncar et al., 1986; Young et al., 1984). This accumulation of beige cells is reported mostly in the subcutaneous fat depots, whereas the epididymal fat is less prone to this "transdifferentiation" (Seale et al., 2011). The

critical component that recruits beige cells in the subcutaneous adipose tissue and is required for the normal adaptations to cold exposure, is fibroblast growth factor 21 (FGF21) (Fisher et al., 2012). Karalis group's studies in *Crh* KO mice showed a robust increase of beige cells numbers in the subcutaneous compartment, when mice were exposed to 4^{o}C accompanied by an increase in β-oxidation marker genes (Karaliota et al., unpublished data). My experiments had the expected outcome (Figures 3.2-1 and 3.2-2), that cold induced a significant reduction in *Fyn* levels due to the increased β-oxidation. The reported increase in glucocorticoid production after longer or shorter periods of exposure to cold (Harper and Austad, 2000; Karp, 2012) could act synergistically to the increased β-oxidation pathway, thus also reducing *Fyn* expression. The cold challenge produced similar results in the presence and absence of glucocorticoids in *Crh* KO mice, indicating a different regulation of *Fyn* at room temperature (22^{o}C) and at 4^{o}C.

The experimental conditions that I used to unravel the association between CRH and Fyn, i.e. glucocorticoid administration and cold exposure, are typical stimulators of BAT thermogenesis and of the ensuing UCP1 expression. Glucocorticoids down-regulate UCP1 (Soumano et al., 2000; Viengchareun et al., 2001), whereas cold temperatures enhance UCP1 expression (Gasparetti et al., 2003; Lim et al., 2012). However, the role of Fyn has not been elucidated in the regulation of BAT homeostasis. Therefore, I sought to determine whether Fyn expression or activity affected BAT thermogenesis. Although Fyn protein (Figure 3.1) and mRNA levels (Figures 3.2-1 and 3.2-2) were unchanged between WT and *Crh* KO BAT under neutral conditions, Fyn kinase activity was not assessed and hence it cannot be excluded that Fyn's activity differed between the genotypes. To evaluate whether Fyn expression or activity are important mediators in brown adipogenesis, I used the T37i brown preadipocyte cell line (Zennaro et al., 1998), which possesses typical characteristics of brown adipocytes (Buyse et al., 2001; Penfornis et al., 2000; Viengchareun et al., 2002; Zennaro et al.,

1998). Differentiation of T37i cells was normal as cells accumulated lipids (Figure 3.4). In addition, Fyn levels remained stable during the differentiation process (Figure 3.5), however, Fyn kinase inhibitor, SU6656, attenuated the differentiation of T37i cells, indicating that Fyn kinase activity was essential in this process. T37i cells treated with SU6656 did not accumulate lipids in the extent of control cells (Figure 3.6) and this was not due to defects in the lipid synthesis (Figure 3.7-3G and H) or lipid storage (Figure 3.7-3F) capacity of the cells. In fact, SU6656-treated cells had impaired thermogenic machinery (Figure 3.7-1A, B and C) accompanied by increased fatty acid oxidation markers (Figure3.7-2D and E), which could explain the inability to accumulate lipids in a physiological manner. The direct association between Fyn and fatty acid oxidation pathway has also been shown with *Fyn* KO mice, which have increased oxidation of lipids (Bastie et al., 2007).

To ensure that the pharmacological inhibition of Fyn in T37i cells was specific, I also used T37i cells where *Fyn* was silenced with the siRNA technology (*Fyn* KD cells). Similarly to the results obtained with SU6656, *Fyn* KD attenuated lipid accumulation (Figure 3.9) in T37i cells and *Ucp1* expression was decreased (Figure 3.10), indicating that Fyn kinase activity was an important regulator of brown adipogenesis. The role of Fyn in adipose tissue differentiation has been suggested (Sun et al., 2005; Tse et al., 2013), but only in white adipocytes. This study described a similar role in brown adipocyte differentiation.

The lipolytic agent, isoproterenol, is a non-specific β-adrenergic receptor agonist used both in rodent and human studies (Ricci et al., 2005), highlighting its role as a sympathomimetic, able to activate BAT thermogenesis. Much effort has been made in order to identify the exact mechanisms of isoproterenol-induced lipolysis. It has the ability to bind to β-adrenergic receptors and stimulate the cAMP-PKA pathway resulting in activation of ATGL and phosphorylation of HSL and the break down of stored lipids. The present study showed that *Fyn* expression was unaffected by isoproterenol exposure

(Figure 3.12), at least for the 10-minute treatment that was performed, which is a time-point traditionally used when studying isoproterenol-induced lipolysis (Girousse et al., 2013; Lucas et al., 2003). Lipolysis, on the other hand, measured by phosphorylation levels of HSL at serine 563, was highly induced in subcutaneous (Figure 3.11A) and epididymal (Figure 3.11B) fat pads, followed by a smaller increase in BAT (Figure 3.11C), whereas liver remained unaffected (Figure 3.11D). Perhaps, this was due to the normal appearance of liver with no excess fat (observations during the dissections), which usually accumulates in older subjects (Ghosh et al., 2012). The differential responses of various adipose tissues to lipolytic agents, such as isoproterenol, or to catecholamines, that normally induce catabolic processes *in vivo*, have been extensively studied in humans and rodents. All β-ARs (β1, β2, β3) are expressed in white and brown adipose tissues (Boyda et al., 2013) and exert their lipolytic effects upon ligand binding. However, β3-AR is the most abundant (Collins et al., 1994); and its expression pattern differs between the fat depots. β3-AR is highly expressed in BAT (Muzzin et al., 1991; Wajchenberg, 2000) and in beige cells which express UCP1 (Krief et al., 1993), whereas epididymal fat not only expresses more β3-AR but also all β-ARs are more active compared to subcutaneous adipose tissue (Arner, 1995). Upon norepinephrine injection in rats, expression of β3-AR was induced in BAT and WAT (Granneman and Lahners, 1992) and it stimulated lipolysis in epididymal fat in a degree greater to subcutaneous (Morimoto et al., 1997), similarly to isoproterenol (Lacasa et al., 1991). Taken together, these reports could explain why in this study, subcutaneous fat (Figure 3.11A) was more sensitive to isoproterenol-induced lipolysis compared to epididymal and brown fats (Figure 3.11B and C, respectively). In particular, the increased numbers of beige cells in the subcutaneous (*Crh* KO had more compared to WT) rather than in the visceral compartment (Karaliota et al., unpublished data) expressed potentially more β3-AR than epididymal adipose tissue. Therefore, despite the increased lipolytic capacity of epididymal depots compared to subcutaneous, reported in the literature, the metabolic phenotype of *Crh* KO mice resulted in an opposite effect. Furthermore, although BAT

was expected to be the most responsive to isoproterenol-induced phosphorylation of HSL due to increased β3-AR expression, the duration of the experiment probably was not sufficient to potentially activate this lipolytic process. It is noteworthy that alterations in the ratio of the anti-lipolytic α2-AR to the lipolytic β-ARs in adipose tissues also regulate lipolysis responses (Anthony et al., 2009), thus making it essential to elucidate the expression levels of adrenergic receptors in WT and *Crh* KO adipose tissues.

The discrepant observations in the adipose tissues were of important biological significance since differences between various white fat depots also reflect their contrasting roles in the pathogenesis of obesity-related disorders (Hamdy et al., 2006). Central obesity, i.e. visceral/epididymal fat, is associated with high risk of type 2 diabetes, dyslipedemia, atherosclerosis and morbidity (Tran et al., 2008). Peripheral obesity, which refers to subcutaneous fat depots, is not associated with the above pathologies but also improves insulin sensitivity (Snijder et al., 2003b; Tran et al., 2008). The reasons for these adipose effects consist of: the anatomical location of visceral fat, which is in close proximity to the portal vein of liver, thus delivering additional free fatty acids, deriving from nutritional imbalance (such as HFD), which create an insulin resistant state for this organ (Bjorntorp, 1991; Despres et al., 1995; Randle, 1998), and the close proximity of subcutaneous fat with muscle mass at the gluteal region, where muscle is an insulin-sensitive tissue (Snijder et al., 2003b; Virtue and Vidal-Puig, 2008); the cell-autonomous characteristics, i.e. secreted factors, like adipokines, of subcutaneous fat which upon transplantation in visceral depots improved body weight and metabolism (Tran et al., 2008); and the effects of adrenal and sex steroids influence the accumulation of fat in the visceral depots (Johannsson and Bengtsson, 1999; Lonn et al., 1994; Nam et al., 2001; Seidell et al., 1997) rather than in the subcutaneous depot. Overall, the subcutaneous compartment of the white fat depots in *Crh* KO mice displayed both the beneficial characteristics on whole-body metabolism

and the increased sensitivity to isoproterenol-induced lipolysis, thus making it important to unravel in detail the mechanisms that regulate the adrenergic system and the expansion capabilities of the white adipose tissues.

The attenuated response of *Crh* KO mice compared to WT (Figure 3.11) could be a result of the already increased fat utilization as shown from the elevated β-oxidation marker genes in the white fat depots of this genotype (Karaliota et al., unpublished data). Furthermore, the possibility of *Crh* KO mice expressing less β3-AR compared to WT in their fat depots cannot be excluded.

In isolated rodent brown adipocytes, isoproterenol stimulated the thermogenic pathway (Atgie et al., 1997; Mattsson et al., 2011; Mohell et al., 1983; Shih and Taberner, 1995). However, this was not achieved in a study with human subjects (Vosselman et al., 2012), which might have been due to a low dose despite the increased heart rate and whole-body energy expenditure, likely mimicking the sympathetic stimulation. Other sympathomimetics used in human studies could not stimulate BAT without the marked effects on the cardiovascular system (Carey et al., 2013; Cypess et al., 2012). The dose of isoproterenol used and duration in this experiment failed to activate thermogenesis in BAT of WT and *Crh* KO mice, as shown by the lack of UCP1 protein expression increase (Figure 3.13). Interestingly, BAT thermogenic activity in WT mice was increased four hours following intraperitoneal injection of isoproterenol in one study (Bachman et al., 2002), pointing perhaps to the necessity of performing time curves.

To summarize, my studies with a mouse model of global *Crh* deficiency suggest that CRH positively regulated Fyn expression, either directly or indirectly through regulation of urocortins expression; and this mechanism was unmasked when mice were subjected to metabolically challenging conditions. However, isoproterenol-induced lipolysis failed to alter Fyn expression levels, suggesting that this process was either

independent of Fyn or longer incubation with isoproterenol was needed. A novel role for Fyn kinase was also revealed using the T37i cell line, where Fyn promoted brown adipogenesis. Further studies are needed in order to elucidate the acute effects of corticosterone replacement on *Fyn* expression. Indirect calorimetry could provide evidence of whole-body energy expenditure after an isoproterenol injection. Subsequent *in vitro* studies will help to further understand how the two molecules, CRH and Fyn, are interacting and/or regulating each other.

Chapter 4

Potential roles of Fyn kinase in CRHR signalling and lipolysis

The *in vivo* experiments using the *Crh* KO mouse model suggested a positive interaction between CRH and Fyn. To further understand the mechanisms that underlie this interaction, I studied isolated primary preadipocytes from WT and *Crh* KO mice's subcutaneous, epididymal and brown adipose tissues.

There are several benefits associated with the use of this experimental model. Isolation of primary preadipocytes and differentiation to mature adipocytes provided a cellular model that maintained its fundamental cellular functions and morphology. In particular, preadipocytes from WT and *Crh* KO mice were able to proliferate in culture for four passages and maintained the fibroblast-like appearance of undifferentiated adipocytes. Induction of differentiation promoted adipogenesis similarly to cell lines, such as the white preadipocyte line 3T3L1 (Green and Meuth, 1974) and the brown preadipocyte line T37i (Zennaro et al., 1998). Despite the similar morphology at the undifferentiated state, the similar proliferation capabilities and the lack of visible differences in differentiation process of WT and *Crh* KO adipocytes, they remained genetically different as they had been exposed to diverse developmental signals due to lack of *Crh* and low levels of corticosterone. Although there is no information about the effects of *Crh* deficiency on preadipocyte fate, it should be noted that the cellular content, such as basal phosphorylation levels of proteins and expression of membrane receptors, could differ between the two genotypes. This effect is also examined in *Crh* KO tissues.

4.1 Signalling pathways activated in differentiated primary brown adipocytes

Signalling molecules, like extracellular signal-regulated kinase (ERK1/2), have been extensively studied for their involvement in adipocyte differentiation. ERK1/2, particularly, was shown to promote adipogenic differentiation (Bost et al., 2002; Prusty et al., 2002; Sale et al., 1995), whereas distinct roles have been attributed to ERK1 and ERK2 (Bost et al., 2005; Donzelli et al., 2011). More specifically, using ERK1 KO mice showed that ERK1 is necessary for adipocyte differentiation, whereas ERK2 promotes proliferation of preadipocytes (Bost et al., 2005). Both isoforms of ERK1/2 have important roles during recruitment into the differentiation program and extent of maturation in human mesenchymal stem cells (Donzelli et al., 2011). Another signalling molecule that is largely implicated in adipocyte differentiation and function is Akt or protein kinase B (PKB). Akt is activated downstream of the insulin receptor in insulin-sensitive tissues, such as adipose tissues, skeletal muscle and liver, and in turn induces translocation of the glucose transporter GLUT4 to the cell surface of fat cells and skeletal muscle cells, resulting in insulin-induced glucose uptake (Garofalo et al., 2003; Gonzalez and McGraw, 2009; Hernandez et al., 2001).

I examined whether CRH or UCN2 signalling machinery involved Akt and/or ERK1/2 regulation in mature brown adipocytes. Both these intracellular protein kinases are activated downstream of CRHRs (Grammatopoulos, 2012). Additionally, I investigated the effects of the Fyn inhibitor, SU6656 (Blake et al., 2000; Yamada et al., 2010), on regulating the protein expression of these signalling molecules, in order to elucidate a potential interaction between Fyn and CRHRs.

Primary preadipocytes from WT and *Crh* KO brown adipose tissues were isolated, cultured and induced to differentiate for 8 days, where they reached approximately 80% of differentiated cells. Cells were treated with 5 μM SU6656 for two

hours before being stimulated with 100 nM CRH or UCN2 for 5 or 15 minutes. Phosphorylation of Akt on serine 473, one of CRHRs' downstream signalling molecules, was measured by immunoblotting (Figures 4.1-1 and 4.1.-2).

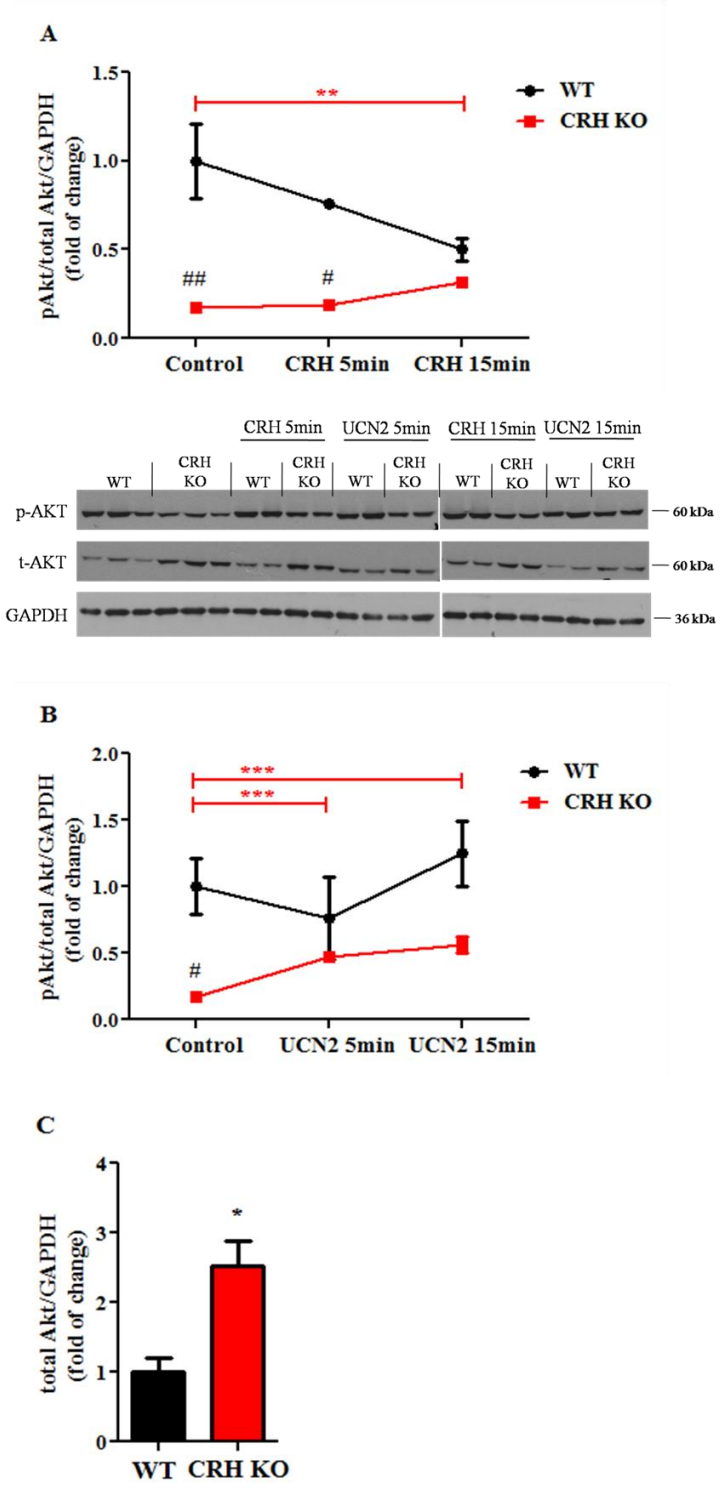

Figure 4.1-1: Effects of CRH and UCN2 on phospho-Akt/total Akt ratio in WT and *Crh* KO differentiated primary brown adipocytes. Primary brown preadipocytes were

differentiated for 8 days. Cells were treated with CRH (A) or UCN2 (B) 100 nM for 5 (A and B) and 15 (A and B) minutes. (C) Total Akt normalized to GAPDH. Immunoblots of phospho-Akt and total Akt are shown. Results were normalized to GAPDH. 15 µg of lysate were used. Data are expressed as mean values ± SEM, n=3 for control cells and n=2 for treated cells, 2-way ANOVA with Bonferroni post-test: * $p<0.05$, ** $p<0.01$, *** $p<0.001$. Black asterisks (*) denote the significant difference to WT control, unless otherwise stated by solid lines. Red asterisks (*), in A and B, denote the significant difference to *Crh* KO control cells. Number signs (#), in A and B, denote the significant difference between WT and *Crh* KO cells. Data are normalized to WT control cells.

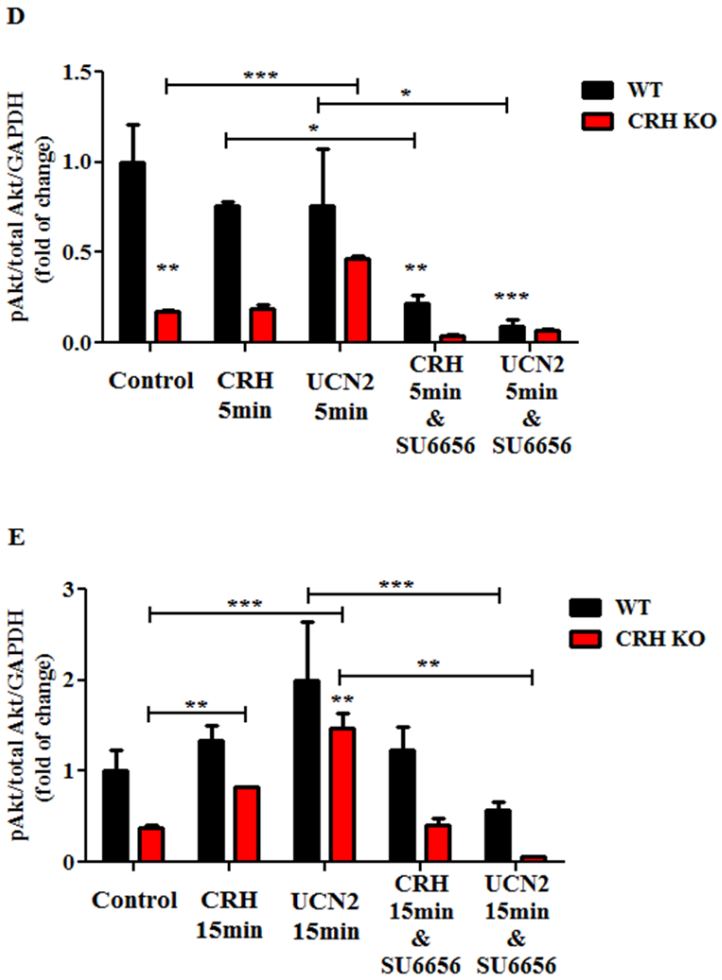

Figure 4.1-2: Effects of CRH and UCN2 on phospho-Akt/total Akt ratio in WT and *Crh* KO differentiated primary brown adipocytes treated with SU6656 5 µM. Primary brown preadipocytes were differentiated for 8 days and were treated with SU6656 5 µM for 2 hours. Next, cells were treated with CRH or UCN2 100 nM for 5 (D) and 15 (E) minutes. Similar description as in Figure 4.1-1.

CRH and UCN2 generated a small effect as measured by phospho-Akt/total Akt ratio in *Crh* KO adipocytes. Time course experiments showed significantly increased phosphorylation after 15-minute treatment with either CRH or UCN2 in *Crh* KO adipocytes (Figure 4.1-1A and B; 2- or 3.3-fold increase, respectively, compared to *Crh* KO control cells), suggesting that CRHR2 was involved in this process, since UCN2 is its natural ligand (Hsu and Hsueh, 2001; Reyes et al., 2001). Further, only *Crhr2* was expressed in brown fat of WT and *Crh* KO mice (Karaliota et al., unpublished data). Phospho-Akt/total Akt ratio in WT cells was unchanged, indicating that either CRH/UCN2 could not activate Akt or there is an impairment in stimulating Akt, perhaps in upstream signalling molecules.

Total Akt levels in *Crh* KO cells were 2.5-fold higher than WT levels (Figure 4.1-1C) and remained unchanged during the experimental treatments (not shown). The former characteristic could be due to the exposure to different signals during development, as mentioned earlier. Additionally, this could have also resulted from the differentiation agents added in the media during differentiation of brown adipocytes, which consist a stimulus for Akt. This is further supported by the similar total Akt levels in WT and *Crh* KO brown adipose tissues (Figure 4.2 immunoblots). Therefore, only *Crh* KO brown adipocytes showed an increase in Akt protein synthesis upon administration of CRH and UCN2.

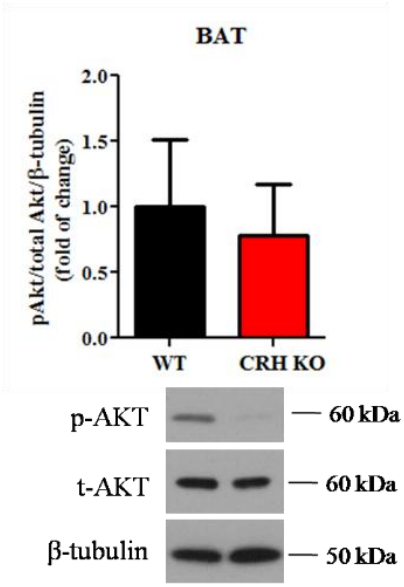

Figure 4.2: Phospho-Akt/total Akt ratio in WT and *Crh* KO brown adipose tissue. BAT was dissected from 3 months old WT and *Crh* KO mice and immunoblots for phospho-Akt and total Akt are shown. Results were normalized to β-tubulin. 30 μg of lysate were used. Data are expressed as mean values ± SEM, n=3 for WT samples and n=4 for *Crh* KO samples, t-test: the results are not significantly different.

In contrast, basal phospho-Akt/total Akt ratio was significantly lower in *Crh* KO adipocytes compared to WT (Figures 4.1-1 and 4.1-2), indicating that *Crh* KO adipocytes had impaired activation of Akt. This was unexpected since my hypothesis was that the glucocorticoid insufficiency of *Crh* KO mice (Muglia et al., 1995) would remove the inhibitory effects of glucocorticoids on phosphorylation of Akt (Buren et al., 2002; Long et al., 2003; Shen et al., 2016). This will be discussed further in section 4.3. Interestingly, phospho-Akt/total Akt ratio was similar between WT and *Crh* KO brown adipose tissues (Figure 4.2), indicating opposite results to the *in vitro* setting, suggesting that glucocorticoids exert their effects only *in vivo* and that this effect was diminished in culture.

SU6656 has been shown to inhibit phosphorylation of Akt at serine 473 (Asano et al., 2005; Cuneo et al., 2006; Ondrusova et al., 2013) and this is in agreement with my results. Inhibition of Fyn activity with SU6656, prior to CRH and UCN2 treatments for

5 minutes, almost totally inhibited phospho-Akt/total Akt ratio for both genotypes (Figure 4.1-2D). Similar results were obtained during the 15-minute UCN2 treatment (Figure 4.1-2E); whereas no change was identified for CRH-treated adipocytes in the same time-point.

Next, phosphorylation of ERK1/2,another downstream signalling molecule of CRHR2 (Grammatopoulos, 2012), was examined. Studies have shown that upon ligand binding (CRH or UCNs), CRHR2 increases phosphorylation of ERK1/2. This was described in various cellular and *in vivo* settings, such as cardiomyocytes and hearts (Brar et al., 2004b; Huang et al., 2009), colorectal cancer cells (Ducarouge et al., 2013) and myometrial cells (Karteris et al., 2004). In the brown adipocyte experiment, immunoblots of phospho-ERK1/2 levels were carried out and results are shown in Figures 4.3-1 and 4.3-2. A time course stimulation showed that CRH for 15 minutes activated ERK1/2 in *Crh* KO adipocytes (Figure 4.3-1A; 2.5-fold increase compared to *Crh* KO control cells), whereas WT levels remained unchanged, indicating that either CRH/UCN2 could not activate ERK1/2 or there is an impairment in stimulating ERK1/2. The latter could also be attributed to lack of Akt activation in WT brown adipocytes, as previously discussed, since Akt has been shown to interact with ERK1/2 (Zhou et al., 2015). UCN2, on the other hand, exerted a more potent effect and significantly increased (4-fold compared to *Crh* KO control cells) phospho-ERK1/2/total ERK1/2 ratio in *Crh* KO cells at 5 minutes, which was the maximal effect, as levels remained stimulated after 15 minutes (Figure 4.3-1B). WT levels showed a delayed response to UCN2 and phospho-ERK1/2/total ERK1/2 ratio was elevated by 3.3-fold compared to untreated cells (Figure 4.3-1B). Similarly to Akt results, these data confirm CRHR2 involvement in activation of ERK1/2.

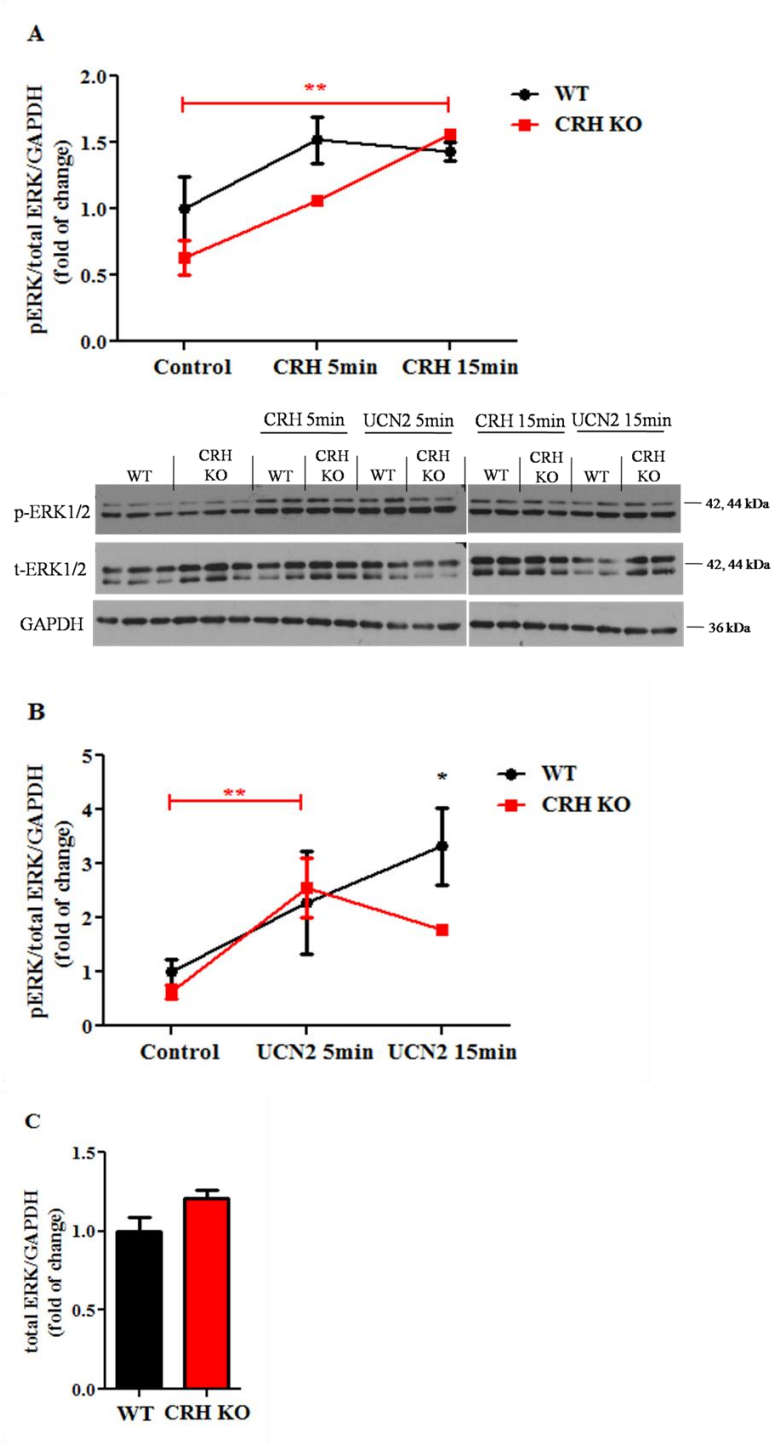

Figure 4.3-1: Effects of CRH and UCN2 on phospho-ERK1/2/total ERK1/2 ratio in WT and *Crh* KO differentiated primary brown adipocytes. Primary brown preadipocytes were differentiated for 8 days. Cells were treated with CRH (A) or UCN2 (B) 100 nM for 5 (A and B) and 15 (A and B) minutes. (C) Total ERK1/2 normalized to GAPDH. Immunoblots of phospho-ERK1/2 and total ERK1/2 are shown. Results were normalized to GAPDH. 15 µg of lysate were used. Data are expressed as mean values ± SEM, n=3 for control cells and n=2 for treated cells, 2-way ANOVA with Bonferroni post-test: * $p<0.05$, ** $p<0.01$. Black asterisks (*) denote the significant difference to WT control, unless otherwise stated by solid lines. Red asterisks (*), in A and B, denote

the significant difference to *Crh* KO control cells. Data are normalized to WT control cells.

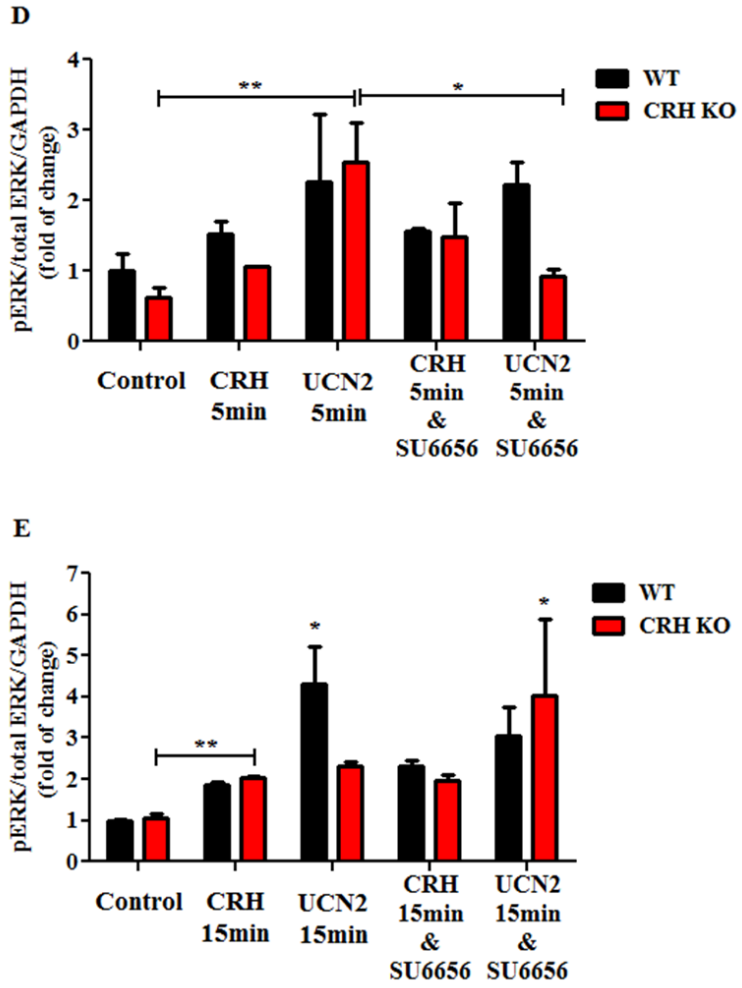

Figure 4.3-2: Effects of CRH and UCN2 on phospho-ERK1/2/total ERK1/2 ratio in WT and *Crh* KO differentiated primary brown adipocytes treated with SU6656 5 μM. Primary brown preadipocytes were differentiated for 8 days and were treated with SU6656 5 μM for 2 hours. Next, cells were treated with CRH or UCN2 100 nM for 5 (D) and 15 (E) minutes. Similar description as in Figure 4.3-1.

Contrary to total Akt levels (Figure 4.1-1C), total ERK1/2 was unchanged between WT and *Crh* KO cells (Figure 4.3-1C) and remained stable throughout the experiment (not shown). Basal phospho-ERK1/2/total ERK1/2 ratio was also similar between WT and *Crh* KO brown adipocytes (Figures 4.3-1 and 4.3-2). Given that the

published evidence on glucocorticoid effects on phospho-ERK1/2 identified both an inhibitory (Gonzalez et al., 2010; Greenberg et al., 2002) and enhancing role (Kumar et al., 2009; Qiu et al., 2001) and the fact that there are no reports on regulation of ERK1/2 in a *Crh* deficient environment, no hypothesis could be made on the anticipated ERK1/2 levels in WT and *Crh* KO brown adipocytes. Similarly to the *in vitro* basal total ERK1/2 levels, brown adipose tissues had similar expression of ERK1/2 (Figure 4.4), suggesting that this signalling molecule was not affected by stimulatory signals that activated Akt, as discussed previously.

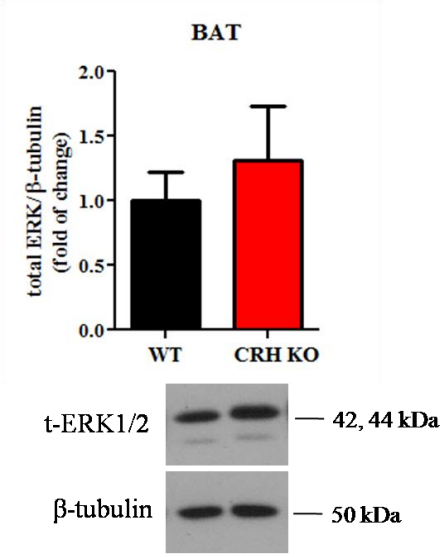

Figure 4.4: Total ERK1/2 in WT and *Crh* KO brown adipose tissue. BAT was dissected from 3 months old WT and *Crh* KO mice and immunoblots for total ERK1/2 are shown. Results were normalized to β-tubulin. 30 μg of lysate were used. Data are expressed as mean values ± SEM, n=3, t-test: the results are not significantly different.

SU6656 has been shown to exert inhibitory effects on phosphorylation of ERK1/2 (Cicha et al., 2014; Garcia-Martin et al., 2013; Tian et al., 2009), similarly to what was described for phospho-Akt/total Akt. Although ERK1/2 activation was shown to be Fyn-dependent in *Crh* KO adipocytes after UCN2 treatment for 5 minutes (Figure 4.3-2D), its activation was Fyn-independent in WT adipocytes (Figure 4.3-2D and E) and *Crh* KO cells during the 15-minute treatments (Figure 4.3-2E).

4.2 Isoproterenol and SU6656 effects on lipolysis in differentiated primary white and brown adipocytes

I examined whether the *in vivo* data (section 3.4) from white and brown adipose tissues could be reproduced *in vitro* and thus if this event was cell-autonomous. Isoproterenol is a lipolytic agent (Girousse et al., 2013; Lucas et al., 2003; Viswanadha and Londos, 2006) widely used both *in vitro* and *in vivo*. Whilst increased fatty acid oxidation is mainly thought to be the reason for the lean phenotype of *Fyn* KO mice, it is possible that increased lipolysis could also participate to this phenomenon. To assess the lipolytic actions of isoproterenol and SU6656 on differentiated primary white and brown adipocytes, phosphorylation levels of HSL at serine 563 (most commonly examined phosphorylation site as discussed in section 3.4) were measured.

Basal lipolysis, assessed by phospho-HSL in PBS-treated cells, was unchanged between WT and *Crh* KO adipocytes (Figure 4.5), similar to the *in vivo* results (Figure 3.11). Isoproterenol induced an increase in phospho-HSL levels (Figure 4.5A, B and C); and this result was more prominent in epididymal and brown adipocytes (Figure 4.5B and C) compared to subcutaneous (Figure 4.5A). This was opposite to the *in vivo* results and might be related to developmental cues that regulate whole-body homeostasis (discussed in section 4.3).

Additionally, phosphorylated HSL was increased in *Crh* KO cells more than in WT, but that was only present in the white and not the brown adipocytes, which displayed the opposite effect (Figure 4.5A, B and C). Since isoproterenol is a non-selective β-adrenergic agonist, the data on WT and *Crh* KO adipocytes could be a result of the different expression of β-adrenergic receptors (β-AR), which will be discussed further in section 4.3. These results were not in agreement with the *in vivo* measurements where *Crh* KO adipose tissues, both white and brown, had an attenuated response to isoproterenol compared to WT (Figure 3.11). Further, subcutaneous tissue

exhibited the strongest increase in phospho-HSL activation, contrary to the smallest effect reported *in vitro*. Despite the possibility that different expression patterns of adrenergic receptors were the main reason for the varying results between WT and *Crh* KO cells or tissues, it is noteworthy that the characteristic metabolic phenotype of *Crh* KO mice consisted the basis for the differences observed between the *in vivo* and *in vitro* results.

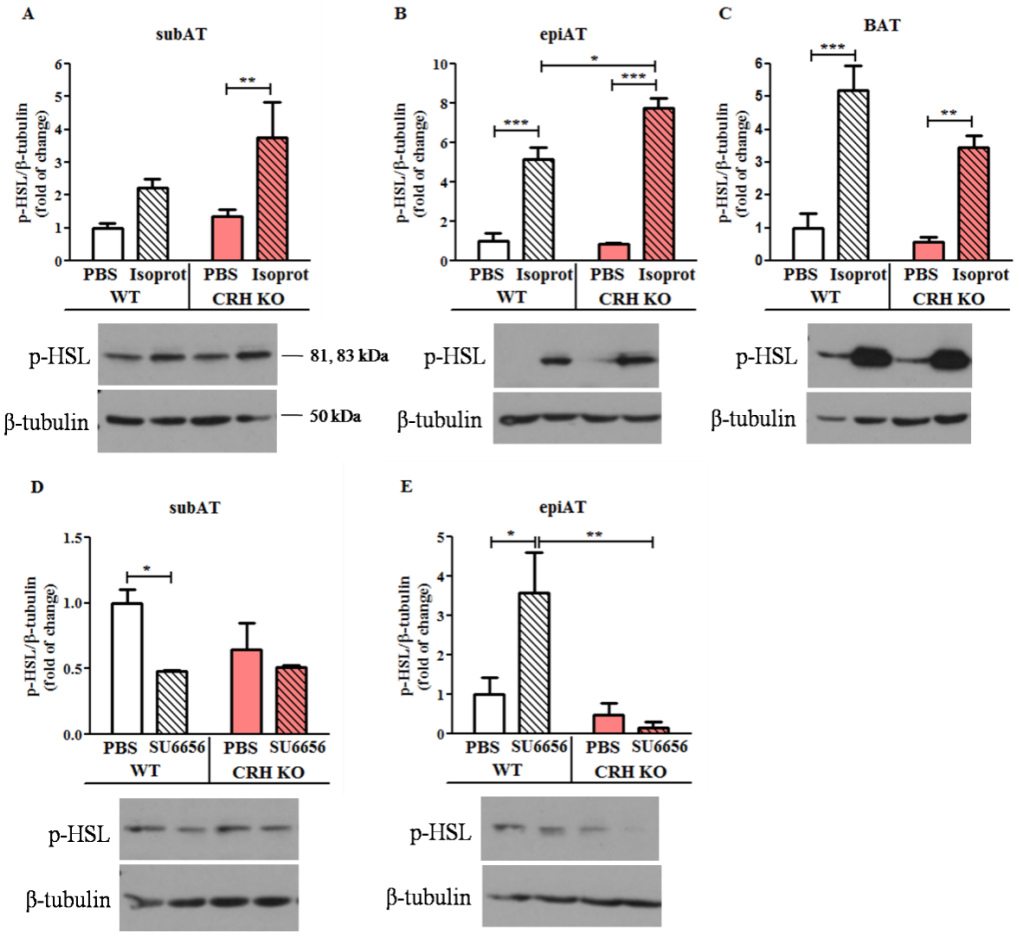

Figure 4.5: Effects of isoproterenol and SU6656 on levels of phospho-HSL expression in WT and *Crh* KO differentiated primary white and brown adipocytes. Primary subcutaneous (A, D), epididymal (B, E) and brown (C) preadipocytes were differentiated for 10 days and were treated next either with isoproterenol 0.1 μM for 15 minutes (A, B, C) or SU6656 5 μM for 2 hours (D, E). Immunoblots of phospho-HSL are shown. Results were normalized to β-tubulin. 15μg of lysate were used. Data are expressed as mean values ± SEM, for subAT and epiAT cells: n=4 for WT PBS and n=2 or 3 for remaining conditions, for BAT cells: n=3, 2-way ANOVA with Bonferroni post-test: * $p<0.05$, ** $p<0.01$, *** $p<0.001$. Data are normalized to WT PBS and the statistical analysis has been performed to WT PBS, unless otherwise stated by solid lines.

Controversial results were obtained with SU6656 since it caused a 50% reduction in phospho-HSL of WT subcutaneous adipocytes (Figure 4.5D) and it further produced an increase in lipolysis of WT epididymal adipocytes (Figure 4.5E), which are more sensitive to isoproterenol-induced lipolysis compared to subcutaneous adipocytes (Arner, 1995; Lacasa et al., 1991). Moreover, Fyn did not mediate the activation of HSL in isoproterenol-treated *Crh* KO epididymal adipocytes (Figure 4.5E).

Similarly to the *in vivo* data (Figure 3.12), Fyn protein expression was not affected by any of the agents used on cultured adipocytes (Figure 4.6), indicating that, perhaps, this process of induced lipolysis was independent of Fyn expression.

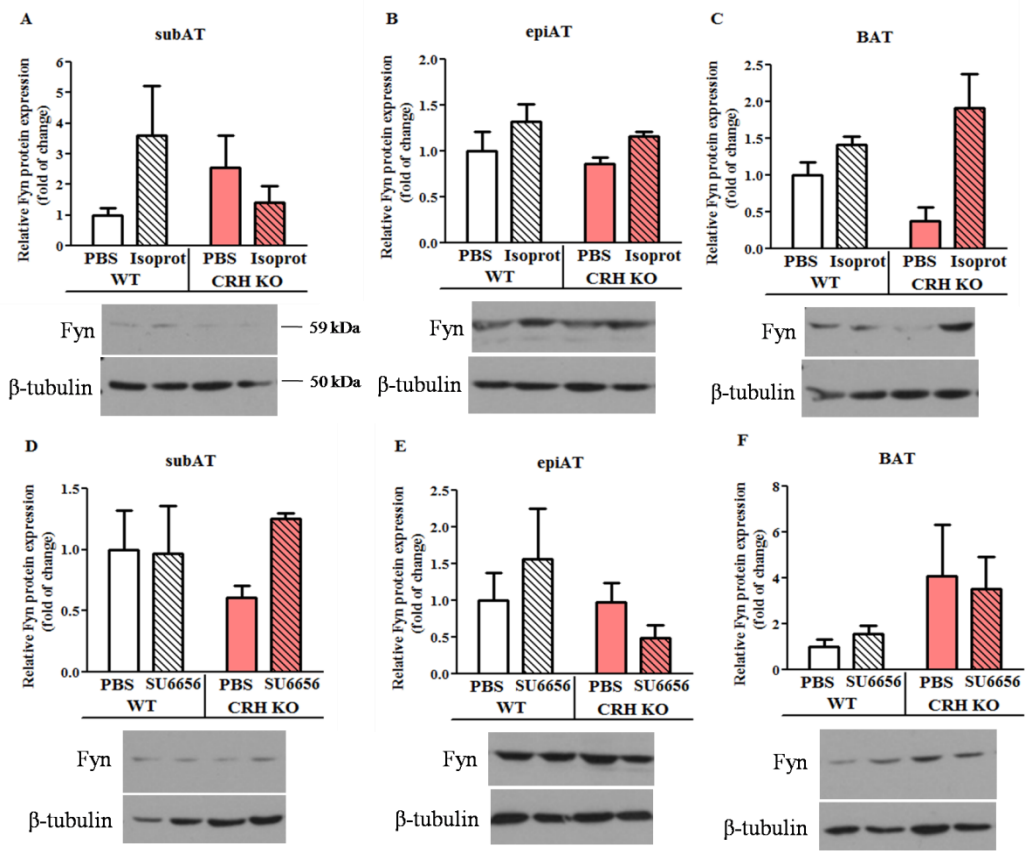

Figure 4.6: Effects of isoproterenol and SU6656 on levels of Fyn expression in WT and *Crh* KO differentiated primary white and brown adipocytes. Primary subcutaneous (A, D), epididymal (B, E) and brown (C, F) preadipocytes were differentiated for 10 days and were treated next either with isoproterenol 0.1 μM for 15 minutes (A, B, C) or SU6656 5 μM for 2 hours (D, E, F). Immunoblots of Fyn are shown. Results were normalized to β-tubulin. 15 μg of lysate were used. Data are expressed as mean values ± SEM, n=2 or 3, 2-way ANOVA with Bonferroni post-test: the results are not significantly different. Data are normalized to WT PBS.

4.3 Discussion

Primary cells are a useful tool in research design as they allow experimental procedures, which are difficult to perform *in vivo*, such as investigate the effects of a kinase inhibitor on a specific cell type independently of other cell types residing in the tissue. Isolating, culturing and differentiating preadipocytes from WT and *Crh* KO white (subcutaneous and epididymal) and brown fat pads provided a cellular model, which allowed investigation of CRHR signalling cascades and quantification of responsiveness to potential lipolytic agents. These experiments addressed the question of whether Fyn is involved in CRHRs signalling. Further, the addition of isoproterenol and SU6656 in the culture media provided evidence of their lipolytic effects and whether these effects were cell-autonomous and Fyn-mediated.

To date, there are no reports of CRHR signalling characteristics in brown adipocytes. The importance of the role of CRHR in brown adipocyte physiology has been highlighted by studies with CRHR knockout mice. Interestingly, these studies have confirmed the CRHRs' involvement in energy balance via regulation of the sympathetic nervous system (SNS) activation and subsequent stimulation of thermogenesis in brown fat (Bale et al., 2003; Carlin et al., 2006). These central effects were abolished in the *in vitro* system used in this study, and therefore, the direct effects of peptides were investigated independently of the central effects they exert *in vivo*, thus providing another beneficial effect for the primary cell cultures. In this study, the WT and *Crh* KO mice strains used did not express *Crhr1* in their brown fat depots (Karaliota et al., unpublished data). *Crhr2*, on the other hand, was expressed and its levels were increased in *Crh* KO compared to control animals (Karaliota et al., unpublished data).

CRH and UCN2 have been shown to activate Akt through binding to CRHR2 in various cellular models. Particularly, CRH stimulated Akt in THP1 human monocytic cells (Chandras et al., 2009), whereas UCN2 exerted similar actions in HEK293 kidney

cells (Markovic et al., 2011), RM-1 prostate cancer cells (Jin et al., 2011) and ventricular myocytes (Walther et al., 2014). Akt, as a signalling molecule has been implicated in a variety of processes. The phosphatidylinositol-3 kinase (PI3K)/Akt pathway is involved in promoting cell growth, proliferation and cell survival (Altomare and Khaled, 2012; Manning and Cantley, 2007). In insulin-sensitive tissues, like skeletal muscle, adipose tissue (white and brown) and liver, upon insulin binding, insulin receptor is tyrosine phosphorylated and in turn, activates the insulin receptor substrate 1 (IRS1)/PI3K/Akt pathway (Shepherd, 2005; Shepherd et al., 1998). This signalling cascade results in glucose transport in cells (Cheatham et al., 1994; Hara et al., 1994; Hernandez et al., 2001; Le Marchand-Brustel et al., 1995; Okada et al., 1994), increases expression of glycogen synthase (Shepherd et al., 1995) and decreases lipolysis (Duncan et al., 2007). This pathway has also been shown to activate phosphodiesterase 3B (PDE), which hydrolyzes cAMP (Jaworski et al., 2007; Wijkander et al., 1998) and thus rendering PKA less active in the hydrolysis pathway (described in the general introduction; Figure 1.1).

The interplay between Akt and glucocorticoids has been studied on the basis that glucocorticoids are responsible for the development of insulin resistance in muscle, adipose tissue and liver (Witchel and DeFranco, 2006). It was shown that, *in vivo*, dexamethasone, a synthetic glucocorticoid, diminished insulin-mediated PI3K/Akt activation in muscle and liver (Giorgino et al., 1993; Ruzzin et al., 2005; Saad et al., 1993). In dexamethasone-treated rat adipocytes (Buren et al., 2002) and upon injection of dexamethasone in rats (Buren et al., 2008), inhibition of insulin-induced Akt phosphorylation has been reported. Furthermore, adrenalectomy, promoting a glucocorticoid deficient environment, was associated with enhanced insulin signalling and Akt in skeletal muscle (Long et al., 2003). In various other experimental settings, where phosphorylation of Akt is not associated with insulin, glucocorticoids have also been shown to inhibit its phosphorylation. For example, through inhibition of Akt,

dexamethasone inhibits osteoblast remodeling (Shen et al., 2016), impairs neurite outgrowth in PC12 cells (Terada et al., 2014) and promotes apoptosis in L6 myoblasts (Singleton et al., 2000). Increased glucocorticoid production in rats with chronic renal failure, resulted in impaired PI3K/Akt activation (Wang et al., 2007).

In the present study, increased phospho-Akt/total Akt ratio was measured for both treatments, CRH and UCN2 (Figure 4.1-1A and B). This suggested involvement of CRHR2, since UCN2 is its natural ligand (Hsu and Hsueh, 2001; Reyes et al., 2001). This was also confirmed by the lack of *Crhr1* expression in brown adipose tissue of WT and *Crh* KO mice (Karaliota et al., unpublished data). The increased *Crhr2* expression in *Crh* KO BAT compared to WT (Karaliota et al., unpublished data) was in agreement with a different mouse model, the *Crhr1* KO, which expressed elevated *Crhr2* in WAT and BAT as a compensatory mechanism to the genetic deletion (Lu et al., 2015). Moreover, glucocorticoids have been shown to down-regulate *Crhr2* in the ventromedial nucleus of hypothalamus (VMH) and not in the paraventricular nucleus (PVN), thus controlling appetite and other eating disorders (Chen et al., 2005), therefore this could also justify how low levels of corticosterone in *Crh* KO mice (Muglia et al., 1995) could have diminished their inhibitory effects on expression of *Crhr2* in this genotype. Since, it was reported that glucocorticoid replacement could reverse the effect of *Crhr1* deletion on *Crhr2* expression (Lu et al., 2015), it remains to be elucidated whether corticosterone supplementation in *Crh* KO mice also reversed the observed effect in BAT and other tissues. The lack of WT responsiveness, measured by phospho-Akt/total Akt ratio, suggested either that the CRHR2 ligands could not activate Akt or that Akt could not be activated, probably due to impairment in upstream signalling molecules. The former scenario could have resulted from various causes: the receptor could be internalized and thus was not able to bind CRH/UCN2 and activate the signalling cascade; a delayed response could be generated as this was also reported for a different cellular model (THP1 monocytic cells), where CRH and UCN2 significantly increased

phospho-Akt/total Akt ratio after 30 minutes of stimulation (Chandras et al., 2009); lastly, it could be possible that WT CRHR2 levels were minimal and ligands were ineffective. Therefore, further studies are needed in order to address some of the hypotheses discussed above, such as perform time- and dose-dependent experiments and determine CRHR2 cellular localization with immunostaining before and after glucocorticoid replacement. The latter scenario that could perhaps explain the lack of WT responsiveness (measured by phospho-Akt/total Akt ratio) to CRH and UCN2 could implicate impairment in the regulators of G protein signalling (RGS). These molecules accelerate GTP hydrolysis catalyzed by Gα G protein subunits upon binding to GPCRs, thus terminating the GPCR signal. It has been shown that various members of the RGS family are involved in enhancing lipolysis (Iankova et al., 2008), in regulating body weight (Waugh et al., 2011) and in promoting obesity and insulin resistance (Deng et al., 2012). Therefore, RGSs could be differentially expressed in WT and *Crh* KO adipose tissue. The latter along with their reported regulation from glucocorticoids (Holden et al., 2011; Holden et al., 2014; Ni et al., 1999) could further enhance these differences and hence resulting in modulation of the CRHR2 signalling.

The characteristic glucocorticoid insufficient environment of *Crh* KO mice could not have directly affected basal phospho-Akt/total Akt ratio in brown adipocytes since the result shown in Figures 4.1-1 and 4.1-2 was opposite to what has already been published and described above, meaning that the reduced corticosterone in *Crh* KO mice was expected to increase basal phospho-Akt/total Akt ratio. Therefore, it should be noted that glucocorticoids could affect other mediators of CRHR2 signalling pathway, such as the RGS as described previously. In the control condition (=no CRH/UCN2 stimulation), the lower levels of phospho-Akt/total Akt ratio in *Crh* KO adipocytes compared to WT indicate that the activation mechanism of Akt in *Crh* KO cells was impaired. However, the significant increase of phospho-Akt/total Akt ratio after CRH and UCN2 treatments indicated that *Crh* KO adipocytes are more sensitive to these

stimuli compared to WT, perhaps due to increased levels of *Crhr2* (Karaliota et al., unpublished data). Total Akt levels were not affected by glucocorticoid treatment in previous studies, suggesting that the elevated *Crh* KO total Akt levels compared to WT levels (Figure 4.1-1C) did not result from low corticosterone levels. Instead, it could be a developmental effect as discussed previously or *Crh* KO brown adipocytes were more insulin sensitive thus resulting in increased Akt levels. Additionally, analysis of whole brown adipose tissues from WT and *Crh* KO mice showed that phospho-Akt/total Akt ratio and total Akt (Figure 4.2) were unchanged between the genotypes. This suggested that the tissue and the isolated, cultured and differentiated preadipocytes had totally different signalling characteristics. Furthermore, this indicated that *Crh* KO brown adipocytes could activate Akt protein synthesis only upon stimulation, for example after the addition of differentiation agents, such as insulin, in the culture media.

The inhibitory actions of SU6656 on phospho-Akt/total Akt ratio were previously reported in pancreatic cancer cells (Asano et al., 2005), in endothelial cells (Cuneo et al., 2006) and in melanoma cells (Ondrusova et al., 2013), where it suppressed tumour growth in time periods as early as 30 minutes and 2 hours. My results are in agreement with these reports. Particularly, phospho-Akt/total Akt ratio was significantly inhibited after SU6656 treatment and the 5-minute CRH and UCN2 stimulations (Figure 4.1-2D). Despite the lack of the proper control condition with only SU6656 treatment, due to very low protein concentration of those samples, the fact that CRH and UCN2 did not have an effect on WT phospho-Akt/total Akt ratio suggested that Fyn was directly associated with Akt and thus inhibition of Fyn resulted in reduction of phospho-Akt/total Akt ratio. The latter association was supported by the reported interaction of Fyn and IRS1 (Myers et al., 1996; Sun et al., 1996), linking Fyn and Akt in the insulin signalling pathway. Significant inhibition of phospho-Akt/total Akt ratio was also reported for the 15-minute UCN2 treatment (Figure 4.1-2E), indicating that this process was also Fyn-dependent. However, no change was measured for the 15-minute CRH treatment,

indicating that SU6656 exerted its effects on the most potent CRHR2 ligand, UCN2, explaining also the reason for detecting these effects at the 15-minute time-point, pointing to the necessity for Fyn being intact at different time-points. Transient effects on phospho-Akt/total Akt ratio, similar to the ones reported here after SU6656 and CRH stimulations, have also been studied. Reports, which performed time course experiments, provided evidence of mechanisms that transiently inhibited phosphorylation of Akt and included the Parkinson's disease mimetic drug, 6-hydroxydopamine (Chen et al., 2004b) or inhibitors of the catalytic subunit, p110, of PI3K (Torbett et al., 2008).

Summarizing my results on Akt in primary brown adipocytes, it was shown that CRH and mainly UCN2 activated CRHR2 and in turn, CRHR2 activated Akt in *Crh* KO adipocytes. On the other hand, CRH and UCN2 stimuli failed to produce any response in WT cells. The fact that Akt was activated only in *Crh* KO adipocytes could have a significant biological role since Akt is an important downstream mediator of the insulin signalling pathway. Therefore, *Crh* KO brown adipocytes could have an increased insulin-insulin receptor-IRS1-PI3K-Akt pathway and thus have increased glucose uptake resulting from the increased insulin sensitivity reported from ITT experiments in *Crh* KO mice (Karaliota et al., unpublished data). In case this hypothesis will be validated, then it would be opposite to the reported inhibitory actions of CRHR2 in skeletal muscle on insulin sensitivity (Chen et al., 2006; Kuperman and Chen, 2008), thus establishing tissue-specificity for CRHR2 on regulating glucose uptake. Further, an additional biological role could be discussed as Akt is negatively regulating lipolysis and this will be analyzed below. Inhibition of Fyn kinase activity by SU6656 provided evidence that Fyn was associated with Akt and there were no interactions with CRHR2.

The ERK1/2 signalling pathway has been extensively studied downstream of CRHR2. All peptides of CRH family have been shown to bind to CRHR2 and stimulate ERK1/2, although the latter was activated to a lesser extend after CRH compared to

UCNs (Wu et al., 2007). The latter could support my results where phospho-ERK1/2/total ERK1/2 ratio was almost unchanged in WT adipocytes (Figure 4.3-1A). However, as discussed for Akt, it is likely that the magnitude of WT ERK1/2 activation might be regulated by the level of CRHR2 expression, signal transduction potential and affinity, independently or combined. Contrary to CRH, UCNs bind to CRHR2 with higher affinity (Bale and Vale, 2004) and activate ERK1/2 very quickly, for example within 5 minutes after addition *in vitro* (Huang et al., 2009; Kageyama et al., 2010; Wu et al., 2007). The role of this pathway has been studied in a plethora of experimental settings: delayed effects of stress on memory formation were mediated by CRHR2-ERK1/2 induction (Sananbenesi et al., 2003); control of human pregnant myometrial cells was displayed by this pathway (Karteris et al., 2004); cardioprotective effects after ischemic reperfusion injury in rat hearts (Schulman et al., 2002) and isolated cardiomyocytes (Brar et al., 2004b) were generated by activation of UCNs-CRHR2-ERK1/2 cascade; pro-inflammatory effects of this pathway regulated the pathophysiology of colitis in humans (Moss et al., 2007); prevention of cancer progression was mediated by UCNs-CRHR2-ERK1/2 pathway (Ducarouge et al., 2013; Kageyama et al., 2010); and this cascade also regulated β-arrestin 1, therefore controlling CRHR2 internalization (Markovic et al., 2011). My results confirmed that UCN2 activated CRHR2-ERK1/2 in brown adipocytes with a rapid response for *Crh* KO cells and lower for WT (Figure 4.3-1B).

The involvement of glucocorticoids in regulation of phospho-ERK1/2 levels presented controversial results, which varied in different experimental settings. More specifically, dexamethasone inhibited ERK1/2 in lung cancer cells to prevent tumour growth (Greenberg et al., 2002); in colon cancer cells to prevent migration (Han et al., 2015); and dexamethasone and cortisol decreased phospho-ERK1/2 during oocyte maturation in lamb (Gonzalez et al., 2010). The enhancing effects of glucocorticoids on ERK1/2 were reported in PC12 neural cells (Qiu et al., 2001), in survival of renal cells

after ischemia reperfusion injury (Kumar et al., 2009) and in ovarian follicular cells where it exerted an anti-apoptotic role (Sasson et al., 2003). Hence, glucocorticoids did not have a similar pattern of action on activation of ERK1/2. Overall, this evidence makes it impossible to ascertain whether *Crh* KO glucocorticoid insufficiency (Muglia et al., 1995) was implicated in the regulation of ERK1/2 levels, both the phosphorylated form (Figures 4.3-1 and 4.3-2) and the total (Figure 4.3-1C), measured in this study under basal conditions.

A small number of studies investigated the role of SU6656 on ERK1/2 activation, but all concluded that this inhibitor reduced phospho-ERK1/2/total ERK1/2 ratio after 24 hours (Cicha et al., 2014; Garcia-Martin et al., 2013; Taniguchi et al., 2013; Tian et al., 2009). In this experiment, SU6656 did not alter phospho-ERK1/2/total ERK1/2 ratio (Figure 4.3-2D and E), although the 2-hour treatment was shown to inhibit Fyn kinase activity (Bastie et al., 2007) and my studies also showed effects on phosphorylation of Akt (Figure 4.1-2D and E). Thus, it seems likely that Fyn was not involved in CRHR2-mediated activation of ERK1/2. The reduction in phospho-ERK1/2/total ERK1/2 ratio observed in the 5-minute UCN2-treated *Crh* KO cells (Figure 4.3-2D), could either have no biological significance or an inhibitory role was unraveled for CRHR2.

In conclusion, CRH activated ERK1/2 to a smaller extent and this response was delayed compared to UCN2 in *Crh* KO cells. The natural ligand of CRHR2, UCN2, activated ERK1/2 in WT adipocytes as well, a result supported by previous studies. The biological significance of these increases in phospho-ERK1/2/total ERK1/2 ratio could link CRHR2 to adipocyte differentiation since it was shown that both isoforms, ERK1 and ERK2, were necessary for maturation of preadipocytes and proliferation (Bost et al., 2005; Bost et al., 2002; Donzelli et al., 2011; Prusty et al., 2002; Sale et al., 1995). Moreover, CRHR2 was shown to promote brown adipocyte differentiation (Lu et al., 2015), thus further strengthening the above notion. Additional supporting information

that ERK1/2 displayed an important role in adipocyte differentiation was provided by the inability to detect phospho-ERK1/2 in whole brown adipose tissue lysates, which consisted mainly from mature adipocytes (immunoblots not shown), suggesting that under basal conditions ERK1/2 was not activated. Total ERK1/2 levels were unchanged between WT and *Crh* KO BAT, as evident from Figure 4.4. Inhibition of Fyn activity did not reverse the effects of CRH and UCN2 on phospho-ERK1/2/total ERK1/2 ratio, concluding that Fyn was not interacting with ERK1/2.

When isolating and culturing primary preadipocytes, it is important to note that although they provide a useful tool in experimental design, the results obtained from such cultures should be treated with caution. The advantages of using primary preadipocytes are that they partially mimic the functions of the adipose tissue and they consist of a cell-autonomous system.

As previously shown (chapter 3), *Crh* KO white and brown adipose tissues had an attenuated response to isoproterenol-induced lipolysis compared to WT (Figure 3.11). This could be explained by the increased fatty acid oxidation of *Crh* KO white adipose tissues (Karaliota et al., unpublished data) and/or by reduced expression of β3-AR compared to WT. The greater effect of isoproterenol on phosphorylation of HSL was reported for the subcutaneous adipose tissue, followed by epididymal and brown adipose tissues (Figure 3.11). As discussed in chapter 3, this could be supported by the metabolic phenotype of *Crh* KO mice (Karaliota et al., unpublished data). In particular, the increased numbers of beige cells in *Crh* KO subcutaneous depots could potentially express more β3-ARs, therefore making the subcutaneous depots more sensitive to isoproterenol-induced lipolysis. Epididymal fat pad, which did not contain beige cells (Karaliota et al., unpublished data), showed less sensitivity to isoproterenol-induced lipolysis in terms of phospho-HSL, compared to the subcutaneous fat, whereas BAT was

the least sensitive of all adipose tissues, as probably more time was needed to stimulate this tissue (detailed discussion in chapter 3).

My *in vitro* data showed that the lipolytic effect of isoproterenol, measured by phosphorylation of HSL Ser563, was more prominent in the epididymal and brown adipocytes followed by the subcutaneous cells (Figure 4.5A, B and C). This was in agreement to the reported increased lipolytic capacity of epididymal adipose tissue due to increased β3-AR compared to subcutaneous fat (Arner, 1995), thus serving as a primary energy pool. The highly expressed β3-AR in BAT compared to WAT (Muzzin et al., 1991; Wajchenberg, 2000), explained why brown adipocytes were more sensitive to isoproterenol compared to subcutaneous, whereas brown adipocytes could not display responses greater to epididymal adipocytes perhaps due to differences in expression of other β-ARs, like β1-AR and/or β2-AR. This also showed that BAT was able to respond to the isoproterenol-induced lipolysis in my *in vivo* experiment, but the time-point used was not sufficient to generate such stimulation, as discussed in chapter 3. These data provided evidence that cultures of preadipocytes produced different results from the systemic response that was measured upon isoproterenol injection in mice. In conclusion, the effect observed by examining whole adipose tissues was not cell-autonomous, rather it resulted from the genetic deletion of *Crh* and the ensuing metabolic phenotype.

In the adipocyte cultures, *Crh* KO cells exhibited greater responses to isoproterenol than WT cells (Figure 4.5A, B and C). But this was only evident in the white and not the brown adipose-deriving cells, indicating that only *Crh* KO white fat had higher levels of β-ARs than WT and not brown, and this was perhaps a result of the different origin of these specific fat pads (Kajimura et al., 2015). This hypothesis remains to be elucidated by measuring the expression profile of β-ARs in WT and *Crh* KO adipose tissues. Additionally, the increased expression of Akt in *Crh* KO brown adipocytes compared to WT (Figure 4.1-1C) could also attenuate lipolysis as reported

elsewhere (Jaworski et al., 2007; Wijkander et al., 1998). As a consequence, the adipocyte cultures unmasked a unique effect of global *Crh* deficiency and of its characteristic reduced circulating corticosterone on regulation of lipolysis processes in adipose tissues.

Fyn KO mice owe their lean phenotype, partly, to the increased fatty acid oxidation in skeletal muscle and adipose tissue (Bastie et al., 2007). However, the lipolytic pathway has not been examined yet and it could also be altered, therefore linking Fyn and hydrolysis of lipids. As a consequence, SU6656 could either increase or decrease the lipolytic processes in this cellular setting. The increase was reported for the WT epididymal adipocytes (Figure 4.5E) and this could be justified by reduced Akt levels in WT epididymal adipocytes compared to *Crh* KO, similarly to brown adipocytes (Figure 4.1-1C). Contrary to that, SU6656 decreased phospho-HSL in WT subcutaneous adipocytes (Figure 4.5D), which remains to be further examined as total expression of HSL needs to be determined and also measure Akt levels, which indirectly regulate lipolytic processes (Jaworski et al., 2007; Wijkander et al., 1998). Similarly to the *in vivo* data (Figure 3.12), Fyn protein expression was not altered upon isoproterenol and SU6656 stimulations (Figure 4.6). Particularly, it has not been shown that inhibition of Fyn activity reduces Fyn expression and the 15-minute treatment with isoproterenol either did not alter Fyn protein expression due to the small incubation time or Fyn did not regulate phosphorylation of HSL.

In summary, in primary differentiated brown adipocytes I examined part of the CRHR2 signalling characteristics and concluded that Fyn was interacting with Akt independently of CRHR2 and that Fyn was not involved in CRHR2-mediated activation of ERK1/2. Further, the combination of the *in vivo* and *in vitro* data upon stimulation of lipolysis processes provided evidence that the *in vivo* effects were not cell-autonomous and resulted from the metabolic phenotype developed due to deletion of *Crh*. More

studies are needed in order to fully elucidate the lipolytic capacities and CRHR signalling cascades of adipose tissues.

Chapter 5

Summary and conclusion

The understanding of the molecular mechanisms that underlie whole-body energy homeostasis is essential as dysregulations cause a large number of diseases, including obesity and cardiovascular diseases that are often associated with increased mortality risk. In this study, I focused on investigating CRH and Fyn kinase, two molecules that are implicated in metabolism and are regulated by the HPA axis. CRH has been examined for the anorexigenic effects upon its exogenous administration in rodents (Arase et al., 1988; Krahn et al., 1990; Morley and Levine, 1982). Furthermore, the induction of the sympathetic nervous system and subsequent increases in thermogenesis, norepinephrine and glucocorticoid release (Cullen et al., 2001) clearly indicated CRH as a mediator of energy availability. All members of the CRH family of peptides have been shown, either by genetic deletions (Bale et al., 2003; Chen et al., 2006; Li et al., 2007; Zalutskaya et al., 2007) or overexpression (Jamieson et al., 2011) and *in vivo* injections (Cullen et al., 2001; Seres et al., 2004), to be potent mediators of metabolic processes. The recent finding that CRH/CRHR1 or UCN2/CRHR2 regulate adipose tissue differentiation to white or beige, respectively, suggested that CRH family of peptides could participate in adipogenesis (Lu et al., 2015). Interestingly, the analysis of the *Crh* KO mice metabolic phenotype (Karaliota et al., unpublished data), revealed increased lipid utilization with increased fatty acid oxidation in white adipose tissues. Additionally, the *Crh* KO mice also displayed an expanded and functional beige compartment in the subcutaneous adipose tissue, which might explain the increased thermogenesis also observed in these mice. These studies strengthened the role of CRH in regulation of energy homeostasis. Finally, a large body of evidence implicates CRH in the development of anxiety-related disorders (Bale and Vale, 2004). Interestingly,

however, *Crh* KO mice display normal anxiety under stressful conditions (Dunn and Swiergiel, 1999; Weninger et al., 1999a), due to compensatory mechanisms, such as urocortins.

Fyn kinase, on the other hand, was reported to play significant role in white adipogenesis (Sun et al., 2005; Tse et al., 2013) and the *Fyn* KO mice displayed a remarkable phenotype characterized by reduced body weight and reduced adiposity in white fat pads accompanied by increased fatty acid oxidation in skeletal muscle and white adipose tissues (Bastie et al., 2007). Lastly, Fyn kinase was shown to be regulated by the HPA axis, suggested by the fact that *Fyn* KO mice displayed increased anxiety (Belzung and Griebel, 2001; Miyakawa et al., 1994) and *Fyn kinase* expression was down-regulated by glucocorticoids (Harr et al., 2010).

My experiments resulted in the discovery of a novel regulation of Fyn kinase by CRH, either directly or indirectly. This positive effect of CRH on Fyn kinase expression, in all the tissues that were examined, was unmasked when *Crh* KO mice were supplemented with corticosterone (Figures 3.2-1 and 3.2-2), the main glucocorticoid in mice, in order to correct the glucocorticoid insufficiency and HPA axis output resulting from the global *Crh* deficiency (Muglia et al., 1995). Activation of catabolic processes through cold exposure decreased *Fyn* expression levels in all tissues examined (Figures 3.2-1 and 3.2-2), suggesting that mobilization of energy reserves affected Fyn. This is particularly in line with the role of Fyn kinase as a regulator of lipid utilization (Bastie et al., 2007), since a reduction of Fyn kinase expression or activity was reported to increase β-oxidation in adipose tissues (and muscle), an event that is undeniably also apparent under cold challenge. Furthermore, low temperatures increased circulating corticosterone (Harper and Austad, 2000; Karp, 2012), which in turn enhanced catabolic processes and further reduced Fyn kinase expression (Harr et al., 2010), therefore affecting β-oxidation pathway. Consequently, examination of the effects of glucocorticoid replacement using indirect calorimetry could be done in the future to

determine whether elevation of blood corticosterone affects energy expenditure, activity and food intake. Since it was shown that alterations in expression of CRH family of peptides occur due to genetic deletions and reversed upon corticosterone delivery (Lu et al., 2015), it is likely that compensatory mechanisms also arose in the *Crh* KO mouse. Therefore, it remains to be elucidated whether urocortins expression was altered and whether this was secondary to the glucocorticoid insufficiency. Significant information could also be collected from the inhibition of Fyn kinase activity using the SU6656 inhibitor in the *Crh* KO mice (Yamada et al., 2010). Indirect calorimetry, mRNA and protein expression levels, after just one SU6656 injection, would help elucidate whether inhibiting Fyn kinase activity in the *Crh* KO mice would result in an even greater lipid oxidation profile than the *Crh* KO mouse. If that was observed, this would suggest a synergistic action of CRH and Fyn kinase. In order to confirm these results, the use of a proper double knockout (with Fyn kinase totally deleted or using tissue-specific deletion) will be necessary.

Stimuli that activate brown adipose tissue have been the basis of experimental studies since brown adipose tissue and the beige compartment generated in white adipose tissues have been reported to exert beneficial effects on obesity, insulin sensitivity and glucose clearance (Kajimura et al., 2015). Despite the efforts to produce drugs that stimulate brown adipose tissue thermogenesis, the adverse effects on the cardiovascular system have put a barrier to this research. One such example of drug with adverse effects is the β-adrenergic agonists which have been used because this pathway plays a key role in activation of brown adipose tissue thermogenesis (Villarroya and Vidal-Puig, 2013). In this study, glucocorticoid replacement and cold exposure were used as potent stimulators of brown adipose tissue thermogenesis (Gasparetti et al., 2003; Lim et al., 2012; Soumano et al., 2000; Viengchareun et al., 2001), thus I sought to determine the role of Fyn kinase in brown adipogenesis. Use of the brown preadipocyte cell line, T37i, enabled the description of a novel role for Fyn, since

inhibition of Fyn kinase activity attenuated adipocyte differentiation, indicating a significant role in promoting maturation and full functionality of brown adipocytes (section 3.3). Although the effects on adipocyte differentiation due to lack of *Crh* were not determined, we could speculate that CRH could play an important role in promoting adipogenesis, similarly to Fyn kinase, a concept that was also supported by unpublished data (Karaliota et al.).

Lipolysis processes, which partly control the availability of lipids as substrates for tissues capable of β-oxidation (adipose tissues and muscles), have also been studied in this project, in terms of recording differences between WT and *Crh* KO mice and determining the involvement of Fyn kinase. Although isoproterenol, a potent stimulator of lipolysis, is known to exert its actions primarily in epididymal fat depots (Lacasa et al., 1991), the *Crh* KO mice generated differential results (Figure 3.11). Importantly, the expanded beige compartment in the subcutaneous adipose tissue (Karaliota et al., unpublished data) increased the response of this depot to isoproterenol-induced lipolysis, thus epididymal fat was less prone to the lipolytic effects of isoproterenol. On the contrary, this susceptibility of epididymal adipocytes to lipolysis was evident in primary cultures of preadipocytes isolated from WT and *Crh* KO mice (Figure 4.5), indicating that the *in vivo* effect of isoproterenol was, very likely counter balanced by additional signals (which still remain to be determined) and thus, it was not cell-autonomous. Furthermore, isoproterenol is reported to activate lipolysis in brown adipose tissue along with thermogenesis, which is evident by increased *Ucp1* expression (Cannon and Nedergaard, 2004). The duration of my *in vivo* experiments limited the actions of isoproterenol in white adipose tissues (Figure 3.11) but the brown adipocytes were responsive in the cellular cultures (Figure 4.5), thus establishing that lipolysis in brown adipose tissue was not impaired in *Crh* KO mice. The absence of effect *in vivo* again suggested that additional mechanisms might diminish the effects of β-adrenergic stimulation of lipolysis. Moreover, the unchanged levels of Fyn kinase upon

isoproterenol injection (Figure 3.12) provided evidence that either hydrolysis of lipids was independent of Fyn kinase or that the incubation was too short to affect (if at all) Fyn protein levels. Both of these events should be addressed in future experiments and Fyn-mediated lipolysis should be examined.

The traditional role of CRH in the hypothalamus-pituitary-adrenal (HPA) axis to control autonomic, behavioural, immune and cognitive responses to stress, as well as its peripheral functions, such as on metabolism, energy homeostasis, gastrointestinal and immune systems, have been mediated via activation of the CRH receptors (CRHRs). The signalling cascades, following ligand binding to CRHRs, have been extensively reviewed (Grammatopoulos, 2012). In my primary brown adipocytes experiment, some of the CRHR2 signalling molecules were investigated, particularly Akt (Figures 4.1-1, 4.1-2 and 4.2) and ERK1/2 (Figures 4.3-1, 4.3-2 and 4.4). Both molecules are implicated in controlling adipocyte development and differentiation (Bost et al., 2005; Bost et al., 2002; Donzelli et al., 2011; Garofalo et al., 2003; Gonzalez and McGraw, 2009; Hernandez et al., 2001; Prusty et al., 2002; Sale et al., 1995). In addition to the differences reported between WT and *Crh* KO adipocytes after CRH and UCN2 stimulations, the effects of Fyn kinase activity inhibition were examined, using the specific inhibitor SU6656. Importantly, the differences between WT and *Crh* KO adipocytes require further investigation in order to elucidate the exact role of *Crh* deficiency and of the ensuing low circulating corticosterone, since the differences were measured in the basal state. Whether developmental cues controlled these events or differential energy needs drive different phosphorylation events, is still unknown. In parallel, and as mentioned previously, compensatory mechanisms due to genetic deletions, such as increased CRHR2 (Lu et al., 2015) in *Crh* KO brown adipose tissue, could be the basis of the phenotypes reported in this study.

The effects of SU6656 on CRHR2 signalling characteristics concluded that although Fyn was associated with Akt, this was not the case with CRHR2 and ERK1/2.

The former characteristic provided another linking point between Fyn, Akt and insulin signalling, complementing previous studies (Liu et al., 2005; Saltiel and Pessin, 2003). In addition to the roles of CRHR2 (Lu et al., 2015) and ERK1/2 (Bost et al., 2005; Bost et al., 2002; Donzelli et al., 2011; Prusty et al., 2002; Sale et al., 1995) in mediating adipocyte differentiation, my results strengthened this notion since CRH and UCN2 increased phospho-ERK1/2/total ERK1/2 ratio in WT and *Crh* KO brown adipocytes (Figures 4.3-1 and 4.3-2).

Results of this thesis provide evidence of a novel positive correlation between CRH and Fyn kinase, which not only strengthens their role in regulating energy balance but also could be used as potential therapeutic targets to treat obesity and/or other metabolic disorders. The latter was evident from animals with genetic deletions of *Crh* or *Fyn kinase*, which display a lean phenotype with beneficial effects in whole-body insulin sensitivity, even under caloric excess (high-fat diet). The important role of Fyn kinase in promoting brown adipogenesis complements its fundamental role in controlling white adipogenesis. The former along with the anti-obesity effects of brown adipose tissue could consist of another plausible approach to increase brown adipose tissue activity and therefore whole-body energy expenditure.

References

Aird, F., Clevenger, C. V., Prystowsky, M. B. & Redei, E. 1993. Corticotropin-releasing factor mRNA in rat thymus and spleen. *Proc Natl Acad Sci U S A,* 90**,** 7104-8.

Altomare, D. A. & Khaled, A. R. 2012. Homeostasis and the importance for a balance between AKT/mTOR activity and intracellular signaling. *Curr Med Chem,* 19**,** 3748-62.

Anthonsen, M. W., Ronnstrand, L., Wernstedt, C., Degerman, E. & Holm, C. 1998. Identification of novel phosphorylation sites in hormone-sensitive lipase that are phosphorylated in response to isoproterenol and govern activation properties in vitro. *J Biol Chem,* 273**,** 215-21.

Anthony, N. M., Gaidhu, M. P. & Ceddia, R. B. 2009. Regulation of visceral and subcutaneous adipocyte lipolysis by acute AICAR-induced AMPK activation. *Obesity (Silver Spring),* 17**,** 1312-7.

Arase, K., York, D. A., Shimizu, H., Shargill, N. & Bray, G. A. 1988. Effects of corticotropin-releasing factor on food intake and brown adipose tissue thermogenesis in rats. *Am J Physiol,* 255**,** E255-9.

Arborelius, L., Owens, M. J., Plotsky, P. M. & Nemeroff, C. B. 1999. The role of corticotropin-releasing factor in depression and anxiety disorders. *J Endocrinol,* 160**,** 1-12.

Arner, P. 1995. Differences in lipolysis between human subcutaneous and omental adipose tissues. *Ann Med,* 27**,** 435-8.

Asano, T., Yao, Y., Shin, S., McCubrey, J., Abbruzzese, J. L. & Reddy, S. A. 2005. Insulin receptor substrate is a mediator of phosphoinositide 3-kinase activation in quiescent pancreatic cancer cells. *Cancer Res,* 65**,** 9164-8.

Atgie, C., D'Allaire, F. & Bukowiecki, L. J. 1997. Role of beta1- and beta3-adrenoceptors in the regulation of lipolysis and thermogenesis in rat brown adipocytes. *Am J Physiol,* 273**,** C1136-42.

Aune, U. L., Ruiz, L. & Kajimura, S. 2013. Isolation and differentiation of stromal vascular cells to beige/brite cells. *J Vis Exp*.

Bachman, E. S., Dhillon, H., Zhang, C. Y., Cinti, S., Bianco, A. C., Kobilka, B. K. & Lowell, B. B. 2002. betaAR signaling required for diet-induced thermogenesis and obesity resistance. *Science,* 297**,** 843-5.

Baigent, S. M. 2001. Peripheral corticotropin-releasing hormone and urocortin in the control of the immune response. *Peptides,* 22**,** 809-20.

Bale, T. L. 2005. Sensitivity to stress: dysregulation of CRF pathways and disease development. *Horm Behav,* 48**,** 1-10.

Bale, T. L., Anderson, K. R., Roberts, A. J., Lee, K. F., Nagy, T. R. & Vale, W. W. 2003. Corticotropin-releasing factor receptor-2-deficient mice display abnormal homeostatic responses to challenges of increased dietary fat and cold. *Endocrinology,* 144**,** 2580-7.

Bale, T. L., Contarino, A., Smith, G. W., Chan, R., Gold, L. H., Sawchenko, P. E., Koob, G. F., Vale, W. W. & Lee, K. F. 2000. Mice deficient for corticotropin-releasing hormone receptor-2 display anxiety-like behaviour and are hypersensitive to stress. *Nat Genet,* 24**,** 410-4.

Bale, T. L., Picetti, R., Contarino, A., Koob, G. F., Vale, W. W. & Lee, K. F. 2002. Mice deficient for both corticotropin-releasing factor receptor 1 (CRFR1) and CRFR2 have an impaired stress response and display sexually dichotomous anxiety-like behavior. *J Neurosci,* 22**,** 193-9.

Bale, T. L. & Vale, W. W. 2004. CRF and CRF receptors: role in stress responsivity and other behaviors. *Annu Rev Pharmacol Toxicol,* 44**,** 525-57.

Bastie, C. C., Zong, H., Xu, J., Busa, B., Judex, S., Kurland, I. J. & Pessin, J. E. 2007. Integrative metabolic regulation of peripheral tissue fatty acid oxidation by the SRC kinase family member Fyn. *Cell Metab,* 5**,** 371-81.

Belzung, C. & Griebel, G. 2001. Measuring normal and pathological anxiety-like behaviour in mice: a review. *Behav Brain Res,* 125**,** 141-9.

Benou, C., Wang, Y., Imitola, J., VanVlerken, L., Chandras, C., Karalis, K. P. & Khoury, S. J. 2005. Corticotropin-releasing hormone contributes to the

peripheral inflammatory response in experimental autoimmune encephalomyelitis. *J Immunol,* 174**,** 5407-13.

Berry, D. C., Stenesen, D., Zeve, D. & Graff, J. M. 2013. The developmental origins of adipose tissue. *Development,* 140**,** 3939-49.

Bjorntorp, P. 1991. Metabolic implications of body fat distribution. *Diabetes Care,* 14**,** 1132-43.

Bjorntorp, P., Gustafson, A. & Persson, B. 1971. Adipose tissue fat cell size and number in relation to metabolism in endogenous hypertriglyceridemia. *Acta Med Scand,* 190**,** 363-7.

Blake, R. A., Broome, M. A., Liu, X., Wu, J., Gishizky, M., Sun, L. & Courtneidge, S. A. 2000. SU6656, a selective src family kinase inhibitor, used to probe growth factor signaling. *Mol Cell Biol,* 20**,** 9018-27.

Blanchette-Mackie, E. J., Dwyer, N. K., Barber, T., Coxey, R. A., Takeda, T., Rondinone, C. M., Theodorakis, J. L., Greenberg, A. S. & Londos, C. 1995. Perilipin is located on the surface layer of intracellular lipid droplets in adipocytes. *J Lipid Res,* 36**,** 1211-26.

Boehme, S. A., Gaur, A., Crowe, P. D., Liu, X. J., Tamraz, S., Wong, T., Pahuja, A., Ling, N., Vale, W., De Souza, E. B. & Conlon, P. J. 1997. Immunosuppressive phenotype of corticotropin-releasing factor transgenic mice is reversed by adrenalectomy. *Cell Immunol,* 176**,** 103-12.

Boggon, T. J. & Eck, M. J. 2004. Structure and regulation of Src family kinases. *Oncogene,* 23**,** 7918-27.

Bornstein, S. R., Webster, E. L., Torpy, D. J., Richman, S. J., Mitsiades, N., Igel, M., Lewis, D. B., Rice, K. C., Joost, H. G., Tsokos, M. & Chrousos, G. P. 1998. Chronic effects of a nonpeptide corticotropin-releasing hormone type I receptor antagonist on pituitary-adrenal function, body weight, and metabolic regulation. *Endocrinology,* 139**,** 1546-55.

Bost, F., Aouadi, M., Caron, L., Even, P., Belmonte, N., Prot, M., Dani, C., Hofman, P., Pages, G., Pouyssegur, J., Le Marchand-Brustel, Y. & Binetruy, B. 2005. The extracellular signal-regulated kinase isoform ERK1 is specifically required for in vitro and in vivo adipogenesis. *Diabetes,* 54**,** 402-11.

Bost, F., Caron, L., Marchetti, I., Dani, C., Le Marchand-Brustel, Y. & Binetruy, B. 2002. Retinoic acid activation of the ERK pathway is required for embryonic stem cell commitment into the adipocyte lineage. *Biochem J,* 361**,** 621-7.

Boyda, H. N., Procyshyn, R. M., Pang, C. C. & Barr, A. M. 2013. Peripheral adrenoceptors: the impetus behind glucose dysregulation and insulin resistance. *J Neuroendocrinol,* 25**,** 217-28.

Bradbury, M. J., McBurnie, M. I., Denton, D. A., Lee, K. F. & Vale, W. W. 2000. Modulation of urocortin-induced hypophagia and weight loss by corticotropin-releasing factor receptor 1 deficiency in mice. *Endocrinology,* 141**,** 2715-24.

Brar, B. K., Chen, A., Perrin, M. H. & Vale, W. 2004a. Specificity and regulation of extracellularly regulated kinase1/2 phosphorylation through corticotropin-releasing factor (CRF) receptors 1 and 2beta by the CRF/urocortin family of peptides. *Endocrinology,* 145**,** 1718-29.

Brar, B. K., Jonassen, A. K., Egorina, E. M., Chen, A., Negro, A., Perrin, M. H., Mjos, O. D., Latchman, D. S., Lee, K. F. & Vale, W. 2004b. Urocortin-II and urocortin-III are cardioprotective against ischemia reperfusion injury: an essential endogenous cardioprotective role for corticotropin releasing factor receptor type 2 in the murine heart. *Endocrinology,* 145**,** 24-35; discussion 21-3.

Brickell, P. M. 1992. The p60c-src family of protein-tyrosine kinases: structure, regulation, and function. *Crit Rev Oncog,* 3**,** 401-46.

Britton, K. T., Lee, G., Vale, W., Rivier, J. & Koob, G. F. 1986. Corticotropin releasing factor (CRF) receptor antagonist blocks activating and 'anxiogenic' actions of CRF in the rat. *Brain Res,* 369**,** 303-6.

Brown, M. R., Fisher, L. A., Rivier, J., Spiess, J., Rivier, C. & Vale, W. 1982. Corticotropin-releasing factor: effects on the sympathetic nervous system and oxygen consumption. *Life Sci,* 30**,** 207-10.

Bruhn, T. O., Engeland, W. C., Anthony, E. L., Gann, D. S. & Jackson, I. M. 1987. Corticotropin-releasing factor in the adrenal medulla. *Ann N Y Acad Sci,* 512**,** 115-28.

Bull, H. A., Brickell, P. M. & Dowd, P. M. 1994. Src-related protein tyrosine kinases are physically associated with the surface antigen CD36 in human dermal microvascular endothelial cells. *FEBS Lett,* 351**,** 41-4.

Buren, J., Lai, Y. C., Lundgren, M., Eriksson, J. W. & Jensen, J. 2008. Insulin action and signalling in fat and muscle from dexamethasone-treated rats. *Arch Biochem Biophys,* 474**,** 91-101.

Buren, J., Liu, H. X., Jensen, J. & Eriksson, J. W. 2002. Dexamethasone impairs insulin signalling and glucose transport by depletion of insulin receptor substrate-1, phosphatidylinositol 3-kinase and protein kinase B in primary cultured rat adipocytes. *Eur J Endocrinol,* 146**,** 419-29.

Buwalda, B., de Boer, S. F., Van Kalkeren, A. A. & Koolhaas, J. M. 1997. Physiological and behavioral effects of chronic intracerebroventricular infusion of corticotropin-releasing factor in the rat. *Psychoneuroendocrinology,* 22**,** 297-309.

Buyse, M., Viengchareun, S., Bado, A. & Lombes, M. 2001. Insulin and glucocorticoids differentially regulate leptin transcription and secretion in brown adipocytes. *FASEB J,* 15**,** 1357-66.

Cannon, B. & Nedergaard, J. 2004. Brown adipose tissue: function and physiological significance. *Physiol Rev,* 84**,** 277-359.

Cantarella, G., Lempereur, L., Lombardo, G., Chiarenza, A., Pafumi, C., Zappala, G. & Bernardini, R. 2001. Divergent effects of corticotropin releasing hormone on endothelial cell nitric oxide synthase are associated with different expression of CRH type 1 and 2 receptors. *Br J Pharmacol,* 134**,** 837-44.

Cao, L., Choi, E. Y., Liu, X., Martin, A., Wang, C., Xu, X. & During, M. J. 2011. White to brown fat phenotypic switch induced by genetic and environmental activation of a hypothalamic-adipocyte axis. *Cell Metab,* 14**,** 324-38.

Cao, W., Medvedev, A. V., Daniel, K. W. & Collins, S. 2001. beta-Adrenergic activation of p38 MAP kinase in adipocytes: cAMP induction of the uncoupling protein 1 (UCP1) gene requires p38 MAP kinase. *J Biol Chem,* 276**,** 27077-82.

Carey, A. L., Formosa, M. F., Van Every, B., Bertovic, D., Eikelis, N., Lambert, G. W., Kalff, V., Duffy, S. J., Cherk, M. H. & Kingwell, B. A. 2013. Ephedrine

activates brown adipose tissue in lean but not obese humans. *Diabetologia,* 56**,** 147-55.

Carlin, K. M., Vale, W. W. & Bale, T. L. 2006. Vital functions of corticotropin-releasing factor (CRF) pathways in maintenance and regulation of energy homeostasis. *Proc Natl Acad Sci U S A,* 103**,** 3462-7.

Carr, D. J., DeCosta, B. R., Jacobson, A. E., Rice, K. C. & Blalock, J. E. 1990. Corticotropin-releasing hormone augments natural killer cell activity through a naloxone-sensitive pathway. *J Neuroimmunol,* 28**,** 53-61.

Chandras, C., Koutmani, Y., Kokkotou, E., Pothoulakis, C. & Karalis, K. P. 2009. Activation of phosphatidylinositol 3-kinase/protein kinase B by corticotropin-releasing factor in human monocytes. *Endocrinology,* 150**,** 4606-14.

Chang, C. P., Pearse, R. V., 2nd, O'Connell, S. & Rosenfeld, M. G. 1993. Identification of a seven transmembrane helix receptor for corticotropin-releasing factor and sauvagine in mammalian brain. *Neuron,* 11**,** 1187-95.

Chatterton, B. E., Mensforth, D., Coventry, B. J. & Cohen, P. 2002. Hibernoma: intense uptake seen on Tc-99m tetrofosmin and FDG positron emission tomographic scanning. *Clin Nucl Med,* 27**,** 369-70.

Chaudhry, A. & Granneman, J. G. 1999. Differential regulation of functional responses by beta-adrenergic receptor subtypes in brown adipocytes. *Am J Physiol,* 277**,** R147-53.

Cheatham, B., Vlahos, C. J., Cheatham, L., Wang, L., Blenis, J. & Kahn, C. R. 1994. Phosphatidylinositol 3-kinase activation is required for insulin stimulation of pp70 S6 kinase, DNA synthesis, and glucose transporter translocation. *Mol Cell Biol,* 14**,** 4902-11.

Chen, A., Blount, A., Vaughan, J., Brar, B. & Vale, W. 2004a. Urocortin II gene is highly expressed in mouse skin and skeletal muscle tissues: localization, basal expression in corticotropin-releasing factor receptor (CRFR) 1- and CRFR2-null mice, and regulation by glucocorticoids. *Endocrinology,* 145**,** 2445-57.

Chen, A., Brar, B., Choi, C. S., Rousso, D., Vaughan, J., Kuperman, Y., Kim, S. N., Donaldson, C., Smith, S. M., Jamieson, P., Li, C., Nagy, T. R., Shulman, G. I.,

Lee, K. F. & Vale, W. 2006. Urocortin 2 modulates glucose utilization and insulin sensitivity in skeletal muscle. *Proc Natl Acad Sci U S A,* 103**,** 16580-5.

Chen, A., Perrin, M., Brar, B., Li, C., Jamieson, P., Digruccio, M., Lewis, K. & Vale, W. 2005. Mouse corticotropin-releasing factor receptor type 2alpha gene: isolation, distribution, pharmacological characterization and regulation by stress and glucocorticoids. *Mol Endocrinol,* 19**,** 441-58.

Chen, F. M., Bilezikjian, L. M., Perrin, M. H., Rivier, J. & Vale, W. 1986. Corticotropin releasing factor receptor-mediated stimulation of adenylate cyclase activity in the rat brain. *Brain Res,* 381**,** 49-57.

Chen, G., Bower, K. A., Ma, C., Fang, S., Thiele, C. J. & Luo, J. 2004b. Glycogen synthase kinase 3beta (GSK3beta) mediates 6-hydroxydopamine-induced neuronal death. *FASEB J,* 18**,** 1162-4.

Chen, R., Lewis, K. A., Perrin, M. H. & Vale, W. W. 1993. Expression cloning of a human corticotropin-releasing-factor receptor. *Proc Natl Acad Sci U S A,* 90**,** 8967-71.

Chondronikola, M., Volpi, E., Borsheim, E., Porter, C., Annamalai, P., Enerback, S., Lidell, M. E., Saraf, M. K., Labbe, S. M., Hurren, N. M., Yfanti, C., Chao, T., Andersen, C. R., Cesani, F., Hawkins, H. & Sidossis, L. S. 2014. Brown adipose tissue improves whole-body glucose homeostasis and insulin sensitivity in humans. *Diabetes,* 63**,** 4089-99.

Chotiwat, C., Kelso, E. W. & Harris, R. B. 2010. The effects of repeated restraint stress on energy balance and behavior of mice with selective deletion of CRF receptors. *Stress,* 13**,** 203-13.

Chrousos, G. P. & Gold, P. W. 1992. The concepts of stress and stress system disorders. Overview of physical and behavioral homeostasis. *JAMA,* 267**,** 1244-52.

Cicha, I., Zitzmann, R. & Goppelt-Struebe, M. 2014. Dual inhibition of Src family kinases and Aurora kinases by SU6656 modulates CTGF (connective tissue growth factor) expression in an ERK-dependent manner. *Int J Biochem Cell Biol,* 46**,** 39-48.

Coll, A. P., Challis, B. G., Lopez, M., Piper, S., Yeo, G. S. & O'Rahilly, S. 2005. Proopiomelanocortin-deficient mice are hypersensitive to the adverse metabolic effects of glucocorticoids. *Diabetes,* 54**,** 2269-76.

Collins, S., Daniel, K. W., Petro, A. E. & Surwit, R. S. 1997. Strain-specific response to beta 3-adrenergic receptor agonist treatment of diet-induced obesity in mice. *Endocrinology,* 138**,** 405-13.

Collins, S., Daniel, K. W., Rohlfs, E. M., Ramkumar, V., Taylor, I. L. & Gettys, T. W. 1994. Impaired expression and functional activity of the beta 3- and beta 1-adrenergic receptors in adipose tissue of congenitally obese (C57BL/6J ob/ob) mice. *Mol Endocrinol,* 8**,** 518-27.

Connolly, E., Nanberg, E. & Nedergaard, J. 1986. Norepinephrine-induced Na+ influx in brown adipocytes is cyclic AMP-mediated. *J Biol Chem,* 261**,** 14377-85.

Contarino, A., Dellu, F., Koob, G. F., Smith, G. W., Lee, K. F., Vale, W. W. & Gold, L. H. 2000. Dissociation of locomotor activation and suppression of food intake induced by CRF in CRFR1-deficient mice. *Endocrinology,* 141**,** 2698-702.

Cooke, M. P. & Perlmutter, R. M. 1989. Expression of a novel form of the fyn proto-oncogene in hematopoietic cells. *New Biol,* 1**,** 66-74.

Coste, S. C., Kesterson, R. A., Heldwein, K. A., Stevens, S. L., Heard, A. D., Hollis, J. H., Murray, S. E., Hill, J. K., Pantely, G. A., Hohimer, A. R., Hatton, D. C., Phillips, T. J., Finn, D. A., Low, M. J., Rittenberg, M. B., Stenzel, P. & Stenzel-Poore, M. P. 2000. Abnormal adaptations to stress and impaired cardiovascular function in mice lacking corticotropin-releasing hormone receptor-2. *Nat Genet,* 24**,** 403-9.

Cousin, B., Cinti, S., Morroni, M., Raimbault, S., Ricquier, D., Penicaud, L. & Casteilla, L. 1992. Occurrence of brown adipocytes in rat white adipose tissue: molecular and morphological characterization. *J Cell Sci,* 103 (Pt 4)**,** 931-42.

Crofford, L. J., Sano, H., Karalis, K., Webster, E. L., Goldmuntz, E. A., Chrousos, G. P. & Wilder, R. L. 1992. Local secretion of corticotropin-releasing hormone in the joints of Lewis rats with inflammatory arthritis. *J Clin Invest,* 90**,** 2555-64.

Cullen, M. J., Ling, N., Foster, A. C. & Pelleymounter, M. A. 2001. Urocortin, corticotropin releasing factor-2 receptors and energy balance. *Endocrinology,* 142**,** 992-9.

Cuneo, K. C., Geng, L., Tan, J., Brousal, J., Shinohara, E. T., Osusky, K., Fu, A., Shyr, Y., Wu, H. & Hallahan, D. E. 2006. SRC family kinase inhibitor SU6656 enhances antiangiogenic effect of irradiation. *Int J Radiat Oncol Biol Phys,* 64**,** 1197-203.

Cypess, A. M., Chen, Y. C., Sze, C., Wang, K., English, J., Chan, O., Holman, A. R., Tal, I., Palmer, M. R., Kolodny, G. M. & Kahn, C. R. 2012. Cold but not sympathomimetics activates human brown adipose tissue in vivo. *Proc Natl Acad Sci U S A,* 109**,** 10001-5.

Cypess, A. M., Haft, C. R., Laughlin, M. R. & Hu, H. H. 2014. Brown fat in humans: consensus points and experimental guidelines. *Cell Metab,* 20**,** 408-15.

Cypess, A. M., Lehman, S., Williams, G., Tal, I., Rodman, D., Goldfine, A. B., Kuo, F. C., Palmer, E. L., Tseng, Y. H., Doria, A., Kolodny, G. M. & Kahn, C. R. 2009. Identification and importance of brown adipose tissue in adult humans. *N Engl J Med,* 360**,** 1509-17.

Cypess, A. M., Weiner, L. S., Roberts-Toler, C., Franquet Elia, E., Kessler, S. H., Kahn, P. A., English, J., Chatman, K., Trauger, S. A., Doria, A. & Kolodny, G. M. 2015. Activation of human brown adipose tissue by a beta3-adrenergic receptor agonist. *Cell Metab,* 21**,** 33-8.

Cypess, A. M., White, A. P., Vernochet, C., Schulz, T. J., Xue, R., Sass, C. A., Huang, T. L., Roberts-Toler, C., Weiner, L. S., Sze, C., Chacko, A. T., Deschamps, L. N., Herder, L. M., Truchan, N., Glasgow, A. L., Holman, A. R., Gavrila, A., Hasselgren, P. O., Mori, M. A., Molla, M. & Tseng, Y. H. 2013. Anatomical localization, gene expression profiling and functional characterization of adult human neck brown fat. *Nat Med,* 19**,** 635-9.

de Kloet, E. R., Joels, M. & Holsboer, F. 2005. Stress and the brain: from adaptation to disease. *Nat Rev Neurosci,* 6**,** 463-75.

Deng, W., Wang, X., Xiao, J., Chen, K., Zhou, H., Shen, D., Li, H. & Tang, Q. 2012. Loss of regulator of G protein signaling 5 exacerbates obesity, hepatic steatosis, inflammation and insulin resistance. *PLoS One,* 7**,** e30256.

Despres, J. P., Lemieux, S., Lamarche, B., Prud'homme, D., Moorjani, S., Brun, L. D., Gagne, C. & Lupien, P. J. 1995. The insulin resistance-dyslipidemic syndrome: contribution of visceral obesity and therapeutic implications. *Int J Obes Relat Metab Disord,* 19 Suppl 1**,** S76-86.

Donzelli, E., Lucchini, C., Ballarini, E., Scuteri, A., Carini, F., Tredici, G. & Miloso, M. 2011. ERK1 and ERK2 are involved in recruitment and maturation of human mesenchymal stem cells induced to adipogenic differentiation. *J Mol Cell Biol,* 3**,** 123-31.

Ducarouge, B., Pelissier-Rota, M., Laine, M., Cristina, N., Vachez, Y., Scoazec, J. Y., Bonaz, B. & Jacquier-Sarlin, M. 2013. CRF2 signaling is a novel regulator of cellular adhesion and migration in colorectal cancer cells. *PLoS One,* 8**,** e79335.

Duncan, J. G., Fong, J. L., Medeiros, D. M., Finck, B. N. & Kelly, D. P. 2007. Insulin-resistant heart exhibits a mitochondrial biogenic response driven by the peroxisome proliferator-activated receptor-alpha/PGC-1alpha gene regulatory pathway. *Circulation,* 115**,** 909-17.

Dunn, A. J. & Swiergiel, A. H. 1999. Behavioral responses to stress are intact in CRF-deficient mice. *Brain Res,* 845**,** 14-20.

Dykstra, M., Cherukuri, A., Sohn, H. W., Tzeng, S. J. & Pierce, S. K. 2003. Location is everything: lipid rafts and immune cell signaling. *Annu Rev Immunol,* 21**,** 457-81.

Egan, J. J., Greenberg, A. S., Chang, M. K., Wek, S. A., Moos, M. C., Jr. & Londos, C. 1992. Mechanism of hormone-stimulated lipolysis in adipocytes: translocation of hormone-sensitive lipase to the lipid storage droplet. *Proc Natl Acad Sci U S A,* 89**,** 8537-41.

Ekman, R., Servenius, B., Castro, M. G., Lowry, P. J., Cederlund, A. S., Bergman, O. & Sjogren, H. O. 1993. Biosynthesis of corticotropin-releasing hormone in human T-lymphocytes. *J Neuroimmunol,* 44**,** 7-13.

Enerback, S., Jacobsson, A., Simpson, E. M., Guerra, C., Yamashita, H., Harper, M. E. & Kozak, L. P. 1997. Mice lacking mitochondrial uncoupling protein are cold-sensitive but not obese. *Nature,* 387**,** 90-4.

Fabbri, A., Tinajero, J. C. & Dufau, M. L. 1990. Corticotropin-releasing factor is produced by rat Leydig cells and has a major local antireproductive role in the testis. *Endocrinology,* 127**,** 1541-3.

Feldmann, H. M., Golozoubova, V., Cannon, B. & Nedergaard, J. 2009. UCP1 ablation induces obesity and abolishes diet-induced thermogenesis in mice exempt from thermal stress by living at thermoneutrality. *Cell Metab,* 9**,** 203-9.

Fisher, F. M., Kleiner, S., Douris, N., Fox, E. C., Mepani, R. J., Verdeguer, F., Wu, J., Kharitonenkov, A., Flier, J. S., Maratos-Flier, E. & Spiegelman, B. M. 2012. FGF21 regulates PGC-1alpha and browning of white adipose tissues in adaptive thermogenesis. *Genes Dev,* 26**,** 271-81.

Garcia-Martin, A., Acitores, A., Maycas, M., Villanueva-Penacarrillo, M. L. & Esbrit, P. 2013. Src kinases mediate VEGFR2 transactivation by the osteostatin domain of PTHrP to modulate osteoblastic function. *J Cell Biochem,* 114**,** 1404-13.

Garofalo, R. S., Orena, S. J., Rafidi, K., Torchia, A. J., Stock, J. L., Hildebrandt, A. L., Coskran, T., Black, S. C., Brees, D. J., Wicks, J. R., McNeish, J. D. & Coleman, K. G. 2003. Severe diabetes, age-dependent loss of adipose tissue, and mild growth deficiency in mice lacking Akt2/PKB beta. *J Clin Invest,* 112**,** 197-208.

Garton, A. J. & Yeaman, S. J. 1990. Identification and role of the basal phosphorylation site on hormone-sensitive lipase. *Eur J Biochem,* 191**,** 245-50.

Gasparetti, A. L., de Souza, C. T., Pereira-da-Silva, M., Oliveira, R. L., Saad, M. J., Carneiro, E. M. & Velloso, L. A. 2003. Cold exposure induces tissue-specific modulation of the insulin-signalling pathway in Rattus norvegicus. *J Physiol,* 552**,** 149-62.

Geerling, J. J., Boon, M. R., van der Zon, G. C., van den Berg, S. A., van den Hoek, A. M., Lombes, M., Princen, H. M., Havekes, L. M., Rensen, P. C. & Guigas, B. 2014. Metformin lowers plasma triglycerides by promoting VLDL-triglyceride clearance by brown adipose tissue in mice. *Diabetes,* 63**,** 880-91.

Gesta, S., Tseng, Y. H. & Kahn, C. R. 2007. Developmental origin of fat: tracking obesity to its source. *Cell,* 131**,** 242-56.

Ghosh, P. M., Shu, Z. J., Zhu, B., Lu, Z., Ikeno, Y., Barnes, J. L., Yeh, C. K., Zhang, B. X., Katz, M. S. & Kamat, A. 2012. Role of beta-adrenergic receptors in regulation of hepatic fat accumulation during aging. *J Endocrinol,* 213**,** 251-61.

Giorgino, F., Almahfouz, A., Goodyear, L. J. & Smith, R. J. 1993. Glucocorticoid regulation of insulin receptor and substrate IRS-1 tyrosine phosphorylation in rat skeletal muscle in vivo. *J Clin Invest,* 91**,** 2020-30.

Girousse, A., Tavernier, G., Valle, C., Moro, C., Mejhert, N., Dinel, A. L., Houssier, M., Roussel, B., Besse-Patin, A., Combes, M., Mir, L., Monbrun, L., Bezaire, V., Prunet-Marcassus, B., Waget, A., Vila, I., Caspar-Bauguil, S., Louche, K., Marques, M. A., Mairal, A., Renoud, M. L., Galitzky, J., Holm, C., Mouisel, E., Thalamas, C., Viguerie, N., Sulpice, T., Burcelin, R., Arner, P. & Langin, D. 2013. Partial inhibition of adipose tissue lipolysis improves glucose metabolism and insulin sensitivity without alteration of fat mass. *PLoS Biol,* 11**,** e1001485.

Goldsmith, J. F., Hall, C. G. & Atkinson, T. P. 2002. Identification of an alternatively spliced isoform of the fyn tyrosine kinase. *Biochem Biophys Res Commun,* 298**,** 501-4.

Gonzalez, E. & McGraw, T. E. 2009. The Akt kinases: isoform specificity in metabolism and cancer. *Cell Cycle,* 8**,** 2502-8.

Gonzalez, R., Ruiz-Leon, Y., Gomendio, M. & Roldan, E. R. 2010. The effect of glucocorticoids on ERK-1/2 phosphorylation during maturation of lamb oocytes and their subsequent fertilization and cleavage ability in vitro. *Reprod Toxicol,* 29**,** 198-205.

Grammatopoulos, D. K. 2012. Insights into mechanisms of corticotropin-releasing hormone receptor signal transduction. *Br J Pharmacol,* 166**,** 85-97.

Grammatopoulos, D. K. & Chrousos, G. P. 2002. Functional characteristics of CRH receptors and potential clinical applications of CRH-receptor antagonists. *Trends Endocrinol Metab,* 13**,** 436-44.

Grammatopoulos, D. K., Dai, Y., Randeva, H. S., Levine, M. A., Karteris, E., Easton, A. J. & Hillhouse, E. W. 1999. A novel spliced variant of the type 1 corticotropin-releasing hormone receptor with a deletion in the seventh transmembrane domain present in the human pregnant term myometrium and fetal membranes. *Mol Endocrinol,* 13**,** 2189-202.

Grammatopoulos, D. K., Randeva, H. S., Levine, M. A., Kanellopoulou, K. A. & Hillhouse, E. W. 2001. Rat cerebral cortex corticotropin-releasing hormone receptors: evidence for receptor coupling to multiple G-proteins. *J Neurochem,* 76**,** 509-19.

Granneman, J. G. & Lahners, K. N. 1992. Differential adrenergic regulation of beta 1- and beta 3-adrenoreceptor messenger ribonucleic acids in adipose tissues. *Endocrinology,* 130**,** 109-14.

Granneman, J. G., Moore, H. P., Granneman, R. L., Greenberg, A. S., Obin, M. S. & Zhu, Z. 2007. Analysis of lipolytic protein trafficking and interactions in adipocytes. *J Biol Chem,* 282**,** 5726-35.

Grauer, W. O., Moss, A. A., Cann, C. E. & Goldberg, H. I. 1984. Quantification of body fat distribution in the abdomen using computed tomography. *Am J Clin Nutr,* 39**,** 631-7.

Green, H. & Meuth, M. 1974. An established pre-adipose cell line and its differentiation in culture. *Cell,* 3**,** 127-33.

Greenberg, A. K., Hu, J., Basu, S., Hay, J., Reibman, J., Yie, T. A., Tchou-Wong, K. M., Rom, W. N. & Lee, T. C. 2002. Glucocorticoids inhibit lung cancer cell growth through both the extracellular signal-related kinase pathway and cell cycle regulators. *Am J Respir Cell Mol Biol,* 27**,** 320-8.

Greenberg, A. S., Shen, W. J., Muliro, K., Patel, S., Souza, S. C., Roth, R. A. & Kraemer, F. B. 2001. Stimulation of lipolysis and hormone-sensitive lipase via the extracellular signal-regulated kinase pathway. *J Biol Chem,* 276**,** 45456-61.

Gregoire, F. M., Smas, C. M. & Sul, H. S. 1998. Understanding adipocyte differentiation. *Physiol Rev,* 78**,** 783-809.

Haemmerle, G., Zimmermann, R., Hayn, M., Theussl, C., Waeg, G., Wagner, E., Sattler, W., Magin, T. M., Wagner, E. F. & Zechner, R. 2002. Hormone-sensitive lipase deficiency in mice causes diglyceride accumulation in adipose tissue, muscle, and testis. *J Biol Chem,* 277**,** 4806-15.

Hamann, A., Benecke, H., Greten, H. & Matthaei, S. 1993. Metformin increases glucose transporter protein and gene expression in human fibroblasts. *Biochem Biophys Res Commun,* 196**,** 382-7.

Hamann, A., Benecke, H., Le Marchand-Brustel, Y., Susulic, V. S., Lowell, B. B. & Flier, J. S. 1995. Characterization of insulin resistance and NIDDM in transgenic mice with reduced brown fat. *Diabetes,* 44**,** 1266-73.

Hamdy, O., Porramatikul, S. & Al-Ozairi, E. 2006. Metabolic obesity: the paradox between visceral and subcutaneous fat. *Curr Diabetes Rev,* 2**,** 367-73.

Han, S., Bui, N. T., Ho, M. T., Kim, Y. M., Cho, M. & Shin, D. B. 2015. Dexamethasone Inhibits TGF-beta1-induced Cell Migration by Regulating the ERK and AKT Pathways in Human Colon Cancer Cells Via CYR61. *Cancer Res Treat*.

Hany, T. F., Gharehpapagh, E., Kamel, E. M., Buck, A., Himms-Hagen, J. & von Schulthess, G. K. 2002. Brown adipose tissue: a factor to consider in symmetrical tracer uptake in the neck and upper chest region. *Eur J Nucl Med Mol Imaging,* 29**,** 1393-8.

Hara, K., Yonezawa, K., Sakaue, H., Ando, A., Kotani, K., Kitamura, T., Kitamura, Y., Ueda, H., Stephens, L., Jackson, T. R. & et al. 1994. 1-Phosphatidylinositol 3-kinase activity is required for insulin-stimulated glucose transport but not for RAS activation in CHO cells. *Proc Natl Acad Sci U S A,* 91**,** 7415-9.

Harada, S., Imaki, T., Naruse, M., Chikada, N., Nakajima, K. & Demura, H. 1999. Urocortin mRNA is expressed in the enteric nervous system of the rat. *Neurosci Lett,* 267**,** 125-8.

Harper, J. M. & Austad, S. N. 2000. Fecal glucocorticoids: a noninvasive method of measuring adrenal activity in wild and captive rodents. *Physiol Biochem Zool,* 73**,** 12-22.

Harr, M. W., McColl, K. S., Zhong, F., Molitoris, J. K. & Distelhorst, C. W. 2010. Glucocorticoids downregulate Fyn and inhibit IP(3)-mediated calcium signaling to promote autophagy in T lymphocytes. *Autophagy,* 6**,** 912-21.

Heinrichs, S. C. & Koob, G. F. 2004. Corticotropin-releasing factor in brain: a role in activation, arousal, and affect regulation. *J Pharmacol Exp Ther,* 311**,** 427-40.

Hernandez, R., Teruel, T. & Lorenzo, M. 2001. Akt mediates insulin induction of glucose uptake and up-regulation of GLUT4 gene expression in brown adipocytes. *FEBS Lett,* 494**,** 225-31.

Hillhouse, E. W. & Grammatopoulos, D. K. 2006. The molecular mechanisms underlying the regulation of the biological activity of corticotropin-releasing hormone receptors: implications for physiology and pathophysiology. *Endocr Rev,* 27**,** 260-86.

Hillhouse, E. W., Randeva, H., Ladds, G. & Grammatopoulos, D. 2002. Corticotropin-releasing hormone receptors. *Biochem Soc Trans,* 30**,** 428-32.

Holden, N. S., Bell, M. J., Rider, C. F., King, E. M., Gaunt, D. D., Leigh, R., Johnson, M., Siderovski, D. P., Heximer, S. P., Giembycz, M. A. & Newton, R. 2011. beta2-Adrenoceptor agonist-induced RGS2 expression is a genomic mechanism of bronchoprotection that is enhanced by glucocorticoids. *Proc Natl Acad Sci U S A,* 108**,** 19713-8.

Holden, N. S., George, T., Rider, C. F., Chandrasekhar, A., Shah, S., Kaur, M., Johnson, M., Siderovski, D. P., Leigh, R., Giembycz, M. A. & Newton, R. 2014. Induction of regulator of G-protein signaling 2 expression by long-acting beta2-adrenoceptor agonists and glucocorticoids in human airway epithelial cells. *J Pharmacol Exp Ther,* 348**,** 12-24.

Holmes, A., Heilig, M., Rupniak, N. M., Steckler, T. & Griebel, G. 2003. Neuropeptide systems as novel therapeutic targets for depression and anxiety disorders. *Trends Pharmacol Sci,* 24**,** 580-8.

Holsboer, F. 1999. The rationale for corticotropin-releasing hormone receptor (CRH-R) antagonists to treat depression and anxiety. *J Psychiatr Res,* 33**,** 181-214.

Hsu, S. Y. & Hsueh, A. J. 2001. Human stresscopin and stresscopin-related peptide are selective ligands for the type 2 corticotropin-releasing hormone receptor. *Nat Med,* 7**,** 605-11.

https://www.jax.org/strain/002783.

Huang, M., Kempuraj, D., Papadopoulou, N., Kourelis, T., Donelan, J., Manola, A. & Theoharides, T. C. 2009. Urocortin induces interleukin-6 release from rat cardiomyocytes through p38 MAP kinase, ERK and NF-kappaB activation. *J Mol Endocrinol,* 42**,** 397-405.

Huang, M. M., Bolen, J. B., Barnwell, J. W., Shattil, S. J. & Brugge, J. S. 1991. Membrane glycoprotein IV (CD36) is physically associated with the Fyn, Lyn,

and Yes protein-tyrosine kinases in human platelets. *Proc Natl Acad Sci U S A,* 88**,** 7844-8.

Iankova, I., Chavey, C., Clape, C., Colomer, C., Guerineau, N. C., Grillet, N., Brunet, J. F., Annicotte, J. S. & Fajas, L. 2008. Regulator of G protein signaling-4 controls fatty acid and glucose homeostasis. *Endocrinology,* 149**,** 5706-12.

Ishibashi, J. & Seale, P. 2010. Medicine. Beige can be slimming. *Science,* 328**,** 1113-4.

Jamieson, P. M., Cleasby, M. E., Kuperman, Y., Morton, N. M., Kelly, P. A., Brownstein, D. G., Mustard, K. J., Vaughan, J. M., Carter, R. N., Hahn, C. N., Hardie, D. G., Seckl, J. R., Chen, A. & Vale, W. W. 2011. Urocortin 3 transgenic mice exhibit a metabolically favourable phenotype resisting obesity and hyperglycaemia on a high-fat diet. *Diabetologia,* 54**,** 2392-403.

Jaworski, K., Sarkadi-Nagy, E., Duncan, R. E., Ahmadian, M. & Sul, H. S. 2007. Regulation of triglyceride metabolism. IV. Hormonal regulation of lipolysis in adipose tissue. *Am J Physiol Gastrointest Liver Physiol,* 293**,** G1-4.

Jessop, D. S., Harbuz, M. S., Snelson, C. L., Dayan, C. M. & Lightman, S. L. 1997. An antisense oligodeoxynucleotide complementary to corticotropin-releasing hormone mRNA inhibits rat splenocyte proliferation in vitro. *J Neuroimmunol,* 75**,** 135-40.

Jessop, D. S., Renshaw, D., Lightman, S. L. & Harbuz, M. S. 1995. Changes in ACTH and beta-endorphin immunoreactivity in immune tissues during a chronic inflammatory stress are not correlated with changes in corticotropin-releasing hormone and arginine vasopressin. *J Neuroimmunol,* 60**,** 29-35.

Jin, L., Zhang, Q., Guo, R., Wang, L., Wang, J., Wan, R., Zhang, R., Xu, Y. & Li, S. 2011. Different effects of corticotropin-releasing factor and urocortin 2 on apoptosis of prostate cancer cells in vitro. *J Mol Endocrinol,* 47**,** 219-27.

Johannsson, G. & Bengtsson, B. A. 1999. Growth hormone and the metabolic syndrome. *J Endocrinol Invest,* 22**,** 41-6.

Kageyama, K., Bradbury, M. J., Zhao, L., Blount, A. L. & Vale, W. W. 1999. Urocortin messenger ribonucleic acid: tissue distribution in the rat and regulation in thymus by lipopolysaccharide and glucocorticoids. *Endocrinology,* 140**,** 5651-8.

Kageyama, K., Hanada, K. & Suda, T. 2010. Differential regulation and roles of urocortins in human adrenal H295R cells. *Regul Pept,* 162**,** 18-25.

Kajimura, S. & Saito, M. 2014. A new era in brown adipose tissue biology: molecular control of brown fat development and energy homeostasis. *Annu Rev Physiol,* 76**,** 225-49.

Kajimura, S., Seale, P. & Spiegelman, B. M. 2010. Transcriptional control of brown fat development. *Cell Metab,* 11**,** 257-62.

Kajimura, S., Spiegelman, B. M. & Seale, P. 2015. Brown and Beige Fat: Physiological Roles beyond Heat Generation. *Cell Metab,* 22**,** 546-59.

Karalis, K., Sano, H., Redwine, J., Listwak, S., Wilder, R. L. & Chrousos, G. P. 1991. Autocrine or paracrine inflammatory actions of corticotropin-releasing hormone in vivo. *Science,* 254**,** 421-3.

Karalis, K. P., Kontopoulos, E., Muglia, L. J. & Majzoub, J. A. 1999. Corticotropin-releasing hormone deficiency unmasks the proinflammatory effect of epinephrine. *Proc Natl Acad Sci U S A,* 96**,** 7093-7.

Karlsson, M., Contreras, J. A., Hellman, U., Tornqvist, H. & Holm, C. 1997. cDNA cloning, tissue distribution, and identification of the catalytic triad of monoglyceride lipase. Evolutionary relationship to esterases, lysophospholipases, and haloperoxidases. *J Biol Chem,* 272**,** 27218-23.

Karp, C. L. 2012. Unstressing intemperate models: how cold stress undermines mouse modeling. *J Exp Med,* 209**,** 1069-74.

Karteris, E., Hillhouse, E. W. & Grammatopoulos, D. 2004. Urocortin II is expressed in human pregnant myometrial cells and regulates myosin light chain phosphorylation: potential role of the type-2 corticotropin-releasing hormone receptor in the control of myometrial contractility. *Endocrinology,* 145**,** 890-900.

Kefalas, P., Brown, T. R. & Brickell, P. M. 1995. Signalling by the p60c-src family of protein-tyrosine kinases. *Int J Biochem Cell Biol,* 27**,** 551-63.

Kiang, J. G. 1997. Corticotropin-releasing factor-like peptides increase cytosolic [Ca2+] in human epidermoid A-431 cells. *Eur J Pharmacol,* 329**,** 237-44.

Kishimoto, T., Radulovic, J., Radulovic, M., Lin, C. R., Schrick, C., Hooshmand, F., Hermanson, O., Rosenfeld, M. G. & Spiess, J. 2000. Deletion of crhr2 reveals an anxiolytic role for corticotropin-releasing hormone receptor-2. *Nat Genet,* 24**,** 415-9.

Klinger, M., Kudlacek, O., Seidel, M. G., Freissmuth, M. & Sexl, V. 2002. MAP kinase stimulation by cAMP does not require RAP1 but SRC family kinases. *J Biol Chem,* 277**,** 32490-7.

Kostich, W. A., Chen, A., Sperle, K. & Largent, B. L. 1998. Molecular identification and analysis of a novel human corticotropin-releasing factor (CRF) receptor: the CRF2gamma receptor. *Mol Endocrinol,* 12**,** 1077-85.

Kotz, C. M., Wang, C., Levine, A. S. & Billington, C. J. 2002. Urocortin in the hypothalamic PVN increases leptin and affects uncoupling proteins-1 and -3 in rats. *Am J Physiol Regul Integr Comp Physiol,* 282**,** R546-51.

Krahn, D. D., Gosnell, B. A. & Majchrzak, M. J. 1990. The anorectic effects of CRH and restraint stress decrease with repeated exposures. *Biol Psychiatry,* 27**,** 1094-102.

Krief, S., Lonnqvist, F., Raimbault, S., Baude, B., Van Spronsen, A., Arner, P., Strosberg, A. D., Ricquier, D. & Emorine, L. J. 1993. Tissue distribution of beta 3-adrenergic receptor mRNA in man. *J Clin Invest,* 91**,** 344-9.

Kumar, S., Allen, D. A., Kieswich, J. E., Patel, N. S., Harwood, S., Mazzon, E., Cuzzocrea, S., Raftery, M. J., Thiemermann, C. & Yaqoob, M. M. 2009. Dexamethasone ameliorates renal ischemia-reperfusion injury. *J Am Soc Nephrol,* 20**,** 2412-25.

Kuperman, Y. & Chen, A. 2008. Urocortins: emerging metabolic and energy homeostasis perspectives. *Trends Endocrinol Metab,* 19**,** 122-9.

Labeur, M. S., Arzt, E., Wiegers, G. J., Holsboer, F. & Reul, J. M. 1995. Long-term intracerebroventricular corticotropin-releasing hormone administration induces distinct changes in rat splenocyte activation and cytokine expression. *Endocrinology,* 136**,** 2678-88.

Lacasa, D., Agli, B., Pecquery, R. & Giudicelli, Y. 1991. Influence of ovariectomy and regional fat distribution on the membranous transducing system controlling lipolysis in rat fat cells. *Endocrinology,* 128**,** 747-53.

Lass, A., Zimmermann, R., Haemmerle, G., Riederer, M., Schoiswohl, G., Schweiger, M., Kienesberger, P., Strauss, J. G., Gorkiewicz, G. & Zechner, R. 2006. Adipose triglyceride lipase-mediated lipolysis of cellular fat stores is activated by CGI-58 and defective in Chanarin-Dorfman Syndrome. *Cell Metab,* 3**,** 309-19.

Lass, A., Zimmermann, R., Oberer, M. & Zechner, R. 2011. Lipolysis - a highly regulated multi-enzyme complex mediates the catabolism of cellular fat stores. *Prog Lipid Res,* 50**,** 14-27.

Le Marchand-Brustel, Y., Heydrick, S. J., Jullien, D., Gautier, N. & Van Obberghen, E. 1995. Effected of insulin and insulin-like growth factor-I on glucose transport and its transporters in soleus muscle of lean and obese mice. *Metabolism,* 44**,** 18-23.

Lederis, K., Letter, A., McMaster, D., Moore, G. & Schlesinger, D. 1982. Complete amino acid sequence of urotensin I, a hypotensive and corticotropin-releasing neuropeptide from Catostomus. *Science,* 218**,** 162-5.

Lee, P., Greenfield, J. R., Ho, K. K. & Fulham, M. J. 2010. A critical appraisal of the prevalence and metabolic significance of brown adipose tissue in adult humans. *Am J Physiol Endocrinol Metab,* 299**,** E601-6.

Lee, P., Smith, S., Linderman, J., Courville, A. B., Brychta, R. J., Dieckmann, W., Werner, C. D., Chen, K. Y. & Celi, F. S. 2014. Temperature-acclimated brown adipose tissue modulates insulin sensitivity in humans. *Diabetes,* 63**,** 3686-98.

Lee, T. W., Kwon, H., Zong, H., Yamada, E., Vatish, M., Pessin, J. E. & Bastie, C. C. 2013. Fyn deficiency promotes a preferential increase in subcutaneous adipose tissue mass and decreased visceral adipose tissue inflammation. *Diabetes,* 62**,** 1537-46.

Lewis, K., Li, C., Perrin, M. H., Blount, A., Kunitake, K., Donaldson, C., Vaughan, J., Reyes, T. M., Gulyas, J., Fischer, W., Bilezikjian, L., Rivier, J., Sawchenko, P. E. & Vale, W. W. 2001. Identification of urocortin III, an additional member of

the corticotropin-releasing factor (CRF) family with high affinity for the CRF2 receptor. *Proc Natl Acad Sci U S A,* 98**,** 7570-5.

Li, C., Chen, P., Vaughan, J., Lee, K. F. & Vale, W. 2007. Urocortin 3 regulates glucose-stimulated insulin secretion and energy homeostasis. *Proc Natl Acad Sci U S A,* 104**,** 4206-11.

Liang, X., Nazarian, A., Erdjument-Bromage, H., Bornmann, W., Tempst, P. & Resh, M. D. 2001. Heterogeneous fatty acylation of Src family kinases with polyunsaturated fatty acids regulates raft localization and signal transduction. *J Biol Chem,* 276**,** 30987-94.

Liaw, C. W., Lovenberg, T. W., Barry, G., Oltersdorf, T., Grigoriadis, D. E. & de Souza, E. B. 1996. Cloning and characterization of the human corticotropin-releasing factor-2 receptor complementary deoxyribonucleic acid. *Endocrinology,* 137**,** 72-7.

Lim, S., Honek, J., Xue, Y., Seki, T., Cao, Z., Andersson, P., Yang, X., Hosaka, K. & Cao, Y. 2012. Cold-induced activation of brown adipose tissue and adipose angiogenesis in mice. *Nat Protoc,* 7**,** 606-15.

Lindquist, J. M. & Rehnmark, S. 1998. Ambient temperature regulation of apoptosis in brown adipose tissue. Erk1/2 promotes norepinephrine-dependent cell survival. *J Biol Chem,* 273**,** 30147-56.

Linton, E. A., Wolfe, C. D., Behan, D. P. & Lowry, P. J. 1988. A specific carrier substance for human corticotrophin releasing factor in late gestational maternal plasma which could mask the ACTH-releasing activity. *Clin Endocrinol (Oxf),* 28**,** 315-24.

Liu, J., Deyoung, S. M., Zhang, M., Dold, L. H. & Saltiel, A. R. 2005. The stomatin/prohibitin/flotillin/HflK/C domain of flotillin-1 contains distinct sequences that direct plasma membrane localization and protein interactions in 3T3-L1 adipocytes. *J Biol Chem,* 280**,** 16125-34.

Livak, K. J. & Schmittgen, T. D. 2001. Analysis of relative gene expression data using real-time quantitative PCR and the 2(-Delta Delta C(T)) Method. *Methods,* 25**,** 402-8.

Loncar, D., Afzelius, B. A. & Cannon, B. 1988a. Epididymal white adipose tissue after cold stress in rats. I. Nonmitochondrial changes. *J Ultrastruct Mol Struct Res,* 101**,** 109-22.

Loncar, D., Afzelius, B. A. & Cannon, B. 1988b. Epididymal white adipose tissue after cold stress in rats. II. Mitochondrial changes. *J Ultrastruct Mol Struct Res,* 101**,** 199-209.

Loncar, D., Bedrica, L., Mayer, J., Cannon, B., Nedergaard, J., Afzelius, B. A. & Svajger, A. 1986. The effect of intermittent cold treatment on the adipose tissue of the cat. Apparent transformation from white to brown adipose tissue. *J Ultrastruct Mol Struct Res,* 97**,** 119-29.

Londos, C., Brasaemle, D. L., Gruia-Gray, J., Servetnick, D. A., Schultz, C. J., Levin, D. M. & Kimmel, A. R. 1995. Perilipin: unique proteins associated with intracellular neutral lipid droplets in adipocytes and steroidogenic cells. *Biochem Soc Trans,* 23**,** 611-5.

Long, W., Barrett, E. J., Wei, L. & Liu, Z. 2003. Adrenalectomy enhances the insulin sensitivity of muscle protein synthesis. *Am J Physiol Endocrinol Metab,* 284**,** E102-9.

Lonn, L., Kvist, H., Ernest, I. & Sjostrom, L. 1994. Changes in body composition and adipose tissue distribution after treatment of women with Cushing's syndrome. *Metabolism,* 43**,** 1517-22.

Lovejoy, D. A., Chang, B. S., Lovejoy, N. R. & del Castillo, J. 2014. Molecular evolution of GPCRs: CRH/CRH receptors. *J Mol Endocrinol,* 52**,** T43-60.

Lovenberg, T. W., Liaw, C. W., Grigoriadis, D. E., Clevenger, W., Chalmers, D. T., De Souza, E. B. & Oltersdorf, T. 1995. Cloning and characterization of a functionally distinct corticotropin-releasing factor receptor subtype from rat brain. *Proc Natl Acad Sci U S A,* 92**,** 836-40.

Lowell, B. B. & Flier, J. S. 1997. Brown adipose tissue, beta 3-adrenergic receptors, and obesity. *Annu Rev Med,* 48**,** 307-16.

Lowell, B. B., V, S. S., Hamann, A., Lawitts, J. A., Himms-Hagen, J., Boyer, B. B., Kozak, L. P. & Flier, J. S. 1993. Development of obesity in transgenic mice after genetic ablation of brown adipose tissue. *Nature,* 366**,** 740-2.

Lowenberg, M., Tuynman, J., Bilderbeek, J., Gaber, T., Buttgereit, F., van Deventer, S., Peppelenbosch, M. & Hommes, D. 2005. Rapid immunosuppressive effects of glucocorticoids mediated through Lck and Fyn. *Blood,* 106**,** 1703-10.

Lowenberg, M., Verhaar, A. P., Bilderbeek, J., Marle, J., Buttgereit, F., Peppelenbosch, M. P., van Deventer, S. J. & Hommes, D. W. 2006. Glucocorticoids cause rapid dissociation of a T-cell-receptor-associated protein complex containing LCK and FYN. *EMBO Rep,* 7**,** 1023-9.

Lu, B., Diz-Chaves, Y., Markovic, D., Contarino, A., Penicaud, L., Fanelli, F., Clark, S., Lehnert, H., Cota, D., Grammatopoulos, D. K. & Tabarin, A. 2015. The corticotrophin-releasing factor/urocortin system regulates white fat browning in mice through paracrine mechanisms. *Int J Obes (Lond),* 39**,** 408-17.

Lucas, S., Tavernier, G., Tiraby, C., Mairal, A. & Langin, D. 2003. Expression of human hormone-sensitive lipase in white adipose tissue of transgenic mice increases lipase activity but does not enhance in vitro lipolysis. *J Lipid Res,* 44**,** 154-63.

MacDougald, O. A. & Mandrup, S. 2002. Adipogenesis: forces that tip the scales. *Trends Endocrinol Metab,* 13**,** 5-11.

Makrigiannakis, A., Psychoyos, A., Zoumakis, E., Margioris, A. N., Stournaras, C. & Gravanis, A. 1997. Endometrial corticotropin-releasing hormone: expression, regulation, and potential physiological implications. *Ann N Y Acad Sci,* 816**,** 116-28.

Makrigiannakis, A., Zoumakis, E., Margioris, A. N., Theodoropoulos, P., Stournaras, C. & Gravanis, A. 1995. The corticotropin-releasing hormone (CRH) in normal and tumoral epithelial cells of human endometrium. *J Clin Endocrinol Metab,* 80**,** 185-9.

Manning, B. D. & Cantley, L. C. 2007. AKT/PKB signaling: navigating downstream. *Cell,* 129**,** 1261-74.

Markovic, D., Punn, A., Lehnert, H. & Grammatopoulos, D. K. 2011. Molecular determinants and feedback circuits regulating type 2 CRH receptor signal integration. *Biochim Biophys Acta,* 1813**,** 896-907.

Martinez-Botas, J., Anderson, J. B., Tessier, D., Lapillonne, A., Chang, B. H., Quast, M. J., Gorenstein, D., Chen, K. H. & Chan, L. 2000. Absence of perilipin results in leanness and reverses obesity in Lepr(db/db) mice. *Nat Genet,* 26**,** 474-9.

Mastick, C. C., Brady, M. J. & Saltiel, A. R. 1995. Insulin stimulates the tyrosine phosphorylation of caveolin. *J Cell Biol,* 129**,** 1523-31.

Mastick, C. C. & Saltiel, A. R. 1997. Insulin-stimulated tyrosine phosphorylation of caveolin is specific for the differentiated adipocyte phenotype in 3T3-L1 cells. *J Biol Chem,* 272**,** 20706-14.

Mastorakos, G., Webster, E. L. & Chrousos, G. P. 1993. Corticotropin-releasing hormone and its receptors in the ovary: physiological implications. *Ann N Y Acad Sci,* 687**,** 20-8.

Mattsson, C. L., Csikasz, R. I., Chernogubova, E., Yamamoto, D. L., Hogberg, H. T., Amri, E. Z., Hutchinson, D. S. & Bengtsson, T. 2011. beta(1)-Adrenergic receptors increase UCP1 in human MADS brown adipocytes and rescue cold-acclimated beta(3)-adrenergic receptor-knockout mice via nonshivering thermogenesis. *Am J Physiol Endocrinol Metab,* 301**,** E1108-18.

McEvoy, A. N., Bresnihan, B., FitzGerald, O. & Murphy, E. P. 2001. Corticotropin-releasing hormone signaling in synovial tissue from patients with early inflammatory arthritis is mediated by the type 1 alpha corticotropin-releasing hormone receptor. *Arthritis Rheum,* 44**,** 1761-7.

McEwen, B. S. 2004. Protection and damage from acute and chronic stress: allostasis and allostatic overload and relevance to the pathophysiology of psychiatric disorders. *Ann N Y Acad Sci,* 1032**,** 1-7.

McGillis, J. P., Park, A., Rubin-Fletter, P., Turck, C., Dallman, M. F. & Payan, D. G. 1989. Stimulation of rat B-lymphocyte proliferation by corticotropin-releasing factor. *J Neurosci Res,* 23**,** 346-52.

Miyakawa, T., Yagi, T., Watanabe, S. & Niki, H. 1994. Increased fearfulness of Fyn tyrosine kinase deficient mice. *Brain Res Mol Brain Res,* 27**,** 179-82.

Miyoshi, H., Perfield, J. W., 2nd, Souza, S. C., Shen, W. J., Zhang, H. H., Stancheva, Z. S., Kraemer, F. B., Obin, M. S. & Greenberg, A. S. 2007. Control of adipose

triglyceride lipase action by serine 517 of perilipin A globally regulates protein kinase A-stimulated lipolysis in adipocytes. *J Biol Chem,* 282**,** 996-1002.

Mohell, N., Nedergaard, J. & Cannon, B. 1983. Quantitative differentiation of alpha- and beta-adrenergic respiratory responses in isolated hamster brown fat cells: evidence for the presence of an alpha 1-adrenergic component. *Eur J Pharmacol,* 93**,** 183-93.

Montecucchi, P. C., Anastasi, A., de Castiglione, R. & Erspamer, V. 1980. Isolation and amino acid composition of sauvagine. An active polypeptide from methanol extracts of the skin of the South American frog Phyllomedusa sauvagei. *Int J Pept Protein Res,* 16**,** 191-9.

Morimoto, A., Nakamori, T., Morimoto, K., Tan, N. & Murakami, N. 1993. The central role of corticotrophin-releasing factor (CRF-41) in psychological stress in rats. *J Physiol,* 460**,** 221-9.

Morimoto, C., Tsujita, T. & Okuda, H. 1997. Norepinephrine-induced lipolysis in rat fat cells from visceral and subcutaneous sites: role of hormone-sensitive lipase and lipid droplets. *J Lipid Res,* 38**,** 132-8.

Morley, J. E. & Levine, A. S. 1982. Corticotrophin releasing factor, grooming and ingestive behavior. *Life Sci,* 31**,** 1459-64.

Moss, A. C., Anton, P., Savidge, T., Newman, P., Cheifetz, A. S., Gay, J., Paraschos, S., Winter, M. W., Moyer, M. P., Karalis, K., Kokkotou, E. & Pothoulakis, C. 2007. Urocortin II mediates pro-inflammatory effects in human colonocytes via corticotropin-releasing hormone receptor 2alpha. *Gut,* 56**,** 1210-7.

Muglia, L., Jacobson, L., Dikkes, P. & Majzoub, J. A. 1995. Corticotropin-releasing hormone deficiency reveals major fetal but not adult glucocorticoid need. *Nature,* 373**,** 427-32.

Muglia, L. J., Jenkins, N. A., Gilbert, D. J., Copeland, N. G. & Majzoub, J. A. 1994. Expression of the mouse corticotropin-releasing hormone gene in vivo and targeted inactivation in embryonic stem cells. *J Clin Invest,* 93**,** 2066-72.

Muller, M. B., Keck, M. E., Zimmermann, S., Holsboer, F. & Wurst, W. 2000. Disruption of feeding behavior in CRH receptor 1-deficient mice is dependent on glucocorticoids. *Neuroreport,* 11**,** 1963-6.

Muzzin, P., Revelli, J. P., Kuhne, F., Gocayne, J. D., McCombie, W. R., Venter, J. C., Giacobino, J. P. & Fraser, C. M. 1991. An adipose tissue-specific beta-adrenergic receptor. Molecular cloning and down-regulation in obesity. *J Biol Chem,* 266**,** 24053-8.

Myers, M. G., Jr., Zhang, Y., Aldaz, G. A., Grammer, T., Glasheen, E. M., Yenush, L., Wang, L. M., Sun, X. J., Blenis, J., Pierce, J. H. & White, M. F. 1996. YMXM motifs and signaling by an insulin receptor substrate 1 molecule without tyrosine phosphorylation sites. *Mol Cell Biol,* 16**,** 4147-55.

Nagano, G., Ohno, H., Oki, K., Kobuke, K., Shiwa, T., Yoneda, M. & Kohno, N. 2015. Activation of classical brown adipocytes in the adult human perirenal depot is highly correlated with PRDM16-EHMT1 complex expression. *PLoS One,* 10**,** e0122584.

Nam, S. Y., Kim, K. R., Cha, B. S., Song, Y. D., Lim, S. K., Lee, H. C. & Huh, K. B. 2001. Low-dose growth hormone treatment combined with diet restriction decreases insulin resistance by reducing visceral fat and increasing muscle mass in obese type 2 diabetic patients. *Int J Obes Relat Metab Disord,* 25**,** 1101-7.

Nawrocki, A. R. & Scherer, P. E. 2004. The delicate balance between fat and muscle: adipokines in metabolic disease and musculoskeletal inflammation. *Curr Opin Pharmacol,* 4**,** 281-9.

Nedergaard, J., Bengtsson, T. & Cannon, B. 2007. Unexpected evidence for active brown adipose tissue in adult humans. *Am J Physiol Endocrinol Metab,* 293**,** E444-52.

Ni, Y. G., Gold, S. J., Iredale, P. A., Terwilliger, R. Z., Duman, R. S. & Nestler, E. J. 1999. Region-specific regulation of RGS4 (Regulator of G-protein-signaling protein type 4) in brain by stress and glucocorticoids: in vivo and in vitro studies. *J Neurosci,* 19**,** 3674-80.

Nishio, H., Takase, I., Fukunishi, S., Takagi, T., Tamura, A., Miyazaki, T. & Suzuki, K. 2005. Evidence for involvement of p59fyn in fasting-induced thymic involution. *Scand J Immunol,* 62**,** 103-7.

Nnodim, J. O. & Lever, J. D. 1988. Neural and vascular provisions of rat interscapular brown adipose tissue. *Am J Anat,* 182**,** 283-93.

Ohno, H., Shinoda, K., Spiegelman, B. M. & Kajimura, S. 2012. PPARgamma agonists induce a white-to-brown fat conversion through stabilization of PRDM16 protein. *Cell Metab,* 15**,** 395-404.

Okada, T., Kawano, Y., Sakakibara, T., Hazeki, O. & Ui, M. 1994. Essential role of phosphatidylinositol 3-kinase in insulin-induced glucose transport and antilipolysis in rat adipocytes. Studies with a selective inhibitor wortmannin. *J Biol Chem,* 269**,** 3568-73.

Okuyama, C., Sakane, N., Yoshida, T., Shima, K., Kurosawa, H., Kumamoto, K., Ushijima, Y. & Nishimura, T. 2002. (123)I- or (125)I-metaiodobenzylguanidine visualization of brown adipose tissue. *J Nucl Med,* 43**,** 1234-40.

Ondrusova, L., Reda, J., Zakova, P. & Tuhackova, Z. 2013. Inhibition of mTORC1 by SU6656, the selective Src kinase inhibitor, is not accompanied by activation of Akt/PKB signalling in melanoma cells. *Folia Biol (Praha),* 59**,** 162-7.

Orava, J., Nuutila, P., Lidell, M. E., Oikonen, V., Noponen, T., Viljanen, T., Scheinin, M., Taittonen, M., Niemi, T., Enerback, S. & Virtanen, K. A. 2011. Different metabolic responses of human brown adipose tissue to activation by cold and insulin. *Cell Metab,* 14**,** 272-9.

Orava, J., Nuutila, P., Noponen, T., Parkkola, R., Viljanen, T., Enerback, S., Rissanen, A., Pietilainen, K. H. & Virtanen, K. A. 2013. Blunted metabolic responses to cold and insulin stimulation in brown adipose tissue of obese humans. *Obesity (Silver Spring),* 21**,** 2279-87.

Osuga, J., Ishibashi, S., Oka, T., Yagyu, H., Tozawa, R., Fujimoto, A., Shionoiri, F., Yahagi, N., Kraemer, F. B., Tsutsumi, O. & Yamada, N. 2000. Targeted disruption of hormone-sensitive lipase results in male sterility and adipocyte hypertrophy, but not in obesity. *Proc Natl Acad Sci U S A,* 97**,** 787-92.

Ouellet, V., Labbe, S. M., Blondin, D. P., Phoenix, S., Guerin, B., Haman, F., Turcotte, E. E., Richard, D. & Carpentier, A. C. 2012. Brown adipose tissue oxidative metabolism contributes to energy expenditure during acute cold exposure in humans. *J Clin Invest,* 122**,** 545-52.

Palacios, E. H. & Weiss, A. 2004. Function of the Src-family kinases, Lck and Fyn, in T-cell development and activation. *Oncogene,* 23**,** 7990-8000.

Penfornis, P., Viengchareun, S., Le Menuet, D., Cluzeaud, F., Zennaro, M. C. & Lombes, M. 2000. The mineralocorticoid receptor mediates aldosterone-induced differentiation of T37i cells into brown adipocytes. *Am J Physiol Endocrinol Metab,* 279**,** E386-94.

Petrovic, N., Walden, T. B., Shabalina, I. G., Timmons, J. A., Cannon, B. & Nedergaard, J. 2010. Chronic peroxisome proliferator-activated receptor gamma (PPARgamma) activation of epididymally derived white adipocyte cultures reveals a population of thermogenically competent, UCP1-containing adipocytes molecularly distinct from classic brown adipocytes. *J Biol Chem,* 285**,** 7153-64.

Pisarchik, A. & Slominski, A. T. 2001. Alternative splicing of CRH-R1 receptors in human and mouse skin: identification of new variants and their differential expression. *FASEB J,* 15**,** 2754-6.

Potter, E., Behan, D. P., Fischer, W. H., Linton, E. A., Lowry, P. J. & Vale, W. W. 1991. Cloning and characterization of the cDNAs for human and rat corticotropin releasing factor-binding proteins. *Nature,* 349**,** 423-6.

Pruett, S. B., Fan, R., Myers, L. P., Wu, W. J. & Collier, S. 2000. Quantitative analysis of the neuroendocrine-immune axis: linear modeling of the effects of exogenous corticosterone and restraint stress on lymphocyte subpopulations in the spleen and thymus in female B6C3F1 mice. *Brain Behav Immun,* 14**,** 270-87.

Prusty, D., Park, B. H., Davis, K. E. & Farmer, S. R. 2002. Activation of MEK/ERK signaling promotes adipogenesis by enhancing peroxisome proliferator-activated receptor gamma (PPARgamma) and C/EBPalpha gene expression during the differentiation of 3T3-L1 preadipocytes. *J Biol Chem,* 277**,** 46226-32.

Punn, A., Levine, M. A. & Grammatopoulos, D. K. 2006. Identification of signaling molecules mediating corticotropin-releasing hormone-R1alpha-mitogen-activated protein kinase (MAPK) interactions: the critical role of phosphatidylinositol 3-kinase in regulating ERK1/2 but not p38 MAPK activation. *Mol Endocrinol,* 20**,** 3179-95.

Qiu, J., Wang, P., Jing, Q., Zhang, W., Li, X., Zhong, Y., Sun, G., Pei, G. & Chen, Y. 2001. Rapid activation of ERK1/2 mitogen-activated protein kinase by corticosterone in PC12 cells. *Biochem Biophys Res Commun,* 287**,** 1017-24.

Randle, P. J. 1998. Regulatory interactions between lipids and carbohydrates: the glucose fatty acid cycle after 35 years. *Diabetes Metab Rev,* 14**,** 263-83.

Redei, E. 1992. Immuno-reactive and bioactive corticotropin-releasing factor in rat thymus. *Neuroendocrinology,* 55**,** 115-8.

Resh, M. D. 1999. Fatty acylation of proteins: new insights into membrane targeting of myristoylated and palmitoylated proteins. *Biochim Biophys Acta,* 1451**,** 1-16.

Reyes, T. M., Lewis, K., Perrin, M. H., Kunitake, K. S., Vaughan, J., Arias, C. A., Hogenesch, J. B., Gulyas, J., Rivier, J., Vale, W. W. & Sawchenko, P. E. 2001. Urocortin II: a member of the corticotropin-releasing factor (CRF) neuropeptide family that is selectively bound by type 2 CRF receptors. *Proc Natl Acad Sci U S A,* 98**,** 2843-8.

Ribon, V., Printen, J. A., Hoffman, N. G., Kay, B. K. & Saltiel, A. R. 1998. A novel, multifuntional c-Cbl binding protein in insulin receptor signaling in 3T3-L1 adipocytes. *Mol Cell Biol,* 18**,** 872-9.

Ricci, M. R., Lee, M. J., Russell, C. D., Wang, Y., Sullivan, S., Schneider, S. H., Brolin, R. E. & Fried, S. K. 2005. Isoproterenol decreases leptin release from rat and human adipose tissue through posttranscriptional mechanisms. *Am J Physiol Endocrinol Metab,* 288**,** E798-804.

Richelsen, B. & Pedersen, S. B. 1987. Antilipolytic effect of prostaglandin E2 in perifused rat adipocytes. *Endocrinology,* 121**,** 1221-6.

Riordan, N. H., Ichim, T. E., Min, W. P., Wang, H., Solano, F., Lara, F., Alfaro, M., Rodriguez, J. P., Harman, R. J., Patel, A. N., Murphy, M. P., Lee, R. R. & Minev, B. 2009. Non-expanded adipose stromal vascular fraction cell therapy for multiple sclerosis. *J Transl Med,* 7**,** 29.

Rivest, S., Deshaies, Y. & Richard, D. 1989. Effects of corticotropin-releasing factor on energy balance in rats are sex dependent. *Am J Physiol,* 257**,** R1417-22.

Rohner-Jeanrenaud, F., Walker, C. D., Greco-Perotto, R. & Jeanrenaud, B. 1989. Central corticotropin-releasing factor administration prevents the excessive body weight gain of genetically obese (fa/fa) rats. *Endocrinology,* 124**,** 733-9.

Rosenwald, M., Perdikari, A., Rulicke, T. & Wolfrum, C. 2013. Bi-directional interconversion of brite and white adipocytes. *Nat Cell Biol,* 15**,** 659-67.

Ross, P. C., Kostas, C. M. & Ramabhadran, T. V. 1994. A variant of the human corticotropin-releasing factor (CRF) receptor: cloning, expression and pharmacology. *Biochem Biophys Res Commun,* 205**,** 1836-42.

Rothwell, N. J. 1990. Central effects of CRF on metabolism and energy balance. *Neurosci Biobehav Rev,* 14**,** 263-71.

Rothwell, N. J. & Stock, M. J. 1997. A role for brown adipose tissue in diet-induced thermogenesis. *Obes Res,* 5**,** 650-6.

Ruzzin, J., Wagman, A. S. & Jensen, J. 2005. Glucocorticoid-induced insulin resistance in skeletal muscles: defects in insulin signalling and the effects of a selective glycogen synthase kinase-3 inhibitor. *Diabetologia,* 48**,** 2119-30.

Saad, M. J., Folli, F., Kahn, J. A. & Kahn, C. R. 1993. Modulation of insulin receptor, insulin receptor substrate-1, and phosphatidylinositol 3-kinase in liver and muscle of dexamethasone-treated rats. *J Clin Invest,* 92**,** 2065-72.

Saito, M., Okamatsu-Ogura, Y., Matsushita, M., Watanabe, K., Yoneshiro, T., Nio-Kobayashi, J., Iwanaga, T., Miyagawa, M., Kameya, T., Nakada, K., Kawai, Y. & Tsujisaki, M. 2009. High incidence of metabolically active brown adipose tissue in healthy adult humans: effects of cold exposure and adiposity. *Diabetes,* 58**,** 1526-31.

Saito, Y. D., Jensen, A. R., Salgia, R. & Posadas, E. M. 2010. Fyn: a novel molecular target in cancer. *Cancer,* 116**,** 1629-37.

Sakamoto, R., Matsubara, E., Nomura, M., Wang, L., Kawahara, Y., Yanase, T., Nawata, H. & Takayanagi, R. 2013. Roles for corticotropin-releasing factor receptor type 1 in energy homeostasis in mice. *Metabolism,* 62**,** 1739-48.

Salans, L. B., Cushman, S. W. & Weismann, R. E. 1973. Studies of human adipose tissue. Adipose cell size and number in nonobese and obese patients. *J Clin Invest,* 52**,** 929-41.

Sale, E. M., Atkinson, P. G. & Sale, G. J. 1995. Requirement of MAP kinase for differentiation of fibroblasts to adipocytes, for insulin activation of p90 S6

kinase and for insulin or serum stimulation of DNA synthesis. *EMBO J,* 14**,** 674-84.

Saltiel, A. R. & Pessin, J. E. 2003. Insulin signaling in microdomains of the plasma membrane. *Traffic,* 4**,** 711-6.

Samovski, D., Sun, J., Pietka, T., Gross, R. W., Eckel, R. H., Su, X., Stahl, P. D. & Abumrad, N. A. 2015. Regulation of AMPK activation by CD36 links fatty acid uptake to beta-oxidation. *Diabetes,* 64**,** 353-9.

Sananbenesi, F., Fischer, A., Schrick, C., Spiess, J. & Radulovic, J. 2003. Mitogen-activated protein kinase signaling in the hippocampus and its modulation by corticotropin-releasing factor receptor 2: a possible link between stress and fear memory. *J Neurosci,* 23**,** 11436-43.

Sarnyai, Z., Shaham, Y. & Heinrichs, S. C. 2001. The role of corticotropin-releasing factor in drug addiction. *Pharmacol Rev,* 53**,** 209-43.

Sasaki, A., Tempst, P., Liotta, A. S., Margioris, A. N., Hood, L. E., Kent, S. B., Sato, S., Shinkawa, O., Yoshinaga, K. & Krieger, D. T. 1988. Isolation and characterization of a corticotropin-releasing hormone-like peptide from human placenta. *J Clin Endocrinol Metab,* 67**,** 768-73.

Sasson, R., Shinder, V., Dantes, A., Land, A. & Amsterdam, A. 2003. Activation of multiple signal transduction pathways by glucocorticoids: protection of ovarian follicular cells against apoptosis. *Biochem Biophys Res Commun,* 311**,** 1047-56.

Scarpace, P. J. & Matheny, M. 1996. Thermogenesis in brown adipose tissue with age: post-receptor activation by forskolin. *Pflugers Arch,* 431**,** 388-94.

Schipper, H. S., Prakken, B., Kalkhoven, E. & Boes, M. 2012. Adipose tissue-resident immune cells: key players in immunometabolism. *Trends Endocrinol Metab,* 23**,** 407-15.

Schulman, D., Latchman, D. S. & Yellon, D. M. 2002. Urocortin protects the heart from reperfusion injury via upregulation of p42/p44 MAPK signaling pathway. *Am J Physiol Heart Circ Physiol,* 283**,** H1481-8.

Schweiger, M., Schreiber, R., Haemmerle, G., Lass, A., Fledelius, C., Jacobsen, P., Tornqvist, H., Zechner, R. & Zimmermann, R. 2006. Adipose triglyceride lipase

and hormone-sensitive lipase are the major enzymes in adipose tissue triacylglycerol catabolism. *J Biol Chem,* 281**,** 40236-41.

Seale, P., Bjork, B., Yang, W., Kajimura, S., Chin, S., Kuang, S., Scime, A., Devarakonda, S., Conroe, H. M., Erdjument-Bromage, H., Tempst, P., Rudnicki, M. A., Beier, D. R. & Spiegelman, B. M. 2008. PRDM16 controls a brown fat/skeletal muscle switch. *Nature,* 454**,** 961-7.

Seale, P., Conroe, H. M., Estall, J., Kajimura, S., Frontini, A., Ishibashi, J., Cohen, P., Cinti, S. & Spiegelman, B. M. 2011. Prdm16 determines the thermogenic program of subcutaneous white adipose tissue in mice. *J Clin Invest,* 121**,** 96-105.

Seasholtz, A. F., Valverde, R. A. & Denver, R. J. 2002. Corticotropin-releasing hormone-binding protein: biochemistry and function from fishes to mammals. *J Endocrinol,* 175**,** 89-97.

Sehringer, B., Zahradnik, H. P., Simon, M., Ziegler, R., Noethling, C. & Schaefer, W. R. 2004. mRNA expression profiles for corticotrophin-releasing hormone, urocortin, CRH-binding protein and CRH receptors in human term gestational tissues determined by real-time quantitative RT-PCR. *J Mol Endocrinol,* 32**,** 339-48.

Seidell, J. C., Han, T. S., Feskens, E. J. & Lean, M. E. 1997. Narrow hips and broad waist circumferences independently contribute to increased risk of non-insulin-dependent diabetes mellitus. *J Intern Med,* 242**,** 401-6.

Seres, J., Bornstein, S. R., Seres, P., Willenberg, H. S., Schulte, K. M., Scherbaum, W. A. & Ehrhart-Bornstein, M. 2004. Corticotropin-releasing hormone system in human adipose tissue. *J Clin Endocrinol Metab,* 89**,** 965-70.

Sharp, L. Z., Shinoda, K., Ohno, H., Scheel, D. W., Tomoda, E., Ruiz, L., Hu, H., Wang, L., Pavlova, Z., Gilsanz, V. & Kajimura, S. 2012. Human BAT possesses molecular signatures that resemble beige/brite cells. *PLoS One,* 7**,** e49452.

Shen, C., Kim, M. R., Noh, J. M., Kim, S. J., Ka, S. O., Kim, J. H., Park, B. H. & Park, J. H. 2016. Glucocorticoid Suppresses Connexin 43 Expression by Inhibiting the Akt/mTOR Signaling Pathway in Osteoblasts. *Calcif Tissue Int,* 99**,** 88-97.

Shen, W. J., Patel, S., Miyoshi, H., Greenberg, A. S. & Kraemer, F. B. 2009. Functional interaction of hormone-sensitive lipase and perilipin in lipolysis. *J Lipid Res,* 50**,** 2306-13.

Shepherd, P. R. 2005. Mechanisms regulating phosphoinositide 3-kinase signalling in insulin-sensitive tissues. *Acta Physiol Scand,* 183**,** 3-12.

Shepherd, P. R., Nave, B. T. & Siddle, K. 1995. Insulin activates glycogen synthase by a novel PI 3-kinase/p70s6k dependent pathway in 3T3-L1 adipocytes. *Biochem Soc Trans,* 23**,** 202S.

Shepherd, P. R., Withers, D. J. & Siddle, K. 1998. Phosphoinositide 3-kinase: the key switch mechanism in insulin signalling. *Biochem J,* 333 (Pt 3)**,** 471-90.

Shih, M. F. & Taberner, P. V. 1995. Selective activation of brown adipocyte hormone-sensitive lipase and cAMP production in the mouse by beta 3-adrenoceptor agonists. *Biochem Pharmacol,* 50**,** 601-8.

Shimizu, Y., Tanishita, T., Minokoshi, Y. & Shimazu, T. 1997. Activation of mitogen-activated protein kinase by norepinephrine in brown adipocytes from rats. *Endocrinology,* 138**,** 248-53.

Singh, L. K., Boucher, W., Pang, X., Letourneau, R., Seretakis, D., Green, M. & Theoharides, T. C. 1999. Potent mast cell degranulation and vascular permeability triggered by urocortin through activation of corticotropin-releasing hormone receptors. *J Pharmacol Exp Ther,* 288**,** 1349-56.

Singleton, J. R., Baker, B. L. & Thorburn, A. 2000. Dexamethasone inhibits insulin-like growth factor signaling and potentiates myoblast apoptosis. *Endocrinology,* 141**,** 2945-50.

Slominski, A., Wortsman, J., Pisarchik, A., Zbytek, B., Linton, E. A., Mazurkiewicz, J. E. & Wei, E. T. 2001. Cutaneous expression of corticotropin-releasing hormone (CRH), urocortin, and CRH receptors. *FASEB J,* 15**,** 1678-93.

Smith, G. W., Aubry, J. M., Dellu, F., Contarino, A., Bilezikjian, L. M., Gold, L. H., Chen, R., Marchuk, Y., Hauser, C., Bentley, C. A., Sawchenko, P. E., Koob, G. F., Vale, W. & Lee, K. F. 1998. Corticotropin releasing factor receptor 1-deficient mice display decreased anxiety, impaired stress response, and aberrant neuroendocrine development. *Neuron,* 20**,** 1093-102.

Snijder, M. B., Dekker, J. M., Visser, M., Bouter, L. M., Stehouwer, C. D., Kostense, P. J., Yudkin, J. S., Heine, R. J., Nijpels, G. & Seidell, J. C. 2003a. Associations of hip and thigh circumferences independent of waist circumference with the incidence of type 2 diabetes: the Hoorn Study. *Am J Clin Nutr,* 77**,** 1192-7.

Snijder, M. B., Dekker, J. M., Visser, M., Yudkin, J. S., Stehouwer, C. D., Bouter, L. M., Heine, R. J., Nijpels, G. & Seidell, J. C. 2003b. Larger thigh and hip circumferences are associated with better glucose tolerance: the Hoorn study. *Obes Res,* 11**,** 104-11.

Soumano, K., Desbiens, S., Rabelo, R., Bakopanos, E., Camirand, A. & Silva, J. E. 2000. Glucocorticoids inhibit the transcriptional response of the uncoupling protein-1 gene to adrenergic stimulation in a brown adipose cell line. *Mol Cell Endocrinol,* 165**,** 7-15.

Sperber, B. R. & McMorris, F. A. 2001. Fyn tyrosine kinase regulates oligodendroglial cell development but is not required for morphological differentiation of oligodendrocytes. *J Neurosci Res,* 63**,** 303-12.

Spiegelman, B. M. & Flier, J. S. 2001. Obesity and the regulation of energy balance. *Cell,* 104**,** 531-43.

Spina, M., Merlo-Pich, E., Chan, R. K., Basso, A. M., Rivier, J., Vale, W. & Koob, G. F. 1996. Appetite-suppressing effects of urocortin, a CRF-related neuropeptide. *Science,* 273**,** 1561-4.

Stanford, K. I., Middelbeek, R. J., Townsend, K. L., Lee, M. Y., Takahashi, H., So, K., Hitchcox, K. M., Markan, K. R., Hellbach, K., Hirshman, M. F., Tseng, Y. H. & Goodyear, L. J. 2015. A novel role for subcutaneous adipose tissue in exercise-induced improvements in glucose homeostasis. *Diabetes,* 64**,** 2002-14.

Stenzel-Poore, M. P., Heinrichs, S. C., Rivest, S., Koob, G. F. & Vale, W. W. 1994. Overproduction of corticotropin-releasing factor in transgenic mice: a genetic model of anxiogenic behavior. *J Neurosci,* 14**,** 2579-84.

Stephanou, A., Jessop, D. S., Knight, R. A. & Lightman, S. L. 1990. Corticotrophin-releasing factor-like immunoreactivity and mRNA in human leukocytes. *Brain Behav Immun,* 4**,** 67-73.

Sterzer, P., Wiegers, G. J. & Reul, J. M. 2004. Long-term in vivo administration of glucocorticoid hormones attenuates their capacity to accelerate in vitro proliferation of rat splenic T cells. *Endocrinology,* 145**,** 3630-8.

Suda, T., Kageyama, K., Sakihara, S. & Nigawara, T. 2004. Physiological roles of urocortins, human homologues of fish urotensin I, and their receptors. *Peptides,* 25**,** 1689-701.

Suda, T., Tomori, N., Tozawa, F., Mouri, T., Demura, H. & Shizume, K. 1984. Distribution and characterization of immunoreactive corticotropin-releasing factor in human tissues. *J Clin Endocrinol Metab,* 59**,** 861-6.

Sudol, M., Greulich, H., Newman, L., Sarkar, A., Sukegawa, J. & Yamamoto, T. 1993. A novel Yes-related kinase, Yrk, is expressed at elevated levels in neural and hematopoietic tissues. *Oncogene,* 8**,** 823-31.

Sun, X. J., Pons, S., Asano, T., Myers, M. G., Jr., Glasheen, E. & White, M. F. 1996. The Fyn tyrosine kinase binds Irs-1 and forms a distinct signaling complex during insulin stimulation. *J Biol Chem,* 271**,** 10583-7.

Sun, Y., Ma, Y. C., Huang, J., Chen, K. Y., McGarrigle, D. K. & Huang, X. Y. 2005. Requirement of SRC-family tyrosine kinases in fat accumulation. *Biochemistry,* 44**,** 14455-62.

Swiergiel, A. H. & Dunn, A. J. 1999. CRF-deficient mice respond like wild-type mice to hypophagic stimuli. *Pharmacol Biochem Behav,* 64**,** 59-64.

Takahashi, K., Totsune, K., Murakami, O., Saruta, M., Nakabayashi, M., Suzuki, T., Sasano, H. & Shibahara, S. 2004. Expression of urocortin III/stresscopin in human heart and kidney. *J Clin Endocrinol Metab,* 89**,** 1897-903.

Taniguchi, K., Xia, L., Goldberg, H. J., Lee, K. W., Shah, A., Stavar, L., Masson, E. A., Momen, A., Shikatani, E. A., John, R., Husain, M. & Fantus, I. G. 2013. Inhibition of Src kinase blocks high glucose-induced EGFR transactivation and collagen synthesis in mesangial cells and prevents diabetic nephropathy in mice. *Diabetes,* 62**,** 3874-86.

Tchernof, A., Belanger, C., Morisset, A. S., Richard, C., Mailloux, J., Laberge, P. & Dupont, P. 2006. Regional differences in adipose tissue metabolism in women: minor effect of obesity and body fat distribution. *Diabetes,* 55**,** 1353-60.

Tchkonia, T., Lenburg, M., Thomou, T., Giorgadze, N., Frampton, G., Pirtskhalava, T., Cartwright, A., Cartwright, M., Flanagan, J., Karagiannides, I., Gerry, N., Forse, R. A., Tchoukalova, Y., Jensen, M. D., Pothoulakis, C. & Kirkland, J. L. 2007. Identification of depot-specific human fat cell progenitors through distinct expression profiles and developmental gene patterns. *Am J Physiol Endocrinol Metab,* 292**,** E298-307.

Terada, K., Kojima, Y., Watanabe, T., Izumo, N., Chiba, K. & Karube, Y. 2014. Inhibition of nerve growth factor-induced neurite outgrowth from PC12 cells by dexamethasone: signaling pathways through the glucocorticoid receptor and phosphorylated Akt and ERK1/2. *PLoS One,* 9**,** e93223.

Theoharides, T. C., Singh, L. K., Boucher, W., Pang, X., Letourneau, R., Webster, E. & Chrousos, G. 1998. Corticotropin-releasing hormone induces skin mast cell degranulation and increased vascular permeability, a possible explanation for its proinflammatory effects. *Endocrinology,* 139**,** 403-13.

Thomas, S. M. & Brugge, J. S. 1997. Cellular functions regulated by Src family kinases. *Annu Rev Cell Dev Biol,* 13**,** 513-609.

Thompson, R. C., Seasholtz, A. F. & Herbert, E. 1987. Rat corticotropin-releasing hormone gene: sequence and tissue-specific expression. *Mol Endocrinol,* 1**,** 363-70.

Thonberg, H., Fredriksson, J. M., Nedergaard, J. & Cannon, B. 2002. A novel pathway for adrenergic stimulation of cAMP-response-element-binding protein (CREB) phosphorylation: mediation via alpha1-adrenoceptors and protein kinase C activation. *Biochem J,* 364**,** 73-9.

Tian, H. P., Huang, B. S., Zhao, J., Hu, X. H., Guo, J. & Li, L. X. 2009. Non-receptor tyrosine kinase Src is required for ischemia-stimulated neuronal cell proliferation via Raf/ERK/CREB activation in the dentate gyrus. *BMC Neurosci,* 10**,** 139.

Timpl, P., Spanagel, R., Sillaber, I., Kresse, A., Reul, J. M., Stalla, G. K., Blanquet, V., Steckler, T., Holsboer, F. & Wurst, W. 1998. Impaired stress response and reduced anxiety in mice lacking a functional corticotropin-releasing hormone receptor 1. *Nat Genet,* 19**,** 162-6.

Torbett, N. E., Luna-Moran, A., Knight, Z. A., Houk, A., Moasser, M., Weiss, W., Shokat, K. M. & Stokoe, D. 2008. A chemical screen in diverse breast cancer cell lines reveals genetic enhancers and suppressors of sensitivity to PI3K isoform-selective inhibition. *Biochem J,* 415**,** 97-110.

Tran, T. T., Yamamoto, Y., Gesta, S. & Kahn, C. R. 2008. Beneficial effects of subcutaneous fat transplantation on metabolism. *Cell Metab,* 7**,** 410-20.

Tse, M. C., Liu, X., Yang, S., Ye, K. & Chan, C. B. 2013. Fyn regulates adipogenesis by promoting PIKE-A/STAT5a interaction. *Mol Cell Biol,* 33**,** 1797-808.

Udelsman, R., Harwood, J. P., Millan, M. A., Chrousos, G. P., Goldstein, D. S., Zimlichman, R., Catt, K. J. & Aguilera, G. 1986. Functional corticotropin releasing factor receptors in the primate peripheral sympathetic nervous system. *Nature,* 319**,** 147-50.

Ulisse, S., Fabbri, A., Tinajero, J. C. & Dufau, M. L. 1990. A novel mechanism of action of corticotropin releasing factor in rat Leydig cells. *J Biol Chem,* 265**,** 1964-71.

Valdenaire, O., Giller, T., Breu, V., Gottowik, J. & Kilpatrick, G. 1997. A new functional isoform of the human CRF2 receptor for corticotropin-releasing factor. *Biochim Biophys Acta,* 1352**,** 129-32.

Vale, W., Spiess, J., Rivier, C. & Rivier, J. 1981. Characterization of a 41-residue ovine hypothalamic peptide that stimulates secretion of corticotropin and beta-endorphin. *Science,* 213**,** 1394-7.

van't Hof, W. & Resh, M. D. 1997. Rapid plasma membrane anchoring of newly synthesized p59fyn: selective requirement for NH2-terminal myristoylation and palmitoylation at cysteine-3. *J Cell Biol,* 136**,** 1023-35.

van't Hof, W. & Resh, M. D. 1999. Dual fatty acylation of p59(Fyn) is required for association with the T cell receptor zeta chain through phosphotyrosine-Src homology domain-2 interactions. *J Cell Biol,* 145**,** 377-89.

van der Lans, A. A., Hoeks, J., Brans, B., Vijgen, G. H., Visser, M. G., Vosselman, M. J., Hansen, J., Jorgensen, J. A., Wu, J., Mottaghy, F. M., Schrauwen, P. & van Marken Lichtenbelt, W. D. 2013. Cold acclimation recruits human brown fat and increases nonshivering thermogenesis. *J Clin Invest,* 123**,** 3395-403.

van Marken Lichtenbelt, W. D., Vanhommerig, J. W., Smulders, N. M., Drossaerts, J. M., Kemerink, G. J., Bouvy, N. D., Schrauwen, P. & Teule, G. J. 2009. Cold-activated brown adipose tissue in healthy men. *N Engl J Med,* 360**,** 1500-8.

Van Pett, K., Viau, V., Bittencourt, J. C., Chan, R. K., Li, H. Y., Arias, C., Prins, G. S., Perrin, M., Vale, W. & Sawchenko, P. E. 2000. Distribution of mRNAs encoding CRF receptors in brain and pituitary of rat and mouse. *J Comp Neurol,* 428**,** 191-212.

Vatish, M., Yamada, E., Pessin, J. E. & Bastie, C. C. 2009. Fyn kinase function in lipid utilization: a new upstream regulator of AMPK activity? *Arch Physiol Biochem,* 115**,** 191-8.

Vaughan, J., Donaldson, C., Bittencourt, J., Perrin, M. H., Lewis, K., Sutton, S., Chan, R., Turnbull, A. V., Lovejoy, D., Rivier, C. & et al. 1995. Urocortin, a mammalian neuropeptide related to fish urotensin I and to corticotropin-releasing factor. *Nature,* 378**,** 287-92.

Venihaki, M. & Majzoub, J. 2002. Lessons from CRH knockout mice. *Neuropeptides,* 36**,** 96-102.

Venihaki, M., Zhao, J. & Karalis, K. P. 2003. Corticotropin-releasing hormone deficiency results in impaired splenocyte response to lipopolysaccharide. *J Neuroimmunol,* 141**,** 3-9.

Viengchareun, S., Penfornis, P., Zennaro, M. C. & Lombes, M. 2001. Mineralocorticoid and glucocorticoid receptors inhibit UCP expression and function in brown adipocytes. *Am J Physiol Endocrinol Metab,* 280**,** E640-9.

Viengchareun, S., Zennaro, M. C., Pascual-Le Tallec, L. & Lombes, M. 2002. Brown adipocytes are novel sites of expression and regulation of adiponectin and resistin. *FEBS Lett,* 532**,** 345-50.

Villarroya, F. & Vidal-Puig, A. 2013. Beyond the sympathetic tone: the new brown fat activators. *Cell Metab,* 17**,** 638-43.

Virtanen, K. A., Lidell, M. E., Orava, J., Heglind, M., Westergren, R., Niemi, T., Taittonen, M., Laine, J., Savisto, N. J., Enerback, S. & Nuutila, P. 2009. Functional brown adipose tissue in healthy adults. *N Engl J Med,* 360**,** 1518-25.

Virtue, S. & Vidal-Puig, A. 2008. It's not how fat you are, it's what you do with it that counts. *PLoS Biol,* 6**,** e237.

Viswanadha, S. & Londos, C. 2006. Optimized conditions for measuring lipolysis in murine primary adipocytes. *J Lipid Res,* 47**,** 1859-64.

Vitali, A., Murano, I., Zingaretti, M. C., Frontini, A., Ricquier, D. & Cinti, S. 2012. The adipose organ of obesity-prone C57BL/6J mice is composed of mixed white and brown adipocytes. *J Lipid Res,* 53**,** 619-29.

Vosselman, M. J., van der Lans, A. A., Brans, B., Wierts, R., van Baak, M. A., Schrauwen, P. & van Marken Lichtenbelt, W. D. 2012. Systemic beta-adrenergic stimulation of thermogenesis is not accompanied by brown adipose tissue activity in humans. *Diabetes,* 61**,** 3106-13.

Wade, G. N. & Gray, J. M. 1979. Gonadal effects on food intake and adiposity: a metabolic hypothesis. *Physiol Behav,* 22**,** 583-93.

Wajchenberg, B. L. 2000. Subcutaneous and visceral adipose tissue: their relation to the metabolic syndrome. *Endocr Rev,* 21**,** 697-738.

Walther, S., Pluteanu, F., Renz, S., Nikonova, Y., Maxwell, J. T., Yang, L. Z., Schmidt, K., Edwards, J. N., Wakula, P., Groschner, K., Maier, L. S., Spiess, J., Blatter, L. A., Pieske, B. & Kockskamper, J. 2014. Urocortin 2 stimulates nitric oxide production in ventricular myocytes via Akt- and PKA-mediated phosphorylation of eNOS at serine 1177. *Am J Physiol Heart Circ Physiol,* 307**,** H689-700.

Wang, H., Hu, L., Dalen, K., Dorward, H., Marcinkiewicz, A., Russell, D., Gong, D., Londos, C., Yamaguchi, T., Holm, C., Rizzo, M. A., Brasaemle, D. & Sztalryd, C. 2009. Activation of hormone-sensitive lipase requires two steps, protein phosphorylation and binding to the PAT-1 domain of lipid droplet coat proteins. *J Biol Chem,* 284**,** 32116-25.

Wang, Q. A., Tao, C., Gupta, R. K. & Scherer, P. E. 2013. Tracking adipogenesis during white adipose tissue development, expansion and regeneration. *Nat Med,* 19**,** 1338-44.

Wang, W., Kissig, M., Rajakumari, S., Huang, L., Lim, H. W., Won, K. J. & Seale, P. 2014. Ebf2 is a selective marker of brown and beige adipogenic precursor cells. *Proc Natl Acad Sci U S A,* 111**,** 14466-71.

Wang, X., Hu, J. & Price, S. R. 2007. Inhibition of PI3-kinase signaling by glucocorticoids results in increased branched-chain amino acid degradation in renal epithelial cells. *Am J Physiol Cell Physiol,* 292**,** C1874-9.

Waugh, J. L., Celver, J., Sharma, M., Dufresne, R. L., Terzi, D., Risch, S. C., Fairbrother, W. G., Neve, R. L., Kane, J. P., Malloy, M. J., Pullinger, C. R., Gu, H. F., Tsatsanis, C., Hamilton, S. P., Gold, S. J., Zachariou, V. & Kovoor, A. 2011. Association between regulator of G protein signaling 9-2 and body weight. *PLoS One,* 6**,** e27984.

Weber, W. A. 2004. Brown adipose tissue and nuclear medicine imaging. *J Nucl Med,* 45**,** 1101-3.

Webster, E. L., Lewis, D. B., Torpy, D. J., Zachman, E. K., Rice, K. C. & Chrousos, G. P. 1996. In vivo and in vitro characterization of antalarmin, a nonpeptide corticotropin-releasing hormone (CRH) receptor antagonist: suppression of pituitary ACTH release and peripheral inflammation. *Endocrinology,* 137**,** 5747-50.

Weninger, S. C., Dunn, A. J., Muglia, L. J., Dikkes, P., Miczek, K. A., Swiergiel, A. H., Berridge, C. W. & Majzoub, J. A. 1999a. Stress-induced behaviors require the corticotropin-releasing hormone (CRH) receptor, but not CRH. *Proc Natl Acad Sci U S A,* 96**,** 8283-8.

Weninger, S. C., Muglia, L. J., Jacobson, L. & Majzoub, J. A. 1999b. CRH-deficient mice have a normal anorectic response to chronic stress. *Regul Pept,* 84**,** 69-74.

Weyer, C., Foley, J. E., Bogardus, C., Tataranni, P. A. & Pratley, R. E. 2000. Enlarged subcutaneous abdominal adipocyte size, but not obesity itself, predicts type II diabetes independent of insulin resistance. *Diabetologia,* 43**,** 1498-506.

Wijkander, J., Landstrom, T. R., Manganiello, V., Belfrage, P. & Degerman, E. 1998. Insulin-induced phosphorylation and activation of phosphodiesterase 3B in rat adipocytes: possible role for protein kinase B but not mitogen-activated protein kinase or p70 S6 kinase. *Endocrinology,* 139**,** 219-27.

Witchel, S. F. & DeFranco, D. B. 2006. Mechanisms of disease: regulation of glucocorticoid and receptor levels--impact on the metabolic syndrome. *Nat Clin Pract Endocrinol Metab,* 2**,** 621-31.

Woeller, C. F., O'Loughlin, C. W., Pollock, S. J., Thatcher, T. H., Feldon, S. E. & Phipps, R. P. 2015. Thy1 (CD90) controls adipogenesis by regulating activity of the Src family kinase, Fyn. *FASEB J,* 29**,** 920-31.

Wu, J., Bostrom, P., Sparks, L. M., Ye, L., Choi, J. H., Giang, A. H., Khandekar, M., Virtanen, K. A., Nuutila, P., Schaart, G., Huang, K., Tu, H., van Marken Lichtenbelt, W. D., Hoeks, J., Enerback, S., Schrauwen, P. & Spiegelman, B. M. 2012. Beige adipocytes are a distinct type of thermogenic fat cell in mouse and human. *Cell,* 150**,** 366-76.

Wu, J., Cohen, P. & Spiegelman, B. M. 2013. Adaptive thermogenesis in adipocytes: is beige the new brown? *Genes Dev,* 27**,** 234-50.

Wu, S. V., Yuan, P. Q., Wang, L., Peng, Y. L., Chen, C. Y. & Tache, Y. 2007. Identification and characterization of multiple corticotropin-releasing factor type 2 receptor isoforms in the rat esophagus. *Endocrinology,* 148**,** 1675-87.

Xue, R., Lynes, M. D., Dreyfuss, J. M., Shamsi, F., Schulz, T. J., Zhang, H., Huang, T. L., Townsend, K. L., Li, Y., Takahashi, H., Weiner, L. S., White, A. P., Lynes, M. S., Rubin, L. L., Goodyear, L. J., Cypess, A. M. & Tseng, Y. H. 2015. Clonal analyses and gene profiling identify genetic biomarkers of the thermogenic potential of human brown and white preadipocytes. *Nat Med,* 21**,** 760-8.

Yamada, E., Bastie, C. C., Koga, H., Wang, Y., Cuervo, A. M. & Pessin, J. E. 2012. Mouse skeletal muscle fiber-type-specific macroautophagy and muscle wasting are regulated by a Fyn/STAT3/Vps34 signaling pathway. *Cell Rep,* 1**,** 557-69.

Yamada, E., Pessin, J. E., Kurland, I. J., Schwartz, G. J. & Bastie, C. C. 2010. Fyn-dependent regulation of energy expenditure and body weight is mediated by tyrosine phosphorylation of LKB1. *Cell Metab,* 11**,** 113-24.

Yamauchi, N., Otagiri, A., Nemoto, T., Sekino, A., Oono, H., Kato, I., Yanaihara, C. & Shibasaki, T. 2005. Distribution of urocortin 2 in various tissues of the rat. *J Neuroendocrinol,* 17**,** 656-63.

Yang, H. B., Yang, X., Cao, J., Li, S., Liu, Y. N., Suo, Z. W., Cui, H. B., Guo, Z. & Hu, X. D. 2011. cAMP-dependent protein kinase activated Fyn in spinal dorsal horn to regulate NMDA receptor function during inflammatory pain. *J Neurochem,* 116**,** 93-104.

Ye, L., Wu, J., Cohen, P., Kazak, L., Khandekar, M. J., Jedrychowski, M. P., Zeng, X., Gygi, S. P. & Spiegelman, B. M. 2013. Fat cells directly sense temperature to activate thermogenesis. *Proc Natl Acad Sci U S A,* 110**,** 12480-5.

Yin, G., Yan, C. & Berk, B. C. 2003. Angiotensin II signaling pathways mediated by tyrosine kinases. *Int J Biochem Cell Biol,* 35**,** 780-3.

Yoneshiro, T., Aita, S., Matsushita, M., Kayahara, T., Kameya, T., Kawai, Y., Iwanaga, T. & Saito, M. 2013. Recruited brown adipose tissue as an antiobesity agent in humans. *J Clin Invest,* 123**,** 3404-8.

Yoneshiro, T., Aita, S., Matsushita, M., Okamatsu-Ogura, Y., Kameya, T., Kawai, Y., Miyagawa, M., Tsujisaki, M. & Saito, M. 2011. Age-related decrease in cold-activated brown adipose tissue and accumulation of body fat in healthy humans. *Obesity (Silver Spring),* 19**,** 1755-60.

Young, P., Wilson, S. & Arch, J. R. 1984. Prolonged beta-adrenoceptor stimulation increases the amount of GDP-binding protein in brown adipose tissue mitochondria. *Life Sci,* 34**,** 1111-7.

Zalutskaya, A. A., Arai, M., Bounoutas, G. S. & Abou-Samra, A. B. 2007. Impaired adaptation to repeated restraint and decreased response to cold in urocortin 1 knockout mice. *Am J Physiol Endocrinol Metab,* 293**,** E259-63.

Zechner, R., Zimmermann, R., Eichmann, T. O., Kohlwein, S. D., Haemmerle, G., Lass, A. & Madeo, F. 2012. FAT SIGNALS--lipases and lipolysis in lipid metabolism and signaling. *Cell Metab,* 15**,** 279-91.

Zennaro, M. C., Le Menuet, D., Viengchareun, S., Walker, F., Ricquier, D. & Lombes, M. 1998. Hibernoma development in transgenic mice identifies brown adipose tissue as a novel target of aldosterone action. *J Clin Invest,* 101**,** 1254-60.

Zhang, G., Sun, Q. & Liu, C. 2016. Influencing Factors of Thermogenic Adipose Tissue Activity. *Front Physiol,* 7**,** 29.

Zhang, J., Tang, H., Zhang, Y., Deng, R., Shao, L., Liu, Y., Li, F., Wang, X. & Zhou, L. 2014. Identification of suitable reference genes for quantitative RT-PCR during 3T3-L1 adipocyte differentiation. *Int J Mol Med,* 33**,** 1209-18.

Zhang, T., He, J., Xu, C., Zu, L., Jiang, H., Pu, S., Guo, X. & Xu, G. 2009. Mechanisms of metformin inhibiting lipolytic response to isoproterenol in primary rat adipocytes. *J Mol Endocrinol,* 42**,** 57-66.

Zhou, J., Du, T., Li, B., Rong, Y., Verkhratsky, A. & Peng, L. 2015. Crosstalk Between MAPK/ERK and PI3K/AKT Signal Pathways During Brain Ischemia/Reperfusion. *ASN Neuro,* 7.

Zimmermann, R., Strauss, J. G., Haemmerle, G., Schoiswohl, G., Birner-Gruenberger, R., Riederer, M., Lass, A., Neuberger, G., Eisenhaber, F., Hermetter, A. & Zechner, R. 2004. Fat mobilization in adipose tissue is promoted by adipose triglyceride lipase. *Science,* 306**,** 1383-6.

Zorrilla, E. P. & Koob, G. F. 2004. The therapeutic potential of CRF1 antagonists for anxiety. *Expert Opin Investig Drugs,* 13**,** 799-828.